Aus der
Klinik für Diagnostische und Interventionelle Radiologie
des Universitätsklinikums Bonn
Direktorin: Univ.-Prof. Dr. Ulrike Attenberger

Multiparametric quantitative magnetic-resonance imaging mapping for the non-invasive assessment of liver fibrosis and disease severity

Habilitationsschrift
Zur Erlangung der Venia Legendi
der Hohen Medizinischen Fakultät
der Rheinischen-Friedrich-Wilhelms-Universität Bonn
für das Lehrgebiet
„Experimentelle Radiologie“

Vorgelegt von
Dr. med. Narine Mesropyan
Wissenschaftliche Mitarbeiterin
an der Rheinischen Friedrich-Wilhelms-Universität Bonn
Bonn 2024

Datum des Habilitationskolloquiums: 22. April 2024

Meiner Familie

The following publications are included in this habilitation thesis

The presented cumulative habilitation thesis is based on the publications listed below. The diagnostic utility of quantitative magnetic resonance imaging (MRI) mapping techniques for the detection and characterization of chronic liver disease in terms of liver fibrosis and function was investigated. In particular, we focused on the investigation of potential non-invasive imaging-based biomarkers of liver disease severity in patients with chronic liver disease (CLD) of different etiologies.

Mesropyan N, Kupczyk P, Dold L, Weismüller TJ, Sprinkart AM, Mädler M, Pieper CC, Kuetting D, Strassburg CP, Attenberger U, Luetkens JA. Non-invasive assessment of liver fibrosis in autoimmune hepatitis: Diagnostic value of liver magnetic resonance parametric mapping including extracellular volume fraction. Abdominal Radiology (NY) 2021 Oct 46(6): 2458–2466 *https://doi.org/10.1007/s00261-020-02822-x.*

Mesropyan N, Kupczyk P, Kukuk GM, Dold L, Weismueller T, Endler C, Isaak A, Faron A, Sprinkart AM, Pieper CC, Kuetting D, Strassburg CP, Attenberger U, Luetkens JA. Diagnostic value of magnetic resonance parametric mapping for non-invasive assessment of liver fibrosis in patients with primary sclerosing cholangitis. BMC Med Imaging 2021 Apr 21(1):65. *https://doi.org/10.1186/s12880- 021-00598-0.*

Mesropyan N*, Kupczyk P*, Dold L, Praktiknjo M, Chang J, Isaak A, Endler C, Kravchenko D, Bischoff LM, Sprinkart AM, Pieper CC, Kuetting D, Jansen C, Attenberger U, Luetkens JA. Assessment of liver cirrhosis severity with extracellular volume fraction MRI. Scientific Reports 2022 Jun 12(1):9422 *https://doi.org/10.1038/s41598-022-13340-9.*

Mesropyan N, Isaak A, Faron A, Praktiknjo M, Jansen C, Kuetting D, Meyer C, Sprinkart AM Chang J, Maedler B, Thomas D, Kupczyk P, Attenberger UI, Luetkens JA. Magnetic resonance parametric mapping of the spleen for non-invasive assessment of portal hypertension. European Radiology 2021 31: 85–93 *https://doi.org/10.1007/s00330-020-07080-5.*

Mesropyan N, Kupczyk P, Isaak A, Endler C, Faron A, Dold L, Sprinkart AM, Pieper CC, Kuetting D, Attenberger UI, Luetkens JA. Synthetic extracellular volume fraction without hematocrit sampling for hepatic applications. Abdominal Radiology (NY) 2021 Oct 46(10):4637-4646 *https://doi.org/10.1007/s00261- 021-03140-6.*

*contributed equally

List of abbreviations

CLD	Chronic liver disease
MRI	Magnetic resonance imaging
CT	Computed tomography
MRE	MR-based Elastography
ECV	Extracellular volume
AUC	Area under the curve
DCE	Dynamic contrast-enhanced
PSC	Primary sclerosing cholangitis
AIH	Autoimmune hepatitis
NASH	Non-alcoholic steatohepatitis
NAFLD	Non-alcoholic liver disease
ALD	Alcoholic liver disease

2 Introduction

2.1 Chronic liver diseases: definition, classification, and epidemiology

Chronic liver diseases (CLDs) include a broad spectrum of pathological conditions characterized by long-term (more than six months) and progressive liver damage, resulting in liver fibrosis and impaired liver function. In CLD, the ongoing inflammatory response of liver tissue, as a protective mechanism, leads to the accumulation of extracellular matrix components within the extracellular space which subsequently expands (hepatic fibrosis). If untreated, over time liver fibrosis leads to liver cirrhosis - a terminal stage, which is characterized by severe scarring of the liver tissue with collagen deposition and failed function. Liver cirrhosis is associated with life-threatening complications such as portal hypertension, spontaneous bacterial peritonitis, ascites, hepatic encephalopathy, and hepatorenal syndrome (Premkumar und Anand, 2022). Hepatic fibrosis was historically considered to be irreversible. However, recent studies indicate that liver fibrosis in the early stages can be reversible resulting in a high clinical interest to develop anti-fibrogenic therapies for liver fibrosis treatment (Nakano et al., 2020) . Therefore, early detection and staging of liver fibrosis are of great clinical importance for well-timed patient management.

CLDs can be classified based on underlying etiology with the following most common etiologies: chronic viral hepatitis (Hepatitis B and C), alcoholic liver disease (ALD), non-alcoholic fatty liver disease (NAFLD)/non-alcoholic steatohepatitis (NASH), genetic causes (Alpha-1 antitrypsin deficiency, hereditary hemochromatosis, Wilson disease), autoimmune liver disease (autoimmune hepatitis (AIH), primary sclerosing cholangitis (PSC), primary biliary cirrhosis), toxic (drug-induced liver disease), and others (idiopathic/cryptogenic, vascular (Budd-Chiari)).

The prevalence and mortality rates of CLDs vary across countries, reflecting country-specific viral hepatitis prevention and treatment, intravenous drug use, alcohol consumption, and obesity rates. The latest data from research investigating the global burden of CLDs released by The Lancet in 2020 show that the disability-adjusted life years caused by CLD in 2019 have increased by 33.0% over the past 30 years, accounting for 1.8% of the global burden (Vento und Cainelli, 2022). Liver cirrhosis is a leading cause of mortality and morbidity across the world, ranking as the 11th leading cause of death and 15th leading cause of morbidity. A

systematic review from the 2019 Global Burden of Diseases, Injuries, and Risk Factors Study (GBD) revealed that the total number of deaths from cirrhosis worldwide reached 1.43 million in 2019, an increase of 8.1% compared to the number of deaths in 2017, according to the GBD 2017 (Cheemerla und Balakrishnan, 2021).

2.2 Diagnosis of chronic liver diseases

Clinical manifestations of CLDs in its early stages with mild to moderate liver fibrosis might be subtle and nonspecific (e.g., fatigue, weakness, weight loss, abdominal pain, etc.) or symptoms may not present themselves until liver damage is severe (e.g., with signs of decompensated liver disease with ascites, encephalopathy, portal hypertension). This poses a challenge in early diagnosis and, therefore, timely initiation of appropriate therapeutic regimens.

Liver biopsy is still considered the gold standard not only for establishing the diagnosis of a particular type of liver disease but more importantly for the assessment of liver disease severity in terms of fibrosis and accompanying inflammation (grading and staging) (Goodman, 2007). The grade of liver disease is considered the degree of inflammation of the hepatocellular injury, which is thought to lead to fibrosis. The stage of liver disease is considered the degree of fibrous scarring of liver parenchyma. Different scoring systems have been developed and used for the assessment of liver disease severity, often considering both activity, grade, and fibrosis stage (including the METAVIR, the Ishak, and the Knodell/histology activity scores) (Chowdhury und Mehta, 2023). According to the most commonly used METAVIR score, there are four fibrosis stages with F0 = no fibrosis, F1 = mild fibrosis with portal fibrosis without septa, F2 = moderate fibrosis with portal fibrosis and few septa, F3 = severe fibrosis with numerous septa without cirrhosis, F4 = cirrhosis. The histologic scoring systems for CLDs are used also to predict disease progression, determine prognosis, and guide physicians in clinical decision-making. However, liver biopsy has its clear drawbacks such as periprocedural complications, inter- and intra- observer variability, sampling errors, as well as low patient acceptance (Chowdhury und Mehta, 2023). Another clear drawback of liver biopsy is that it is not suitable for follow-up examinations, and therefore, monitoring of disease progression over time. In addition, histologic changes obtained at a single time point and localization may not reflect overall disease activity and severity, which may vary.

Therefore, more appropriate, non-invasive, and accurate approaches allowing comprehensive assessment of liver disease severity, including liver fibrosis, disease activity, and liver function in the same setting are highly desirable. Intensive research in this field has been done over the last decades (Baranova et al., 2011). From the clinical perspective, the ideal liver disease severity marker should be liver-specific, readily available, easy to implement, and standardized, also not be influenced by confounders such as inflammation and fibrotic processes outside the liver, intrahepatic fat, iron, and copper deposition. The ability to accurately identify and differentiate between different liver fibrosis stages is also of clinical importance.

Non-invasive tools for the assessment of liver disease and fibrosis severity include serum blood markers (e.g., biochemical and hematological tests and scoring systems) and imaging techniques (e.g., ultrasonography, magnetic resonance imaging (MRI), and computed tomography (CT)).

There is a broad spectrum of serological tests for the assessment of live disease severity, including fibrosis, and dysfunction. They are widely available, easy to obtain, and cost-effective. Biochemical tests for the assessment of liver fibrosis severity include direct and indirect serum markers and panels (please see also ***Figure 1***), which also can be used for the assessment of liver function (Papastergiou et al., 2012). These markers can be categorized into direct, which represent extracellular matrix components, and indirect, which are based on routine laboratory data and reflect the consequences of liver damage. Additionally, a combination of direct and indirect laboratory parameters may be used. Furthermore, due to the poor accuracy of individual markers, algorithms or indices combining panels of markers have been developed and validated (Rossi et al., 2007).

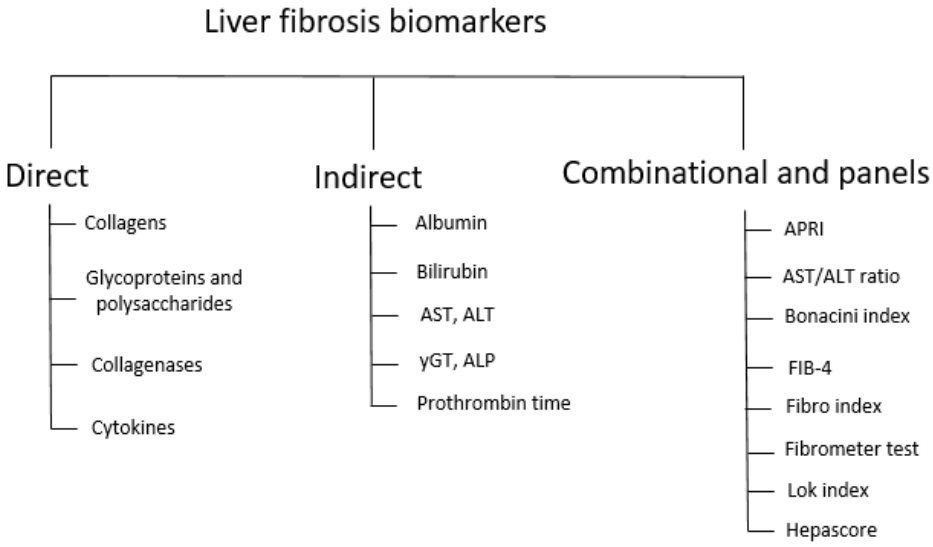

Figure 1 *Overview of non-invasive methods for the assessment of liver fibrosis severity.*
Abbreviations: ALT: alanine aminotransferase; AST: aspartate aminotransferase; yGT: gamma-glutamyl transferase; ALP: alkaline phosphatase; APRI: the aspartate aminotransferase to platelet ratio index; FIB-4: the Fibrosis-4 Index.

Despite the non-invasiveness, repeatability, high availability, and low costs of serum markers, there are several critical issues that should be considered when using them. The main disadvantage of the laboratory tests is that they are not entirely liver-specific and might be influenced by factors outside the liver (Patel und Sebastiani, 2020). For instance, fibrotic and inflammatory changes outside the liver may contribute to false positive results. Furthermore, serum models primarily achieve their best results principally for identifying two groups of patients: those with minimal or no fibrosis and those with advanced fibrosis or cirrhosis. However, the accuracy for intermediate fibrosis is relatively poor (Bissell, 2004). Another potential limitation of serological blood markers is that they were primarily validated in chronic viral hepatitis, NASH/NAFLD, and ALD, which may limit their general applicability in patients with CLDs of other, less common etiologies (Aleknavičiūtė-Valienė und Banys, 2022).

2.3 Imaging of liver fibrosis and cirrhosis: state-of-the-art

Imaging belongs to the standard of care in patients with CLDs, mainly for malignancy exclusion and for the assessment of complications related to liver cirrhosis. Ultrasound traditionally represents a first-line imaging modality in the diagnosis and management of patients with CLDs.

In the last decade, cross-sectional imaging methods, including MRI and CT have undergone a fast evolution and now also represent an important pillar in terms of clinical management, risk stratification, prognosis estimation, and procedural planning in patients with CLDs and cirrhosis. Imaging techniques for liver fibrosis assessment can be divided into elastography methods (ultrasound- and MRI-based) and both semi-quantitative and quantitative methods (MRI-, CT-based).

Ultrasonography

Ultrasound-based elastography is an imaging technique used to evaluate the mechanical properties of tissue according to the propagation of mechanical waves. Different ultrasound-based elastography methods including acoustic radiation force impulse (ARFI) imaging, shear wave elastography (SWE), and transient elastography (TE), have shown promising results in non-invasive liver fibrosis assessment and have been widely implemented into clinical practice due to their inherent advantages, such as wide availability (also at the bedside), and relatively low cost. A number of meta-analyses have shown good to excellent diagnostic accuracy using transient elastography in determining significant and severe liver fibrosis when the results were correlated with pathological classification of liver fibrosis with Area Under the Curve (AUC) of 0.82–0.88 for significant fibrosis and 0.91–0.93 for severe fibrosis (Xu et al., 2015; Li et al., 2016a; Chon et al., 2012).

However, several technical limitations hinder their reproducibility and the accuracy of measurements. These limitations can be tracked back to general ultrasound limitations, e.g., shadowing, reverberation, clutter artifacts, operator-dependent nature of free-hand ultrasound systems. High technical failure rate ranges from 5% to 30% across the studies due to severe ascites, or obesity (Sigrist et al., 2017). Further, limited accuracy in the assessment of deeper tissue or organs, biliary obstruction, acute inflammation, fatty liver, and narrow intercostal spaces also lead to incorrect and/or insufficient measurements. Another strong limitation is the lack of uniformity in commercial system design and settings, which makes comparing measurements from different systems impossible (Sigrist et al., 2017). Biased results can be produced if not standardized across different patient groups with CLDs of different etiologies.

Computed tomography

CT is another widely accessible, reproducible technique with high spatial and temporal resolution and multiple postprocessing options. CT currently belongs to the most commonly used imaging modalities in abdominal/liver imaging with a wide variety of indications. Further, there are some CT-based approaches proposed for the assessment of CLD severity including liver fibrosis. These approaches include semiquantitative and quantitative methods, e.g., analysis of liver surface nodularity, liver segmental volume ratio, splenic volume, and liver texture analysis (Lubner und Pickhardt, 2018).

CT cannot directly quantify liver fibrosis as fibrosis has similar attenuation patterns to the rest of the parenchyma. Therefore, contrast-enhanced CT with calculation of the extracellular volume (ECV) fraction and perfusion has been suggested. Quantification of hepatic ECV fraction on the equilibrium phase in routine liver contrast-enhanced CT is an emerging technique for liver fibrosis assessment, which however still needs extensive validation (Guo et al., 2017).

Perfusion CT of the liver is another promising technique for the staging of fibrosis because it captures perfusion changes that occur during fibrosis (Ronot et al., 2020). Through the acquisition of serial images at high temporal resolution after injection of a bolus of iodinated contrast media followed by post-processing, quantitative and semi-quantitative tissue perfusion parameters (e.g., blood flow, blood volume, mean transit time, portal liver perfusion, arterial liver perfusion, and hepatic perfusion index) can be extracted (Ronot et al., 2020). Other CT techniques proposed for liver fibrosis staging with post-processing software include quantitative measures of liver surface nodularity and the liver segmental volume ratio as well as the combination of laboratory values, liver surface nodularity, and radiomics (Smith et al., 2016). In particular, reported AUCs in case of radiomics demonstrated AUCs of 0.96, 0.97, and 0.95 for ≥ F2, ≥ F3, and F4, respectively. In one of the multicenter studies, the diagnostic accuracy, sensitivity, and specificity of CT for liver cirrhosis were 67–86%, 77–84%, and 53–68%, respectively (Choi et al., 2018).

However, the main disadvantages of CT-based approaches for liver fibrosis and disease severity assessment are ionizing radiation and, in many cases, the need for intravenous iodine-based contrast agent application. This must be taken into account when choosing CT as an imaging modality, especially in patients with impaired renal function, hyperthyroidism, and undergoing follow-up examinations. Another clear disadvantage of contrast-enhanced CT

methods is a high variability of acquisition parameters across the institutions and between different vendors limiting the general applicability of these methods.

2.4 MRI techniques for liver fibrosis and disease severity assessment

Over the past decades, MRI techniques have significantly advanced from a qualitative to a quantitative approach, offering the opportunity for the development of objective and reproducible imaging-based biomarkers that can be incorporated into clinical routine. MRI techniques such as MRI-based elastography (MRE), diffusion-weighted imaging (DWI), texture analysis, and perfusion imaging have been proposed for liver fibrosis and function assessment. To date, MRE is considered to be a safe non-invasive technique with excellent diagnostic accuracy for liver fibrosis assessment. Compared to ultrasound-based elastography, MRE offers wide-field imaging coverage and can also be performed as a 3D technique. According to the meta-analysis mean AUC values (and 95% confidence intervals) for diagnosis of any (≥stage 1), significant (≥stage 2), or advanced fibrosis (≥stage 3), and cirrhosis, were 0.84 (0.76–0.92), 0.88 (0.84–0.91), 0.93 (0.90–0.95), and 0.92 (0.90–0.94), respectively (Singh et al., 2015; Low et al., 2016). Similar diagnostic performance was observed in stratified analysis based on sex, obesity, and etiology of CLD. Also, good repeatability and inter- and intra-rater agreement were demonstrated. The overall rate of technical failure of MRE ranges between 1,5% to 4.3% (Hoodeshenas et al., 2018). MRE has high accuracy for the diagnosis of significant liver fibrosis, independent of BWI and etiology of CLD. Moreover, MRE is usually performed as a part of diagnostic MRI and also in conjunction with other quantitative MRI techniques for liver fat and iron quantification to provide the most comprehensive assessment of the liver.
However, there are some limitations to the broader clinical application of MRE. Obtaining and reporting accurate and reliable liver stiffness measurements with MRE require optimal imaging technique, quality control of images, and know-how with proper interpretation and reporting of elastogram findings (Hoodeshenas et al., 2018). Another technical limitation of MRE is longer scanning time, which may be impractical in patients with claustrophobia and reduced general condition. MRE is currently not widely implemented and available in routine clinical practice as it requires additional expensive hard- and software, and therefore would add costs to the examination.

Diffusion-weighted imaging (DWI) is another non-invasive non-contrast imaging MRI technique, which currently belongs to the imaging standard in liver MRI and does not require additional hardware (Shin et al., 2019). DWI measures the Brownian motion of water molecules in the extracellular space. The apparent diffusion coefficient (ADC) can be calculated from diffusion parameters using a monoexponential model. Alternatively, intravoxel incoherent motion analysis can be performed. According to the intravoxel incoherent motion theory, using multiple b-values diffusion and perfusion parameters can be separated and analyzed assuming a biexponential model (Le Bihan et al., 1988). This results in three parameters: D, or the diffusion coefficient, $D*$, or the perfusion or pseudo-diffusion coefficient, and f, the perfusion fraction. The ability of DWI-derived parameters in the detection and staging of liver fibrosis has been controversially discussed in the literature. Accumulation of extracellular matrix components (collagen fibers, glycosaminoglycans, and proteoglycans) by liver fibrosis theoretically leads to restricted water diffusion and, therefore, decreased ADC values. According to the meta-analysis of 10 studies including 613 patients, AUCs of 0.86 for staging fibrosis stage ≥1, 0.83 for fibrosis stage ≥2, and 0.86 for fibrosis stage ≥3 were found (Wang et al., 2012). Other studies concluded that DWI can only differentiate between healthy and diseased in terms of liver cirrhosis (Bonekamp et al., 2011; Kong et al., 2021; Zhu et al., 2008). Further, DWI suffers from some limitations, such as sensitivity to image noise and motion artifacts, which are especially pronounced in the left liver lobe due to cardiac motion, thus making measurements unreliable. Another clear limitation of the DWI method is the lack of standardization across the institutions (different b values and analysis techniques), and vendor-specific parameters. DWI can be also affected by insufficient fat saturation and iron deposition (Wang et al., 2021). Therefore, further optimization and standardization of DWI techniques for liver fibrosis assessment is required.

MRI-based texture analysis is another proposed MRI-based approach for liver fibrosis assessment. Similar to CT texture analysis, various texture features from images of the liver tissue can be quantified. For texture analysis, any type of image can be applied, e.g., non-contrast and contrast-enhanced, T1- and T2-weighted images, and proton-density weighted imaging. Using various types of analyses, different texture features can be extracted and analyzed using different algorithms. According to studies focusing on this technique, diagnostic performance of texture analysis, the AUCs vary from as low as 0.40 for the

detection of fibrosis stage ≥3, and as high as 1.00 for the staging of cirrhosis. The main limitation of texture analysis is lack of standardization, dependence on image quality, and ROI-placement (Petitclerc et al., 2017).

Dynamic contrast-enhanced MRI (DCE-MRI) using a gadolinium-based contrast agent is another functional imaging method. It is able to characterize both morphological and functional aspects of biological tissues by using both, the temporal and spatial information provided by DCE-MRI. Similar to CT DCE-MRI includes perfusion imaging and hepatocellular functional imaging, but using a gadolinium-based extracellular contrast agent perfusion parameters. According to the studies, with higher fibrosis stages arterial fraction increases, whereas the portal fraction decreases (Ou et al., 2013; Choi et al., 2013). Gadolinium-based hepatocyte-specific (hepatobiliary) contrast agent allows additional assessment of hepatocyte function. Given that liver fibrosis induces hepatic hemodynamic changes and functional damage, concurrently DCE-MRI with a hepatocyte-specific contrast agent helps to diagnose and distinguish between different stages of liver fibrosis (Verloh et al., 2015). At least two images are needed, one before the injection of the contrast agent and a second one 20 minutes after the injection, when the uptake reaches the hepatobiliary phase. Relative enhancement of the tissue or hepatocyte fraction can be calculated, as both of them increase with an increase of fibrosis stage. There is insufficient data on the diagnostic performance of DCE-MRI in a larger population, also in patients with rarer etiologies of liver disease. According to existing data, the AUCs range from 0.63 to 0.93 for liver fibrosis detection using DCE MRI with hepatobiliary contrast agent (Motosugi et al., 2011; Goshima et al., 2012).

2.5 Quantitative MRI mapping and the concept of extracellular volume fraction

Quantitative MRI mapping, or MR-relaxometry, is another promising technique for the assessment of liver fibrosis. Quantitative T1 and T2 mapping techniques have been first proposed and validated against histology in cardiac MRI for the detection and quantification of cardiac fibrosis and inflammation (Diao et al., 2016). Currently, quantitative T1 and T2 mapping are extensively used and considered the gold standard in cardiac imaging for the non-invasive assessment of myocardial fibrosis and edema (Messroghli et al., 2017) .The concept of evaluating the T1 relaxation times in differentiating normal from diseased liver was

first introduced in the 1980s (Thomsen et al., 1990; 1987). Recently there has been increasing interest in MRI–derived mapping parameters as potential imaging-based biomarkers for liver fibrosis and disease severity assessment.

The molecular environment of water molecules in the tissue influences T1 relaxation times. The excessive accumulation of extracellular matrix components with an increase in the collagen volume fraction leads to an increase of T1 relaxation times as shown in myocardial fibrosis (Perea et al., 2015; Mewton et al., 2011). Similarly, increased T1 relaxation times have been shown to correlate with increased hepatic fibrosis due to the accumulation of extracellular matrix components and water caused by fibrosis (Ulmenstein et al., 2022; Luetkens et al., 2018). T1 relaxation times may also be influenced by hepatic inflammation as shown in recent studies on patients with acute liver disease (Hoad et al., 2015; Ulmenstein et al., 2022).

T1 relaxation times can also be measured before and after the administration of an extracellular contrast agent, which allows the additional calculation of the extracellular volume (ECV) fraction. ECV corresponds to the volume fraction of tissue that is not occupied by cells. ECV values are calculated from the change in relaxation rate (R1 = 1/T1) of blood and parenchyma corrected for the hematocrit using the following equation (Schelbert und Messroghli, 2016; Luetkens et al., 2018): ECV = (1 − hematocrit)*(1/T1 parenchyma post-contrast − 1/T1 parenchyma pre-contrast)/(1/T1 aortic post-contrast − 1/T1 aortic pre-contrast). However, ECV calculation requires hematocrit sampling, which might hinder its broader implementation into routine clinical practice. Further, the longitudinal reflexivity (R1 = 1/T1) of blood is known to be in a linear relationship with blood hematocrit. It is determined by the water fractions of plasma and the erythrocyte cytoplasm, which undergo fast water exchange (Spees et al., 2001; Piechnik et al., 2013). Previous cardiac MRI studies showed that ECV quantification without blood sampling, assuming a linear relationship between blood hematocrit and longitudinal T1 relaxation times (1/T1blood), is feasible (Treibel et al., 2016; Raucci et al., 2017). A synthetic ECV calculation for hepatic applications would be beneficial considering the fact that liver fibrosis assessment and staging using T1 mapping techniques could be performed completely non-invasively and time-efficient directly after the MRI examination.

Various T1 mapping techniques have been applied for T1 mapping, e.g., Look-Locker and modified Look-Locker inversion recovery (MOLLI) sequences, saturation recovery-based T1

mapping approaches (Nacif et al., 2011). Color-coded T1 and ECV maps without the need for additional software can be easily generated on the scanner console. T1 maps depict every relatively small variation of T1 within the liver to highlight tissue pathology. The concept of ECV is presented in the ***Figure 1***.

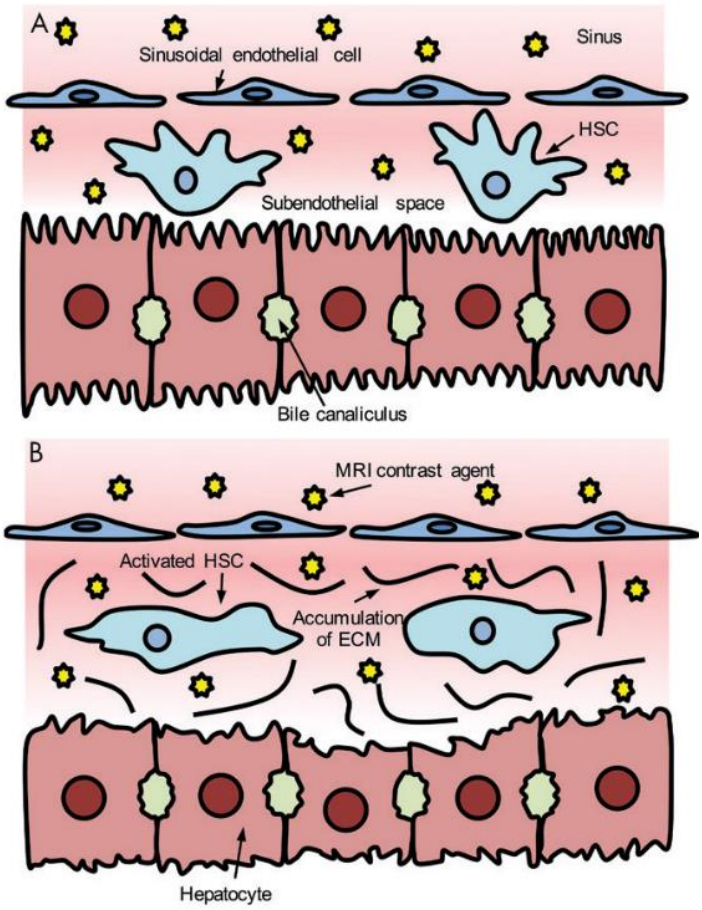

Figure 1 *Illustrated concept of extracellular volume (ECV) measurement in the, A, normal healthy liver and in, B, liver fibrosis. ECV assessment exploits the nature of extracellular MRI contrast agents (yellow) to stay in the extracellular compartments. In a state of dynamic equilibrium with equal contrast concentrations between the blood and the extracellular space, ECV can dichotomize the liver into its mainly interstitial and cellular components. In liver fibrosis (B), chronic liver injury results in hepatocyte dysfunction and increased deposition of extracellular matrix (ECM) components (primarily collagen type I because of activation of hepatic stellate cells [HSC]). Compared with the healthy liver (A), the increased amount of extracellular MRI contrast agents (because of the increased extracellular compartment) in areas of liver fibrosis (B) translates into a more pronounced shortening of T1 values at postcontrast T1 mapping. Luetkens et al. Radiology.*

There are already studies demonstrating the ability of T1 mapping with ECV calculation in the detection of liver fibrotic changes in animals and humans (Luetkens et al., 2018; Li et al., 2016b; Cassinotto et al., 2015; Heye et al., 2012; Wang et al., 2019). In some previous experimental studies, native T1 mapping alone has shown to be a valuable tool for non-invasive fibrosis assessment with good repeatability and reproducibility and a similar to

elastography's high accuracy for fibrosis staging (Li et al., 2020). The potential of T1 mapping in the assessment of liver function can be explained by known direct correlations between the severity of liver fibrosis and liver function. This would allow for a comprehensive assessment of liver fibrosis and function in the same imaging setting. Previous studies have demonstrated the diagnostic utility of T1 mapping with ECV calculation for the assessment of liver fibrosis in patients with CLD of different etiologies (Ulmenstein et al., 2022). However, most of these studies were focusing on patients with chronic viral hepatitis, NAFLD/NASH and/or ALD (Obmann et al., 2021). Data, describing the diagnostic utility of T1 mapping in patients with CLD of other, more rare etiologies are still insufficient or missing.

Similarly, T2 mapping has been reported to be useful in measuring hepatic fibrosis and potentially in differentiating between different stages of liver fibrosis in human and animal studies (Guimaraes et al., 2016). Prolonged T2 relaxation times in regions of fibrosis are potentially attributable to the coexistent inflammation and high water content of the advanced fibrosis. For hepatic T2 mapping different commercially available sequences are currently available, e.g., single-shot T2-prepared bSSFP or T2p-GRE, multi-echo fast spin echo (multi-echo FSE), or gradient spin echo (GraSE) (O'Brien et al., 2022).

A clear advantage of MR-relaxometry is that the relaxation times (T1, T2) are inherent parameters of tissue (organ-specific) and are determined by their physical, chemical, and biological characteristics (Lu et al., 2022). Other advantages of mapping are its robustness in patients with high BMI or ascites, and it does require any additional hardware. Furthermore, there are a number of ongoing efforts aimed at standardization of T1 and T2 measurements between sites and vendors to allow broader clinical implementation and comparability of mapping parameters.

2.6 Objectives

The global aim of this habilitation thesis was, on the one hand, to further investigate the diagnostic value of MRI-derived quantitative mapping parameters for the assessment of liver fibrosis severity in patients with specific etiologies of CLDs (i.e., AIH and PSC), which to date have been insufficiently described in the literature. On the other hand, to investigate the potential value of MRI-derived quantitative mapping parameters for the assessment of liver disease/cirrhosis severity in patients with CLDs of different etiologies. The use of MRI-derived quantitative mapping parameters for the assessment of liver disease/cirrhosis severity will allow to expand the clinical application of the MRI-mapping by providing valuable additional information beyond morphology in the same imaging setting.

The aim of the first study was to explore the diagnostic utility of MRI-derived mapping parameters in liver fibrosis assessment in patients with AIH. In the second study, we focused on patients with PSC. Similar to the first study, we investigated the potential value and diagnostic ability of MRI-derived mapping parameters in differentiation between different fibrosis stages using MRE and ultrasound-based elastography (TE) as the reference standards. In the next two studies, we focused on the potential value and diagnostic utility of MRI-derived mapping parameters for the assessment of liver disease severity in patients with CLDs and cirrhosis of different etiologies (including autoimmune liver disease, NASH/NAFLD, ALD, chronic viral hepatitis, and others). In the first study, the diagnostic utility of T1 mapping and ECV to predict liver cirrhosis severity based on established clinical scores of cirrhosis severity was investigated. In the last exploratory study, the diagnostic ability of spleen mapping parameters in the assessment of the severity of portal hypertension using invasive portal pressure gradient measurements as the reference standard was investigated.

In the above-mentioned studies ECV was calculated and corrected to blood hematocrit, using the established equation (Luetkens et al., 2018). However, the need for hematocrit sampling limits the clinical application of ECV. Therefore, our last study was aimed to generate synthetic ECV for hepatic applications without the need for hematocrit sampling using the known linear relationship between blood hematocrit and longitudinal T1 relaxation times. We investigated whether synthetic ECV is a reliable and accurate alternative to conventional ECV.

Imaging belongs to the standard of care in patients with CLDs and liver cirrhosis of different etiologies. Development and establishment of imaging-based, reliable, accurate, and at the same time reproducible biomarkers for the comprehensive assessment of liver fibrosis and

disease/cirrhosis severity in the same imaging setting without adding any costs and burdens in patients' care are of high clinical importance. An early diagnosis and monitoring of liver fibrosis severity would allow for early therapeutic interventions prior to the development of irreversible and potentially fatal complications. Additionally, the use of synthetic ECV may potentially overcome an important barrier for the broader clinical implementation of hepatic ECV.

3 Results

3.1 Quantitative parametric mapping for the assessment of liver fibrosis severity in patients with autoimmune hepatitis. *Abdominal Radiology (NY) 2021*

"Non-invasive assessment of liver fibrosis in autoimmune hepatitis: Diagnostic value of liver magnetic resonance parametric mapping including extracellular volume fraction"
Mesropyan N, Kupczyk P, Dold L, Weismüller TJ, Sprinkart AM, Mädler M, Pieper CC, Kuetting D, Strassburg CP, Attenberger U, Luetkens JA.
Published in *Abdominal Radiology (NY)* 2021 Oct 46(6): 2458–2466

Purpose - The aim of this study was to determine the diagnostic value of T1 and T2 mapping as well as extracellular volume fraction (ECV) for non-invasive assessment of liver fibrosis in AIH patients.

Methods - In this prospective study, 27 patients (age range: 19–77 years) with AIH underwent liver MRI. T1 and T2 relaxation times as well as ECV were quantified by mapping techniques. The presence of significant fibrosis (≥ F2) was defined as magnetic resonance elastography (MRE)-based liver stiffness ≥ 3.66 kPa. MRE was used as reference standard, against which the diagnostic performance of MRI-derived mapping parameters was tested. Diagnostic performance was compared by utilizing receiver-operating characteristic (ROC) analysis.

Results - MRE-based liver stiffness correlated with both, hepatic native T1 ($r = 0.69$; $P < 0.001$) as well as ECV ($r = 0.80$; $P < 0.001$). For the assessment of significant fibrosis, ECV yielded a sensitivity of 85.7% (95% confidence interval (CI): 60.1–96.0%) and a specificity of 84.6% (CI 60.1–96.0%); hepatic native T1 yielded a sensitivity of 85.7% (CI 60.1–96.0%); and a specificity of 76.9% (CI 49.7–91.8%). Diagnostic performance of hepatic ECV (area under the curve (AUC): 0.885), native hepatic T1 (AUC: 0.846) for assessment of significant fibrosis was similar compared to clinical fibrosis scores (APRI (AUC: 0.852), FIB-4 (AUC: 0.758), and AAR (0.654) ($P > 0.05$ for each comparison)).

Conclusions - Quantitative mapping parameters such as T1 and ECV can identify significant fibrosis in AIH patients. Future studies are needed to explore the value of parametric mapping for the evaluation of different disease stages.

Abdominal Radiology (2021) 46:2458–2466
https://doi.org/10.1007/s00261-020-02822-x

SPECIAL SECTION: DIFFUSE LIVER DISEASE

Non-invasive assessment of liver fibrosis in autoimmune hepatitis: Diagnostic value of liver magnetic resonance parametric mapping including extracellular volume fraction

Narine Mesropyan[1,2] · Patrick Kupczyk[1,2] · Leona Dold[3] · Tobias J. Weismüller[3] · Alois M. Sprinkart[1,2] · Burkhart Mädler[4] · Claus C. Pieper[1] · Daniel Kuetting[1,2] · Christian P. Strassburg[3] · Ulrike Attenberger[1] · Julian A. Luetkens[1,2]

Received: 16 July 2020 / Revised: 7 October 2020 / Accepted: 10 October 2020 / Published online: 19 October 2020

Abstract

Purpose Autoimmune hepatitis (AIH) is an immune-mediated chronic liver disease that leads to severe fibrosis and cirrhosis. The aim of this study was to determine the diagnostic value of T1 and T2 mapping as well as extracellular volume fraction (ECV) for non-invasive assessment of liver fibrosis in AIH patients.

Methods In this prospective study, 27 patients (age range: 19–77 years) with AIH underwent liver MRI. T1 and T2 relaxation times as well as ECV were quantified by mapping techniques. The presence of significant fibrosis (≥F2) was defined as magnetic resonance elastography (MRE)-based liver stiffness ≥ 3.66 kPa. MRE was used as reference standard, against which the diagnostic performance of MRI-derived mapping parameters was tested. Diagnostic performance was compared by utilizing receiver-operating characteristic (ROC) analysis.

Results MRE-based liver stiffness correlated with both, hepatic native T1 ($r = 0.69$; $P < 0.001$) as well as ECV ($r = 0.80$; $P < 0.001$). For the assessment of significant fibrosis, ECV yielded a sensitivity of 85.7% (95% confidence interval (CI): 60.1–96.0%) and a specificity of 84.6% (CI 60.1–96.0%); hepatic native T1 yielded a sensitivity of 85.7% (CI 60.1–96.0%); and a specificity of 76.9% (CI 49.7–91.8%). Diagnostic performance of hepatic ECV (area under the curve (AUC): 0.885), native hepatic T1 (AUC: 0.846) for assessment of significant fibrosis was similar compared to clinical fibrosis scores (APRI (AUC: 0.852), FIB-4 (AUC: 0.758), and AAR (0.654) ($P > 0.05$ for each comparison)).

Conclusion Quantitative mapping parameters such as T1 and ECV can identify significant fibrosis in AIH patients. Future studies are needed to explore the value of parametric mapping for the evaluation of different disease stages.

Keywords Autoimmune hepatitis · Magnetic resonance imaging · Magnetic resonance elastography

Abbreviations

AIH	Autoimmune Hepatitis
MRE	Magnetic resonance elastography
ECV	Extracellular volume fraction

Introduction

Autoimmune hepatitis (AIH) is an immune-mediated chronic liver disease that may lead to severe liver fibrosis and cirrhosis. AIH is relatively rare and predominantly affects females [1]. According to current guidelines, liver biopsy is recommended in patients with AIH to establish diagnosis, evaluate the presence of fibrosis, and make further treatment decision [2]. However, despite being considered the gold standard for diagnosis, liver biopsy in AIH patients

✉ Julian A. Luetkens
julian.luetkens@ukbonn.de

1 Department of Diagnostic and Interventional Radiology, University Hospital Bonn, Venusberg-Campus 1, 53127 Bonn, Germany

2 Quantitative Imaging Lab Bonn (QILaB), Venusberg-Campus 1, 53127 Bonn, Germany

3 Department of Internal Medicine I, University Hospital Bonn, Venusberg-Campus 1, 53127 Bonn, Germany

4 Philips GmbH Germany, Roentgenstrasse 22, 22335 Hamburg, Germany

has clear disadvantages, which include high clinical expertise, high intra- and interobserver variability, risk of severe periprocedural complications, and high cost. Also, serial liver biopsies are not practical for long-term monitoring of a patient's treatment response. As fibrosis detection and staging are important for treatment decisions and prognosis estimation reliably non-invasive measurements are needed, in these patients [1].

Magnetic resonance elastography (MRE) is currently regarded the most accurate non-invasive technique for the detection and staging of liver fibrosis [3–5]. Several studies have demonstrated that the diagnostic performance of MRE in this role is superior to that of transient elastography (TE) [4, 6]. In particular, MRE is notable for its ability to accurately diagnose mild fibrosis, which is difficult by TE [7]. However, also MRE has its drawbacks due to high technical failures rate, i.e., in patients with severe ascites or iron overload [6, 8].

The concept of evaluating the T1 relaxation times in differentiating normal from diseased livers was introduced in the 1980s [9, 10]. Hepatic inflammation and fibrosis are believed to increase the T1 relaxation time of liver parenchyma due to an increase in extracellular matrix and water and protein concentration [11]. T1 mapping can depict even small variations of T1 within a tissue and has been used in cardiac imaging to detect myocardial edema, iron overload, myocardial infarcts, and scarring [12]. Furthermore, T1 relaxation times can also be measured before and after the administration of an extracellular contrast agent, which allows the additional calculation of the extracellular volume (ECV). ECV is a measure of the extracellular space and represents the tissue volume, which is not taken by cells [13]. ECV values are calculated from the change in relaxation rate (R1 = 1/T1) of blood and parenchyma corrected for the hematocrit [14, 15]. Similarly, T2 mapping has been reported to be useful in measuring hepatic fibrosis and potentially in differentiating between different stages of liver fibrosis in human and animal studies [15, 16, 22, 23]. Prolonged T2 relaxation times in regions of fibrosis are potentially attributable to the coexistent inflammation and high water content of the advanced fibrosis. There have been several studies showing correlations between hepatic T1, T2, and ECV with liver fibrosis in both animal and human models [15–21].

Therefore, the purpose of our explorative prospective study was to evaluate the diagnostic utility of different quantitative parametric magnetic resonance imaging (MRI) parameters (T1, T2, and ECV) to diagnose liver fibrosis in patients with AIH using MRE-based liver stiffness as a reference standard.

Material and methods

The institutional review board approved this prospective study, and all study participants provided written informed consent prior to MRI examination. From June 2019 to March 2020, patients with AIH diagnosis were consequently included in this study. Diagnosis of AIH was based on diagnostic criteria of AIH, established by the International Autoimmune Hepatitis Group (IAIHG) [24]. Also patients with overlap syndromes, which implies that the predominant disease is AIH and that the concurrent cholestatic features are background components [25], were included.

All patients included in the study had no acute exacerbation at the time of MRI examination based on clinical and laboratory findings with a good response to immunosuppressive therapy. Model for end-stage liver disease (MELD) was analyzed, and laboratory markers were retrieved from the institutional medical information system. Also, non-invasive scoring systems based on laboratory tests for assessment of liver fibrosis (aspartate aminotransferase-to-platelet ratio index (ARPI), fibrosis index based on the 4 factor (FIB-4), and aspartate aminotransferase and alanine aminotransferase ratio (AST/ALT ratio (de-Ritis)) were calculated as previously described [26–28].

Multiparametric magnetic resonance imaging

All imaging was performed on a clinical whole-body 1.5 T MRI system (Ingenia, Philips Healthcare) equipped with 32-channel abdominal coil with digital interface for signal reception. Besides morphological sequences, patients underwent MRE and parametric mapping of the liver.

Liver MRE was implemented by 2D gradient-recalled echo to acquire liver elasticity maps with motion-encoding gradients (MEGs). Sequence parameters were as follows: time of repetition (TR) 50 ms, time of echo (TE) 20 ms, flip angle (FA) 20°, parallel imaging factor 2.3, active driver frequency 60 Hz, active driver power 100%, acquired voxel size $1.5 \times 4.74 \times 10$ mm, reconstructed voxel size 1.17×1.17 x 10 mm, scan duration/breath hold 15.3 s, and 3 slices. The system configuration was based on a pneumatically powered active wave driver and a tube-connected and strap-secured passive driver placed over the right liver lobe. Generated shear waves at a fixed vibration frequency were coursing through the liver and created tissue displacements, which could be detected to generate magnitude and phase images. Phase shift of magnetic resonance signal was measured at four different phase offsets over one cycle of motion. Further analysis

by integrated software (MR elastography View, Philips Healthcare) allowed the creation of a quantitative elastogram (liver stiffness map). For hepatic T1 mapping a heart rate-independent 10-(2)-7-(2)-5-(2)-3-(2), modified Look-locker inversion recovery (MOLLI) acquisition scheme [29] with internal triggering was implemented. The following technical parameters were applied: TR 1.92 ms, TE 0.84 ms, FA 20°, parallel imaging factor 2, acquired voxel size 1.98 × 2.45 × 10 mm, reconstructed voxel size 1.13 × 1.13 × 10 mm, and scan duration/breath hold 14.0 s. Post-contrast T1 maps using the same imaging technique were performed 10 min after contrast injection in the same positions as pre-contrast examinations. For contrast enhancement, the extracellular contrast agent Gadobutrol (1.0 mmol/ml solution with 0.1 mmol per kilogram of body weight, Gadovist, Bayer Healthcare Pharmaceuticals) was injected as a bolus at a rate of 1.5 ml/s and followed by a 10 ml saline flush. For hepatic T2 mapping, a six-echo gradient spin echo sequence (GraSE) was used [30], and scan parameters: TR 450 ms, inter-echo spacing 16 ms, FA 90°, parallel imaging factor 2.5, acquired voxel size 1.98 × 2.01 × 10 mm, reconstructed voxel size 0.88 × 0.88 × 10 mm, scan duration/breath h hold 15/3 × 5 s. T1 and T2 mapping were performed in transversal views covering liver parenchyma at the level of the portal bifurcation. T1 and T2 relaxation maps were reconstructed at the scanner console. Maps of proton density fat fraction (PDFF) and T2* were achieved with a six-echo 3D gradient-echo sequence (mDixon Quant, Philips Healthcare).The following parameters were applied: TR 7.8 ms, TE 1.1 ms, FA 5°, parallel imaging factor 2, acquired voxel size 1.99 × 1.99 × 6 mm, reconstructed voxel size 0.99 × 0.99 × 3 mm, scan duration/breath hold 15.0 s.

Image analysis

Image analyses were performed by an experienced board-certified radiologist (J.A.L, 8 years of experience in abdominal MRI), blinded for the clinical information. For the assessment of T1 and T2 relaxation times and PDFF, three representative round regions of interest (ROIs) (minimum of one cm^2) were drawn centrally in three hepatic segments (segments 2, 4a, and 7), and mean relaxation times were calculated [31]. T1 values of the blood pool were obtained from the abdominal aorta on the transversal maps. ECV values were normalized for hematocrit and calculated with regions of interest from pre- and post-contrast T1 values using the following equation [32]: ECV = (1 − hematocrit)*(1/T1 parenchyma post-contrast − 1/T1 parenchyma pre-contrast)/(1/T1 aortic post-contrast − 1/T1 aortic pre-contrast). Blood hematocrit levels were determined on the day of examination. Liver tissue stiffness values were derived from stiffness confidence map by drawing the largest possible freehand ROIs (minimum of one cm^2) in three different representative regions of the liver. All patients were divided into two groups, without (< fibrosis stage (F) 2) and with significant fibrosis (≥ F2) according to the MRE-based liver stiffness. According to the literature, a cut-off of 3.66 kPa was chosen to differentiate between patients without and with significant liver fibrosis. The cut-off values for F2, F3, and F4 were 3.66, 4.11, and 4.71 kPa, respectively[4, 33].

Statistical analysis

Statistical analysis was performed using SPSS Statistics (Version 25, IBM) and MedCalc (Version 19.1.3, MedCalc Software). Patient characteristics are presented as mean ± standard deviation or as absolute frequency. Continuous variables between two groups were compared using Student *t* test. Dichotomous variables were compared using the $\chi 2$ test (with the cell count greater than five) and Fisher test (with a cell count less than or equal to five). The bivariate Pearson correlation coefficient (*r*) was used for a correlation analyses. Receiver operating characteristic analysis (ROC) was performed to calculate areas under the curve (AUC). AUCs were compared using the method proposed by DeLong et al. [34]. Sensitivity, specificity, and accuracy were calculated. MRE-based liver stiffness was the reference standard against which the diagnostic performance of MRI-derived mapping parameters of liver was tested. A *P* value < 0.05 was considered statistically significant.

Results

Cohort characteristics

A total of 27 patients with AIH diagnosis were included in this study. 9/27 (33.3%) patients had an overlap syndrome. At the time of MRI examination, 13/27 (48.1%) patients received immunosuppressive therapy with budesonide alone; 8/27 (29.6%) patients received a combination of budesonide with azathioprine; and 3/27 (11.1%) patients received immunosuppressive therapy with azathioprine alone. There were also 3/27 (11.1%) patients, who received no therapy at the time of MRI examination. 13/27 (48.2%) patients had no or not significant (< F2), and 14/27 (51.8%) had significant (≥ F2) fibrosis. 1/14 (7.1%), 4/14 (28.6%), and 9/14 (64.3%) patients had fibrosis stages F2, F3, and F4, respectively. The mean age of patients with no significant fibrosis according to the MRE was 46.6 ± 18.6 years (range: 20–74 years), with significant fibrosis 42.6 ± 18.6 years (range: 19–77 years). The mean body mass index (BMI) in patients with no significant fibrosis was 26.9 ± 4.3 kg/m^2, in patients with significant fibrosis 23.5 ± 2.9 kg/m^2 ($P = 0.047$). Age and sex did not differ in both groups ($P > 0.05$). No significant

Table 1 Clinical characteristics of patients without significant fibrosis (< F2) and with significant fibrosis (≥ F2)

Variable	Patients with AIH and no significant fibrosis (< F2, n = 13)	Patients with AIH and significant fibrosis (≥ F2, n = 14)	*P* value
Age (years)	46.6 ± 18.6	42.6 ± 18.6	0.585
Body mass index (kg/m^2)	26.9 ± 4.3	23.5 ± 2.9	0.047
Sex			0.385
Male	2 (15.4%)	5 (35.7%)	
Female	11 (84.6%)	9 (64.3%)	
Hematocrit level (%)	39.9 ± 6.8	40.2 ± 2.2	0.911
MELD	7.4 ± 2.8	7.9 ± 3.1	0.666
Bilirubin (mg/dl)	0.56 ± 0.49	1.27 ± 0.78	0.011
ALT (U/l)	42.3 ± 35.7	145.6 ± 188.2	0.063
AST (U/l)	30.3 ± 16.5	90.6 ± 97.1	0.045
GGT (U/l)	93.5 ± 145.1	171.7 ± 189.9	0.243
Platelets cells × 10^9/l	291.3 ± 81.5	178.8 ± 100.8	0.003
C-reactive protein level (mg/l)	7.2 ± 5.3	5.1 ± 8.8	0.539
AP (U/l)	98.9 ± 75.6	129.2 ± 127.3	0.468
Creatinine (mg/dl)	0.71 ± 0.16	0.79 ± 0.21	0.315
Albumin (g/l)	41.3 ± 4.0	42.3 ± 6.3	0.717
International normalized ratio	1.12 ± 0.35	1.08 ± 0.08	0.708
ASL/ALT (de-Ritis)	1.07 ± 0.49	0.85 ± 0.35	0.183
FIB-4	1.03 ± 0.50	2.26 ± 1.38	0.006
APRI	0.58 ± 1.02	1.32 ± 1.08	0.084

Continuous data are means ± standard deviations. Nominal data are absolute frequencies with percentages in parentheses

MELD score model of end-stage liver disease, *ALT* alanine aminotransferase, *AST* aspartate aminotransferase, *AP* alkaline phosphatase, *GGT* gamma-glutamyltransferase, *APRI* aspartate aminotransferase-to-platelet ratio index, *FIB-4* Fibrosis-4-Score, *ASL/ALT (de-Ritis)* De-Ritis-Quotient

differences were found between clinical fibrosis scores APRI and AST/ALT ratio in both groups ($P > 0.05$). FIB-4 was higher in the group with significant fibrosis (≥ F2) compared to the group with no significant fibrosis (< F2) ($P = 0.006$). Clinical characteristics are summarized in Table 1.

MRI results

Compared to patients with AIH and no significant fibrosis (< F2), patients with significant fibrosis (≥ F2) had markedly increased hepatic native T1 relaxations times (548.8 ± 40.7 ms vs. 620.3 ± 66.3 ms; $P = 0.003$) and hepatic ECV values (27.1 ± 3.2% vs. 38.7 ± 18.9%; $P = 0.039$). There were no significant differences in hepatic T2 relaxation times between both groups (50.7 ± 4.2 ms vs. 50.5 ± 6.5 ms; $P = 0.920$). Also, no significant difference in fat fraction was present in both groups (5.3 ± 4.6% vs. 3.2 ± 1.5%, $P = 0.135$). MRE-based liver stiffness and hepatic parametric MRI results are given in Table 2. Furthermore, we found a strong correlation between MRE-based liver stiffness and hepatic native T1 ($r = 0.69$, $P < 0.001$) as well as hepatic ECV ($r = 0.80$, $P < 0.001$, see also Fig. 1). There were also

Table 2 Hepatic magnetic resonance elastography characteristics of patients without (< F2) and with significant fibrosis (≥ F2)

Variable	Patients with AIH and no significant fibrosis (< F2, n = 13)	Patients with AIH and significant fibrosis (≥ F2, n = 14)	*P* value
MRE-based liver stiffness (kPa)	2.6 ± 0.6	5.6 ± 1.8	< 0.001
Hepatic native T1 relaxation time (ms)	548.8 ± 40.7	620.3 ± 66.3	0.003
Hepatic extracellular volume fraction (%)	27.1 ± 3.2	38.7 ± 18.9	0.039
Hepatic T2 relaxation time (ms)	50.7 ± 4.2	50.5 ± 6.5	0.920
Hepatic T2* relaxation time (ms)	31.1 ± 5.2	32.5 ± 5.9	0.537
Proton density fat fraction (%)	5.3 ± 4.6	3.2 ± 1.5	0.135

Continuous data are means ± standard deviations

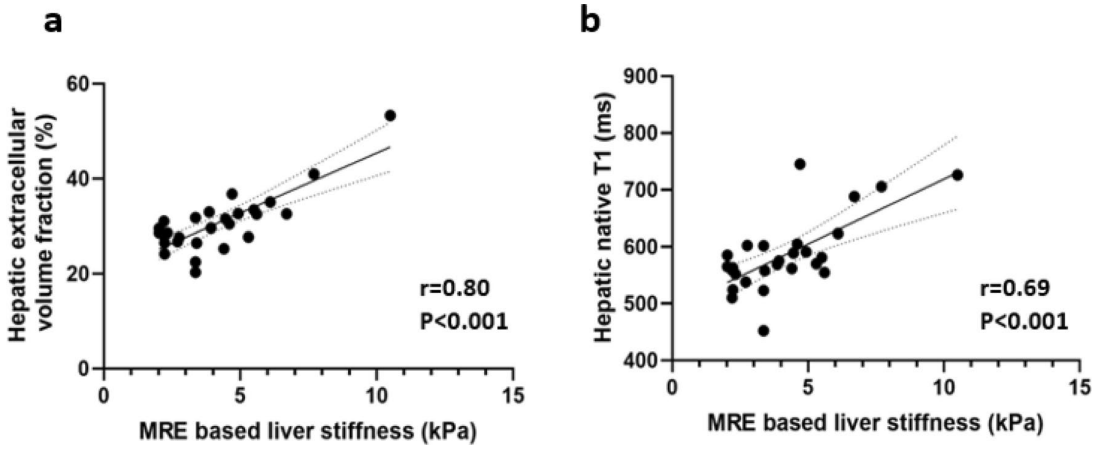

Fig. 1 Scatter plots shows correlations between magnetic resonance elastography (MRE)-based liver stiffness and hepatic extracellular volume fraction (**a**) and hepatic native T1 (**b**). Regression line is given with 95% confidence interval

significant correlations between clinical fibrosis scores such as FIB-4 and APRI and hepatic native T1 (for both scores, $r = 0.49$, $P < 0.05$). Also, hepatic ECV showed a significant correlation with FIB-4 score ($r = 0.39$, $P = 0.04$). We found no correlations between hepatic T2 and MRE-based liver stiffness as well as clinical fibrosis scores (FIB-4 and AST/ALT Ratio). A correlation matrix is given in Table 3. Representative images from patients with and without significant fibrosis are given in Fig. 2.

Diagnostic performance of parametric mapping parameters

Several parametric mapping parameters were evaluated regarding the diagnostic performance to diagnose significant fibrosis (≥F2). Regarding the overall diagnostic performance, hepatic ECV revealed the highest diagnostic performance with an AUC of 0.885, a sensitivity of 85.7%, and a specificity of 84.6% (cut-off value: > 29.5%). There were no significant differences in diagnostic performance of hepatic ECV and clinical fibrosis scores for diagnosing significant fibrosis: APRI ($P = 0.702$), FIB-4 ($P = 0.138$), and AST/ALR ratio (de-Ritis) ($P = 0.058$). Hepatic native T1 showed also a high diagnostic performance with an AUC of 0.846, a sensitivity of 85.7%, and a specificity of 76.9% to diagnose significant fibrosis (cut-off value: > 565 ms). There were no significant differences in diagnostic performance of hepatic ECV and native T1 ($P = 0.550$). Diagnostic performance of hepatic native T1 also differs not significant compared to the clinical fibrosis scores: APRI ($P = 0.956$) and FIB-4 ($P = 0.346$), AAR ($P = 0.123$). Diagnostic performance of hepatic T2 (AUC: 0.566) was significantly lower than that of hepatic native T1 ($P = 0.006$) and ECV ($P = 0.004$). Parameters of diagnostic performance for all other evaluated parameters with sensitivities, specificities, accuracies, positive and negative predictive values are given in Table 4. A ROC curves graph for diagnosis of significant fibrosis is given in Fig. 3.

Discussion

The purpose of our study was to evaluate the diagnostic utility of different quantitative parametric MRI parameters for the assessment of liver fibrosis using MRE-based liver stiffness as a reference standard in patients with AIH. The main

Table 3 Correlation matrix for quantitative MRI parameters and clinical fibrosis scores

Variable	Hepatic native T1		Hepatic T2		Hepatic ECV	
	r value	*P* value	*r* value	*P* value	*r* value	*P* value
MRE-based liver stiffness	0.69	< 0.001	0.03	0.903	0.80	< 0.001
FIB-4	0.49	0.010	− 0.09	0.625	0.39	0.04
APRI	0.49	0.009	0.42	0.031	0.23	0.25
AST/ALT ratio (de-Ritis)	− 0.06	0.775	− 0.23	0,260	0.02	0.92

ECV extracellular volume fraction, *MRE* magnetic resonance elastography, *FIB-4* Fibrosis-4-Score, *ASL/ALT ratio (de-Ritis)* De-Ritis-Quotient, *APRI* aspartate aminotransferase-to-platelet ratio index

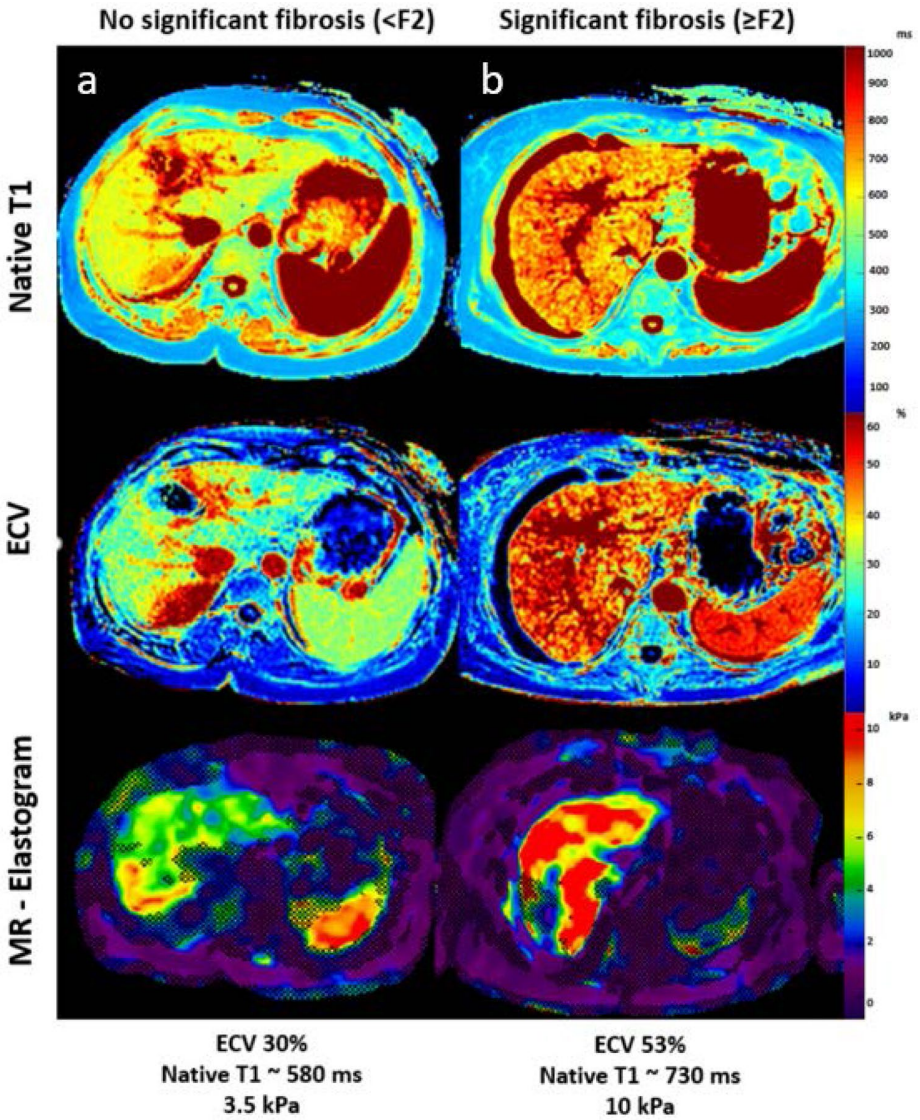

Fig. 2 Representative images of hepatic native T1 and extracellular volume (ECV) maps and magnetic resonance elastogram (MRE) from patients with no significant fibrosis (< F2, **a**) and patient with significant fibrosis (≥ F2, **b**). *ECV* extracellular volume fraction, *F* fibrosis stage

findings of our study are that (1) hepatic ECV a native T1 showed a strong correlation with MRE-based liver stiffness and, (2) hepatic ECV and T1 showed a high diagnostic performance to diagnose significant fibrosis (≥ F2) in patients with AIH.

The development of liver fibrosis is a dynamic process characterized by the excessive extracellular matrix accumulation produced by fibrogenic cell populations in response to injury and inflammation. Advanced liver disease is characterized by increased production and decreased destruction of the extracellular matrix [35]. Consequently, an increased ECV leads to increased accumulation of extracellular MRI contrast agent in the extracellular space. Therefore, fibrosis is believed to increase the T1 relaxation time and ECV of the liver due to an increase in extracellular water and protein concentration. Moreover, recently published studies have already shown positive correlations between hepatic T1, T2, and ECV with liver fibrosis in both animal and human models [15, 18–20, 36]. There are also studies showing positive correlations between T1, T2 mapping parameters and MRE with liver fibrosis, however, without focusing on AIH patients [21, 37]. One of the most studied tools for non-invasive assessment of liver fibrosis in patients with AIH is liver stiffness measurement derived by TE (FibroScan) [38, 39]. Yet, it has limited diagnostic value and poor reproducibility and observer dependency, especially in patients with ascites and obesity [40]. There is one study, mentioning quantitative MRI techniques for prediction of portal hypertension in children and young adults with autoimmune liver disease [41]. There is still no literature directly showing correlations between MRE-based liver stiffness

Table 4 Diagnostic performance of different quantitative MRI parameters for assessment of MRE-derived liver stiffness in patients with autoimmune hepatitis and without (< F2) and with significant (≥ F2) fibrosis

Variable	AUC	Cutoff value	Sensitivity (%)	Specificity (%)	PPV (%)	NPV (%)	Accuracy (%)
Hepatic extracellular volume fraction (%)	0.885 (0.703–0.973)	> 29.5	85.7 (60.1–96.0)	84.6 (57.8–95.7)	85.7 (60.1–96.0)	84.6 (57.8–95.7)	85.2 (67.5–94.1)
Hepatic native T1 (ms)	0.846 (0.656–0.954)	> 565	85.7 (60.1–96.0)	76.9 (49.7–91.8)	85.7 (60.1–96.0)	76.9 (49.7–91.8)	81.5 (63.3–91.8)
Hepatic T2 (ms)	0.566 (0.363–0.754)	≤ 49.2	50.0 (26.8–73.2)	69.2 (42.4–87.3)	63.6 (35.4–84.8)	56.3 (33.2–76.9)	59.3 (40.7–75.5)
APRI score	0.852 (0.662–0.957)	> 0.521	85.7 (60.1–96.0)	76.9 (49.7–91.8)	80.0 (54.8–93.0)	83.3 (55.2–95.3)	81.5 (63.3–91.8)
FIB-4 score	0.758 (0.556–0.900)	> 2.055	57.1 (32.6–78.6)	92.3 (66.7–98.6)	61.5 (35.5–82.3)	85.7 (60.1–96.0)	74.1 (55.3–86.8)
ALT/AST ratio (de-Ritis)	0.654 (0.448–0.825)	≤ 0.976	78.6 (52.4–92.4)	53.8 (29.1–76.8)	64.7 (41.3–82.7)	70.0 (39.7–89.2)	66.7 (47.8–81.4)
MELD score	0.654 (0.448–0.825)	> 6	78.6 (52.4–92.4)	61.5 (35.5–82.3)	68.8 (44.4–85.8)	72.7 (43.4–90.3)	70.4 (51.5–84.1)

Data in parentheses are 95% confidence interval

PPV positive predictive value, *NPV* negative predictive value, *MELD* score model of end stage liver disease, *APRI* aspartate aminotransferase to platelet ratio index, *FIB-4* fibrosis-4-score; ASL/ALT ratio (de-Ritis): De-Ritis-Quotient

and MRI mapping parameter and its potential for detecting and staging liver fibrosis, focusing on patients with AIH.

Taken MRE-based liver stiffness as a reference standard, we found a strong correlation between hepatic ECV and liver stiffness ($r = 0.80$; $P < 0.001$) in patients with AIH. Furthermore, hepatic ECV showed a high diagnostic performance for detecting a significant fibrosis (F ≥ 2) in patients with AIH with an AUC of 0.885. Moreover, although it is not statistically significant, the diagnostic performance of hepatic ECV was higher to that of all non-invasive serologic tests. One drawback of the clinical scores is that fibrotic and inflammatory changes outside of the liver contribute to false positive results and, therefore, cannot be considered as liver specific. At the same time, quantitative mapping parameters, including ECV reflects directly the changes in the liver parenchyma itself. Furthermore, the use of ECV measurements seems to be beneficial, because on the one side, compared with conventional hepatic T1 and T2 mapping, it does not depend on parameters in image acquisition and the magnetic field strength. Therefore, ECV is physiologically normalized measure. Moreover, compared to MRE, its diagnostic quality might not be affected by obesity or ascites. Also, ECV calculation is possible on every MRI system, and no an additional expensive hardware is needed, which might be another advantage over MRE. The other mapping parameter, which showed high diagnostic performance in diagnosing significant fibrosis, is native hepatic T1 (AUC 0.846). Like ECV, T1 mapping seems to be more liver specific than laboratory markers as changes in hepatic T1 are measured directly in the liver parenchyma. In contrast to a previous study [21], which also showed positive correlation between MRE-based liver stiffness and hepatic T1 mapping ($r = 0.49$), our correlation was stronger ($r = 0.69$), likely because of the heterogeneous group of patients in the previous study with liver disease of different etiologies (including hepatitis B and C, non-alcoholic fatty liver

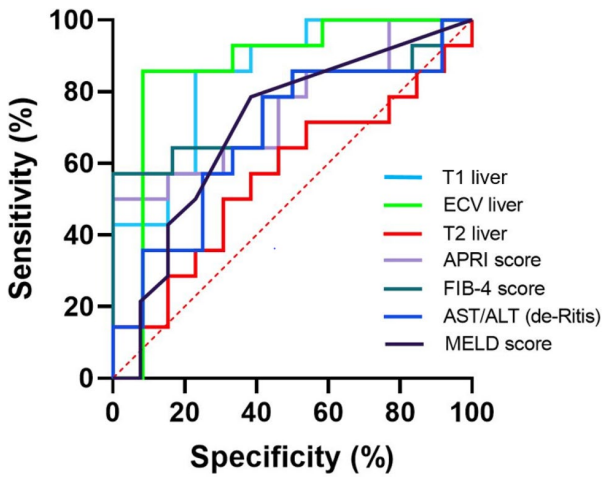

Fig. 3 Graph show receiver-operating characteristic curves for diagnosis of significant fibrosis in patients with autoimmune hepatitis (≥ F2). Curves are given for hepatic T1 relaxation times (area under curve [AUC]: 0.846), hepatic ECV (AUC: 0.885), hepatic T2 relaxation times (AUC: 0.566), APRI (AUC: 0.852), FIB-4 score (0.758), ALT/AST ratio (de-Ritis) (AUC: 0.654), and MELD score (AUC: 0.654)

disease, AIH, primary sclerosing cholangitis, and primary biliary cholangitis).

In contrast to previous data [21], we did not find significant correlation between T2 relaxation times and MRE-based liver stiffness in patients with AIH. Nevertheless, in the previous study, just poor to moderate correlation between T2 and T1 mapping as well as MRE was found. Generally, T2 mapping of the liver has not been validated in the clinical setting. Just a limited number of animal and human studies have shown that fibrosis can prolong the T2 relaxation time of the liver [21, 23]. It might be assumed that T2 relaxation time, similar to cardiac imaging, is might be increased in regions of fibrosis with coexistence of inflammation, due to increased water content [23]. Therefore, the absence of significant differences in both groups can be explained by the same inflammatory activity in the liver at the time of examination.

There are several limitations in this study. The main limitation was the absence of liver biopsy as a reference standard at the time of MRI examination. Liver biopsy with its clear drawbacks was performed only once for initial diagnosis. Liver biopsies for follow-up, however, are not routine clinical practice in our clinic, and therefore, ethics committee approval would have been unobtainable. Therefore, MRE-based liver stiffness was considered as a reference standard for the assessment of different liver fibrosis stages. T1 and T2 maps were acquired in a single transverse section at the level of the bifurcation of portal vein and, therefore, may have missed other significant changes, which probably occurred in other planes. Furthermore, our T1 measurements were not corrected for hepatic steatosis or hepatic/splenic iron overload, which might impair correct assessment of T1 values. However, there was no patient in our study collective with relevant steatosis as well as iron overload. Another limitation of our study was that the reading of all cases was performed only by one experienced radiologist. Additionally, the sample size was rather small and most patients in the advanced fibrosis group had F4 fibrosis, which might limit the overall applicability of our results. The study results have to be considered as preliminary, and further prospective studies using liver biopsy as the reference standard are necessary to confirm the accuracy and usefulness of ECV and other MRI parameters for assessment and follow-up of liver fibrosis in patients with AIH.

In conclusion, in our prospective study, we found strong correlations between quantitative hepatic MRI-derived mapping parameters including ECV and MRE-based liver stiffness. T1 mapping techniques with ECV calculation might provide additional diagnostic information over conventional MRI and over laboratory markers by non-invasive quantification and assessment of fibrotic liver changes in patients with AIH, without the need of additional equipment.

Funding Open Access funding enabled and organized by Projekt DEAL.

Compliance with ethical standards

Conflict of interest The authors declare that they have no conflict of interest.

Ethical approval The study was approved by the ethics committee of the University Hospital Bonn.

Informed consent Written informed consent was obtained prior to the study.

Consent for publication Written informed consent to publish this information was obtained from study participants.

References

1. van Gerven NM, Boer YS de, Mulder CJ, van Nieuwkerk CM, Bouma G (2016) Auto immune hepatitis. World J Gastroenterol 22(19):4651–61.
2. EASL Clinical Practice Guidelines: Autoimmune hepatitis (2015). J Hepatol 63(4):971–1004.
3. Venkatesh SK, Yin M, Ehman RL (2013) Magnetic resonance elastography of liver: technique, analysis, and clinical applications. J Magn Reson Imaging 37(3):544–55.
4. Singh S, Venkatesh SK, Wang Z et al. (2015) Diagnostic performance of magnetic resonance elastography in staging liver fibrosis: a systematic review and meta-analysis of individual participant data. Clin Gastroenterol Hepatol 13(3):440-451.e6.
5. Horowitz JM, Venkatesh SK, Ehman RL et al. (2017) Evaluation of hepatic fibrosis: a review from the society of abdominal radiology disease focus panel. Abdom Radiol (NY) 42(8):2037–53.
6. Guo Y, Parthasarathy S, Goyal P, McCarthy RJ, Larson AC, Miller FH (2015) Magnetic resonance elastography and acoustic radiation force impulse for staging hepatic fibrosis: a meta-analysis. Abdom Imaging 40(4):818–34.
7. Bonekamp S, Kamel I, Solga S, Clark J (2009) Can imaging modalities diagnose and stage hepatic fibrosis and cirrhosis accurately? J Hepatol 50(1):17–35.
8. Wagner M, Corcuera-Solano I, Lo G et al. (2017) Technical Failure of MR Elastography Examinations of the Liver: Experience from a Large Single-Center Study. Radiology 284(2):401–12.
9. Thomsen C, Christoffersen P, Henriksen O, Juhl E (1990) Prolonged T1 in patients with liver cirrhosis: An in vivo MRI study. Magnetic Resonance Imaging 8(5):599–604.

10. (1987) Magnetic resonance imaging of parenchymal liver disease: a comparison with ultrasound, radionuclide scintigraphy and X-ray computed tomography. Clinical Radiology 38(5):495–502.
11. Li Z, Sun J, Hu X et al. (2016) Assessment of liver fibrosis by variable flip angle T1 mapping at 3.0T. J Magn Reson Imaging 43(3):698–703.
12. Radenkovic D, Weingärtner S, Ricketts L, Moon JC, Captur G (2017) T1 mapping in cardiac MRI. Heart Fail Rev 22(4):415–30.
13. Moon JC, Messroghli DR, Kellman P et al. (2013) Myocardial T1 mapping and extracellular volume quantification: a Society for Cardiovascular Magnetic Resonance (SCMR) and CMR Working Group of the European Society of Cardiology consensus statement. J Cardiovasc Magn Reson 15:92.
14. Flett AS, Hayward MP, Ashworth MT et al. (2010) Equilibrium contrast cardiovascular magnetic resonance for the measurement of diffuse myocardial fibrosis: preliminary validation in humans. Circulation 122(2):138–44.
15. Luetkens JA, Klein S, Träber F et al. (2018) Quantification of Liver Fibrosis at T1 and T2 Mapping with Extracellular Volume Fraction MRI: Preclinical Results. Radiology 288(3):748–54.
16. Luetkens JA, Klein S, Traeber F et al. (2018) Quantitative liver MRI including extracellular volume fraction for non-invasive quantification of liver fibrosis: a prospective proof-of-concept study. Gut 67(3):593–4.
17. Luetkens JA, Klein S, Träber F et al. (2019) Quantification of liver fibrosis: extracellular volume fraction using an MRI bolus-only technique in a rat animal model. Eur Radiol Exp 3(1):22.
18. Hoy AM, McDonald N, Lennen RJ et al. (2018) Non-invasive assessment of liver disease in rats using multiparametric magnetic resonance imaging: a feasibility study. Biol Open 7(7).
19. McDonald N, Eddowes PJ, Hodson J et al. (2018) Multiparametric magnetic resonance imaging for quantitation of liver disease: a two-centre cross-sectional observational study. Sci Rep 8(1):9189.
20. Müller A, Hochrath K, Stroeder J et al. (2017) Effects of Liver Fibrosis Progression on Tissue Relaxation Times in Different Mouse Models Assessed by Ultrahigh Field Magnetic Resonance Imaging. Biomed Res Int 2017:8720367.
21. Hoffman DH, Ayoola A, Nickel D, Han F, Chandarana H, Shanbhogue KP (2020) T1 mapping, T2 mapping and MR elastography of the liver for detection and staging of liver fibrosis. Abdom Radiol (NY) 45(3):692–700.
22. Wang H-Q, Jin K-P, Zeng M-S et al. (2019) Assessing liver fibrosis in chronic hepatitis B using MR extracellular volume measurements: Comparison with serum fibrosis indices. Magnetic Resonance Imaging 59:39–45.
23. Guimaraes AR, Siqueira L, Uppal R et al. (2016) T2 relaxation time is related to liver fibrosis severity. Quant Imaging Med Surg 6(2):103–14.
24. Liberal R, Grant CR, Longhi MS, Mieli-Vergani G, Vergani D (2014) Diagnostic criteria of autoimmune hepatitis. Autoimmun Rev 13(4-5):435–40.
25. Czaja AJ (2013) Diagnosis and management of the overlap syndromes of autoimmune hepatitis. Can J Gastroenterol 27(7):417–23.
26. Li J, Gordon SC, Rupp LB et al. (2014) The validity of serum markers for fibrosis staging in chronic hepatitis B and C. J Viral Hepat 21(12):930–7.
27. Sterling RK, Lissen E, Clumeck N et al. (2006) Development of a simple noninvasive index to predict significant fibrosis in patients with HIV/HCV coinfection. Hepatology 43(6):1317–25.
28. Imperiale TF, Born LJ (2001) Clinical utility of the AST/ALT ratio in chronic hepatitis C. Am J Gastroenterol 96(3):919–20.
29. Messroghli DR, Radjenovic A, Kozerke S, Higgins DM, Sivananthan MU, Ridgway JP (2004) Modified Look-Locker inversion recovery (MOLLI) for high-resolution T1 mapping of the heart. Magn Reson Med 52(1):141–6.
30. Sprinkart AM, Luetkens JA, Träber F et al. (2015) Gradient Spin Echo (GraSE) imaging for fast myocardial T2 mapping. J Cardiovasc Magn Reson 17:12.
31. Isaak A, Praktiknjo M, Jansen C et al. (2020) Myocardial Fibrosis and Inflammation in Liver Cirrhosis: MRI Study of the Liver-Heart Axis. Radiology 297(1):51–61.
32. Schelbert EB, Messroghli DR (2016) State of the Art: Clinical Applications of Cardiac T1 Mapping. Radiology 278(3):658–76.
33. Hoodeshenas S, Yin M, Venkatesh SK (2018) Magnetic Resonance Elastography of Liver: Current Update. Top Magn Reson Imaging 27(5):319–33.
34. DeLong ER, DeLong DM, Clarke-Pearson DL (1988) Comparing the areas under two or more correlated receiver operating characteristic curves: a nonparametric approach. Biometrics 44(3):837–45.
35. Lee YA, Wallace MC, Friedman SL (2015) Pathobiology of liver fibrosis: a translational success story. Gut 64(5):830–41.
36. Li J, Liu H, Zhang C et al. (2020) Native T1 mapping compared to ultrasound elastography for staging and monitoring liver fibrosis: an animal study of repeatability, reproducibility, and accuracy. Eur Radiol 30(1):337–45.
37. Besa C, Wagner M, Lo G et al. (2018) Detection of liver fibrosis using qualitative and quantitative MR elastography compared to liver surface nodularity measurement, gadoxetic acid uptake, and serum markers. J Magn Reson Imaging 47(6):1552–61.
38. Wu S, Yang Z, Zhou J et al. (2019) Systematic review: diagnostic accuracy of non-invasive tests for staging liver fibrosis in autoimmune hepatitis. Hepatol Int 13(1):91–101.
39. Xu Q, Sheng L, Bao H et al. (2017) Evaluation of transient elastography in assessing liver fibrosis in patients with autoimmune hepatitis. J Gastroenterol Hepatol 32(3):639–44.
40. Perazzo H, Veloso VG, Grinsztejn B, Hyde C, Castro R (2015) Factors That Could Impact on Liver Fibrosis Staging by Transient Elastography. Int J Hepatol 2015:624596.
41. Dillman JR, Serai SD, Trout AT et al. (2019) Diagnostic performance of quantitative magnetic resonance imaging biomarkers for predicting portal hypertension in children and young adults with autoimmune liver disease. Pediatr Radiol 49(3):332–41.

3.2 Quantitative parametric mapping for the assessment of liver fibrosis severity in patients with primary sclerosing cholangitis. *BMC Medical Imaging 2021*

"Diagnostic value of magnetic resonance parametric mapping for non-invasive assessment of liver fibrosis in patients with primary sclerosing cholangitis"
Mesropyan N, Kupczyk P, Kukuk GM, Dold L, Weismueller T, Endler C, Isaak A, Faron A, Sprinkart AM, Pieper CC, Kuetting D, Strassburg CP, Attenberger U, Luetkens JA.
Published in *BMC Medical Imaging* 2021 Apr 21(1):65

Purpose - The purpose of this study was to investigate the utility of T1 and T2 mapping parameters, including extracellular volume fraction (ECV) for non-invasive assessment of fibrosis severity in patients with PSC.

Methods -In this prospective study, patients with PSC diagnosis were consecutively enrolled from January 2019 to July 2020 and underwent liver MRI. Besides morphological sequences, MR elastography (MRE), and T1 and T2 mapping were performed. ECV was calculated from T1 relaxation times. The presence of significant fibrosis (≥ F2) was defined as MRE-derived liver stiffness ≥ 3.66 kPa and used as the reference standard, against which the diagnostic performance of MRI mapping parameters was tested. Student t test, ROC analysis and Pearson correlation were used for statistical analysis.

Results - 32 patients with PSC (age range 19-77 years) were analyzed. Both, hepatic native T1 ($r = 0.66$; $P < 0.001$) and ECV ($r = 0.69$; $P < 0.001$) correlated with MRE-derived liver stiffness. To diagnose significant fibrosis (≥ F2), ECV revealed a sensitivity of 84.2% (95% confidence interval (CI) 62.4-94.5%) and a specificity of 84.6% (CI 57.8-95.7%); hepatic native T1 revealed a sensitivity of 52.6% (CI 31.7-72.7%) and a specificity of 100.0% (CI 77.2-100.0%). Hepatic ECV (area under the curve (AUC) 0.858) and native T1 (AUC 0.711) had an equal or higher diagnostic performance for the assessment of significant fibrosis compared to serologic fibrosis scores (APRI (AUC 0.787), FIB-4 (AUC 0.588), AAR (0.570)).

Conclusions - Hepatic T1 and ECV can diagnose significant fibrosis in patients with PSC. Quantitative mapping has the potential to be a new non-invasive biomarker for liver fibrosis assessment and quantification in PSC patients.

Mesropyan *et al. BMC Med Imaging* (2021) 21:65
https://doi.org/10.1186/s12880-021-00598-0

BMC Medical Imaging

RESEARCH Open Access

Diagnostic value of magnetic resonance parametric mapping for non-invasive assessment of liver fibrosis in patients with primary sclerosing cholangitis

Narine Mesropyan[1], Patrick Kupczyk[1], Guido M. Kukuk[2], Leona Dold[3], Tobias Weismueller[3], Christoph Endler[1], Alexander Isaak[1], Anton Faron[1], Alois M. Sprinkart[1], Claus C. Pieper[1], Daniel Kuetting[1], Christian P. Strassburg[3], Ulrike I. Attenberger[1] and Julian A. Luetkens[1*]

Abstract

Background: Primary sclerosing cholangitis (PSC) is a chronic cholestatic liver disease, characterized by bile duct inflammation and destruction, leading to biliary fibrosis and cirrhosis. The purpose of this study was to investigate the utility of T1 and T2 mapping parameters, including extracellular volume fraction (ECV) for non-invasive assessment of fibrosis severity in patients with PSC.

Methods: In this prospective study, patients with PSC diagnosis were consecutively enrolled from January 2019 to July 2020 and underwent liver MRI. Besides morphological sequences, MR elastography (MRE), and T1 and T2 mapping were performed. ECV was calculated from T1 relaxation times. The presence of significant fibrosis (≥ F2) was defined as MRE-derived liver stiffness ≥ 3.66 kPa and used as the reference standard, against which the diagnostic performance of MRI mapping parameters was tested. Student *t* test, ROC analysis and Pearson correlation were used for statistical analysis.

Results: 32 patients with PSC (age range 19–77 years) were analyzed. Both, hepatic native T1 ($r = 0.66$; $P < 0.001$) and ECV ($r = 0.69$; $P < 0.001$) correlated with MRE-derived liver stiffness. To diagnose significant fibrosis (≥ F2), ECV revealed a sensitivity of 84.2% (95% confidence interval (CI) 62.4–94.5%) and a specificity of 84.6% (CI 57.8–95.7%); hepatic native T1 revealed a sensitivity of 52.6% (CI 31.7–72.7%) and a specificity of 100.0% (CI 77.2–100.0%). Hepatic ECV (area under the curve (AUC) 0.858) and native T1 (AUC 0.711) had an equal or higher diagnostic performance for the assessment of significant fibrosis compared to serologic fibrosis scores (APRI (AUC 0.787), FIB-4 (AUC 0.588), AAR (0.570)).

Conclusions: Hepatic T1 and ECV can diagnose significant fibrosis in patients with PSC. Quantitative mapping has the potential to be a new non-invasive biomarker for liver fibrosis assessment and quantification in PSC patients.

Keywords: Primary sclerosing cholangitis, Magnetic resonance elastography, Extracellular volume fraction

Background

Primary sclerosing cholangitis (PSC) is a rare cholestatic liver disease, leading to biliary fibrosis and cirrhosis. PSC is believed to be immune-mediated, however, the etiopathogenesis of the disease has still not been completely investigated and remains unclear. The main feature of

*Correspondence: julian.luetkens@ukbonn.de
[1] Department of Diagnostic and Interventional Radiology, University Hospital Bonn, Venusberg-Campus 1, 53127 Bonn, Germany
Full list of author information is available at the end of the article

PSC is a long-term, progressive inflammation followed by fibrosis of the intra- and extrahepatic bile ducts [1, 2]. PSC has a strong male predominance and is often associated with other immune-mediated diseases such as inflammatory bowel disease (IBD, e.g. ulcerative colitis) and autoimmune hepatitis (AIH). To date, there are several reports of therapy showing effect in PSC, but no established medical therapy with proven effect on transplant-free survival [3, 4]. According to the guidelines of the European (EASL) and American (AASLD) Associations for the Study of Liver Diseases, magnetic resonance imaging (MRI) including MR-cholangiography has been established as the standard imaging modality when PSC is suspected [5, 6]. As for any other chronic liver disease, early detection of fibrotic changes of liver parenchyma with fibrosis staging, evaluation of disease activity and severity, prognosis estimation as well as malignancy exclusion (e.g. cholangiocarcinoma and/or hepatocellular carcinoma) are of great clinical importance. Therefore, diagnostic approaches enabling these efficiently and non-invasively in the same clinical setting without adding costs and burdens in patients' care are required [7, 8].

Over the last decades, MRI techniques have undergone significant advancement from a qualitative to quantitative approach, offering the opportunity for the development of objective and reproducible imaging biomarkers that can be incorporated into clinical routine [9]. To date, magnetic resonance elastography (MRE) is considered to be a safe noninvasive technique with excellent diagnostic accuracy for liver fibrosis assessment [10–13], and routine liver biopsy is no longer recommended for fibrosis staging in PSC [5, 6]. However, MRE requires additional expensive equipment and is only available in specialized centers. Therefore, ubiquitously available quantitative imaging techniques might be desirable that can encompass a major portion of the liver.

Initially extensively used in cardiac imaging for the detection and quantification of cardiac fibrosis and inflammation, quantitative T1 and T2 mapping techniques [14], might also be promising MRI techniques for the evaluation of liver parenchyma. According to current studies, hepatic fibrosis increases the T1 and T2 relaxation time of liver parenchyma due to an increase of extracellular matrix and protein concentration [15–17]. T1 mapping techniques also allow the estimation of extracellular volume fraction (ECV) from native and post-contrast T1. ECV is a biomarker of the extracellular space and reflects tissue volume which is not taken by cells [18]. ECV can be calculated from the change in relaxation rate (R1 = 1/T1) of blood and parenchyma corrected for the hematocrit [17, 19]. Although several studies investigated the role of T1 and T2 mapping techniques as well as ECV for liver fibrosis assessment [16, 17, 20–23], reliable data investigating these techniques in patients with PSC are still missing. Therefore, the goal of the present study was to explore the diagnostic value of MRI mapping parameters, including ECV to diagnose significant fibrosis in PSC patients using MRE-derived liver stiffness as a reference standard.

Methods

This study was approved by the institutional review board and was conducted in compliance with the ethical standards set in the 1964 Declaration of Helsinki as well as its later amendments. Written informed consent was obtained from all participants prior to MRI examination. Consecutive patients of the University Hospital of Bonn with diagnosis of PSC were prospectively enrolled from January 2019 to July 2020. Diagnosis of PSC was based on diagnostic criteria of PSC established by the EASL [6]. Patients with additional features of AIH and accompanying IBD were also included. Exclusion criteria were as follows: (1) concomitant diagnosis of other chronic liver diseases, including hepatic steatosis and iron overload; (2) contraindications for MRI; (3) acute ascending cholangitis; (4) cholangiocarcinoma or hepatocellular carcinoma; (5) previous liver transplant; (6) small-duct PSC; (7) insufficient imaging quality or absence of laboratory tests at the time of MRI examination. Additionally, data of liver stiffness measurements derived by transient elastography (TE, FibroScan) were analyzed. A cut-off value of 8.6 kPa was chosen to differentiate between patients without (< F2) and with (≥ F2) significant fibrosis [24]. Biochemical blood analyses were performed using standard tests and non-invasive serologic fibrosis scores (aspartate aminotransferase to platelet ratio index (APRI), fibrosis index based on the 4 factor (FIB-4) and aspartate aminotransferase and alanine aminotransferase ratio (AST/ALT ratio (de-Ritis)) were calculated [25–27]. All clinical data and laboratory markers were recorded from the patient charts. None of the patients of the study cohort had acute exacerbation of PSC, IBD and AIH at the time of MRI examination based on clinical and laboratory findings and received symptomatic therapy according to current guidelines [6].

Multiparemetric MRI

All liver MRI were performed on a clinical whole-body 1.5 T system (Ingenia, Philips Healthcare) equipped with 32-channel abdominal coil with digital interface for signal reception. Liver MRE and T1 and T2 mapping were performed in addition to morphological sequences. For liver MRE, a 2D gradient-recalled echo with added cyclic motion encoding gradients (MEGs) sequence with the following parameters was applied: time of repetition (TR)/time of echo (TE) 50/20 ms,

flip angle (FA) 20°, parallel imaging factor 2.3, active driver frequency 60 Hz, active driver power 100%, field of view (FOV) $450 \times 403 \times 32$ mm, acquired voxel size $1.50 \times 4.74 \times 10$ mm, reconstructed voxel size $1.17 \times 1.17 \times 10$ mm^3, scan duration/breath hold 15.3 s, 3 slices. The system configuration was based on an active pneumatic driver connected via plastic tube with a passive driver, which was placed at the patient's right upper quadrant. MRE involves (a) generation of shear waves in the tissue, (b) acquisition of MR images, (c) depicting the propagation of the induced shear waves, and (d) postprocessing of the share waves to generate quantitative liver stiffness maps using implemented vendor´s software (MR elastography View, Philips Healthcare). For hepatic T1 mapping, we used a heart rate independent 10-(2)-7-(2)-5-(2)-3-(2) modified Look-Locker inversion recovery (MOLLI) acquisition scheme with internal triggering [28]. Technical parameters were as follows: TR/TE 1.92/0.84 ms, FA 20°, parallel imaging factor 2, acquired voxel size $1.98 \times 2.45 \times 10$ mm^3, reconstructed voxel size $1.13 \times 1.13 \times 10$ mm^3, scan duration/breath hold 14 s. For the post-contrast T1 maps the same technique was used after 10 min of contrast agent application in the same positions as pre-contrast examinations. For contrast enhanced T1 mapping, a gadolinium-based contrast agent (Gadobutrol, 1.0 mmol/ml solution with 0.1 mmol per kilogram of body weight, Gadovist, Bayer Healthcare Pharmaceuticals) was administered as a single bolus with an injection rate of 1.5 ml/s. Hepatic T2 mapping was performed using a six-echo gradient spin echo sequence (GraSE) with the following parameters [29]: TR/TE 450/16 ms, inter-echo spacing 16 ms, FA 90°, parallel imaging factor 2.5, acquired voxel size $1.98 \times 2.01 \times 10$ mm, reconstructed voxel size $0.88 \times 0.88 \times 10$ mm, scan duration/breath hold $15/3 \times 5$ s. Hepatic quantitative maps were acquired in a single transversal slice slightly above the liver hilum. Relaxation maps were reconstructed at the scanner console.

Image analysis

An experienced board-certified radiologist (J.A.L, 8 years of experience in abdominal MRI) performed image analyses, blinded to the clinical data. For the assessment of T1 and T2 relaxation times, the mean relaxation time of three representative regions of interest (ROI) was calculated. ROIs were drawn centrally in the hepatic segments II, IVa and VII within liver parenchyma away from confounding factors like organ borders, vessels or bile ducts. Blood pool T1 values were derived from the abdominal aorta. ECV was calculated with ROI-based on pre- and post-contrast T1 values according to the previously published equation [30]. Hematocrit samples were derived on the same day prior to MRI examination. Liver tissue stiffness values were derived from stiffness confidence map by drawing largest possible ROIs (≥ 1 cm^2) in at least three different representative regions of the liver. Based on MRE-derived liver stiffness, all study participants were divided into two groups, first, without ($<$ fibrosis stage F2) and second, with significant fibrosis ($\geq$ F2). To differentiate between patients with and without significant liver fibrosis a cutoff value of 3.66 kPa was chosen [31].

Statistical analysis

All data were analyzed using software (SPSS Statistics, version 25, IBM, MedCalc, version 19.1.3, MedCalc). Patient characteristics are presented as mean $\pm$ standard deviation, as absolute frequency or median, as appropriate. Student *t* test was used for comparison of continuous variables between two different groups. Dichotomous variables were compared using the χ^2 test (with the cell count >5) and Fisher test (with a cell count ≤ 5). Bivariate Pearson correlation coefficient or Spearman's rank correlation coefficient were used for a correlation analyses, as appropriate. Receiver operating characteristic analysis (ROC) was used to determine the cut-points with the highest combined sensitivity and specificity, positive predictive values (PPV), negative predictive values (NPV) and accuracy using MRE-derived liver stiffness as a reference standard. DeLong method was used to compare areas under the curves (AUCs) [32]. MRE-derived liver stiffness as well as liver stiffness derived by TE were the reference standards against which the diagnostic performance of MRI-derived mapping parameters of liver was tested. The level of statistical significance was set to $P < 0.05$.

Results

Cohort characteristics

A total of 32 patients with diagnosis of large-duct PSC were included in this study. Based on MRE-derived stiffness values, 40.6% (13/32) patients had no ($<$F2) and 59.4% (19/32) had significant ($\geq$ F2) fibrosis. 15.8% (3/19), 21.1% (4/19), and 63.1% (12/19) patients had fibrosis stages F2, F3 and F4, respectively. 18.7% (6/32) patients had additional features of AIH. There were 61.5% (8/13) patients with intrahepatic biliary changes only and 38.5% (5/13) patients with both intra- and extrahepatic bile duct changes in patients without significant fibrosis ($<$F2) and 73.7% (14/19) and 26.3% (5/19) in the group of patients with significant fibrosis ($\geq$F2), respectively. In patients without significant fibrosis ($<$F2), there were 15.4% (2/13) patients with and 84.6% (11/13) with no imaging features of portal hypertension (varices, splenomegaly, and/ or ascites). In patients with significant fibrosis

(≥ F2) there were 52.6% (10/19) patients with and 47.4% (9/19) patients without imaging features of portal hypertension ($P=0.03$). The mean age of the disease onset in the group of patients without significant fibrosis was 38.4 ± 7.5 years, with significant fibrosis 31.1 ± 12.5 years. At the time of MRI examination, 40.6% (13/32) patients received therapy with ursodeoxycholic acid (UDCA) alone; 31.3% (10/32) patients received a combination of 5-aminosalicylic acid (5-ASA) with UDCA due to accompanying IBD; 12.5% (4/32) patient the combination of corticosteroids (budesonide) with UDCA due to overlap with AIH. 20.0% (5/32) patients received no therapy at the time of MRI examination. Clinical characteristics are summarized in Table1. Additionally, 18/32 patients had TE examination within 6 month to MRI examination (the mean interval between MRI examination and TE was 66.3 ± 48.0 days).

Transient elastography results

Based on liver stiffness measurements derived by TE 44.4% (8/18) patients had no (< F2) and 55.6% (10/18) had significant fibrosis (≥ F2). The mean value of liver stiffness measurements derived by TE in patients without (< F2) was 5.7 ± 0.8 kPa and in patients with significant fibrosis (≥ F2) 23.1 ± 20.3 kPa ($P=0.024$). We found significant correlations between liver stiffness measurements derived by TE and MRE (r = 0.78, $P<0.001$) as well as hepatic ECV (r = 0.52, $P=0.026$). ECV was significant higher in patients with significant fibrosis according to TE (32.2 ± 5.7% vs. 27.1 ± 1.4%; $P=0.023$).

Based on TE analysis, hepatic ECV revealed a diagnostic performance with an AUC of 0.815, a sensitivity of 77.8% and a specificity of 66.7% to diagnose significant fibrosis (cutoff value: 27.7%). Hepatic native T1 showed also high diagnostic performance with an AUC of 0.870, a sensitivity of 77.8% and a specificity of 88.9% to diagnose significant fibrosis (cutoff value: > 559 ms). Hepatic T2 achieved an AUC of 0.753, a sensitivity of 55.6% and a specificity of 100.0% (cutoff value: > 53.3 ms).

MRI results

Hepatic native T1 as well as ECV were remarkably increased in the group of patients with significant fibrosis (≥ F2) compared to the group of patients without significant fibrosis (< F2): 559.6 ± 56.3 ms vs. 522.8 ± 33.2 ms, $P=0.043$, and 30.5 ± 4.4% vs. 26.3 ± 1.9%, $P=0.003$, respectively (see also Fig. 1). We found no significant differences in hepatic T2 relaxation times between

Table 1 Clinical characteristics of patients without significant fibrosis (< F2) and with significant fibrosis (≥ F2)

Variable	PSC patients without significant fibrosis (< F2, n = 13)	PSC patients with significant fibrosis (≥ F2, n = 19)	*P* value
Age (years)	43.1 ± 12.8	39.5 ± 17.5	0.531
Body mass index (kg/m^2)	23.8 ± 2.9	24.8 ± 3.8	0.439
Sex			0.246
Male	7 (53.8%)	4/19 (21.1%)	
Female	6 (46.2%)	15 (78.9%)	
Hematocrit level (%)	43 ± 4	42 ± 6	0.526
Bilirubin (mg/dl)	0.56 ± 0.25	1.19 ± 0.98	0.031
ALT (U/l)	52.1 ± 55.3	118.1 ± 92.9	0.029
AST (U/l)	33.4 ± 11.4	81.9 ± 46.6	0.001
GGT (U/l)	155.5 ± 116.7	240.3 ± 180.5	0.147
Platelets cells × 10^9/l	291.2 ± 81.1	248.5 ± 130.7	
C-reactive protein level (mg/l)	12.4 ± 22.8	2.1 ± 1.5	0.221
AP (U/l)	285.8 ± 181.6	140.8 ± 45.4	0.013
Creatinine (mg/dl)	0.79 ± 0.09	0.79 ± 0.14	0.946
Albumin (g/l)	45.9 ± 3.2	42.8 ± 5.3	
International normalized ratio	1.08 ± 0.28	1.05 ± 0.12	0.683
ASL/ALT (de-Ritis)	0.85 ± 0.28	0.82 ± 0.33	0.798
FIB-4	0.85 ± 0.62	1.84 ± 2.86	0.232
MELD	6.69 ± 2.21	7.47 ± 2.46	0.919
APRI	0.31 ± 0.19	0.94 ± 1.10	0.052
Mayo score	− 1.09 ± 0.54	0.03 ± 1.34	0.012

Continuous data are means ± standard deviations. Nominal data are absolute frequencies with percentages in parentheses

MELD, Score Model of End Stage Liver Disease; ALT, Alanine aminotransferase; AST, Aspartate aminotransferase; AP, Alkaline phosphatase, GGT, Gamma-glutamyltransferase; APRI, aspartate aminotransferase to platelet ratio index; FIB-4, Fibrosis-4-Score; ASL/ALT (de-Ritis), De-Ritis ratio

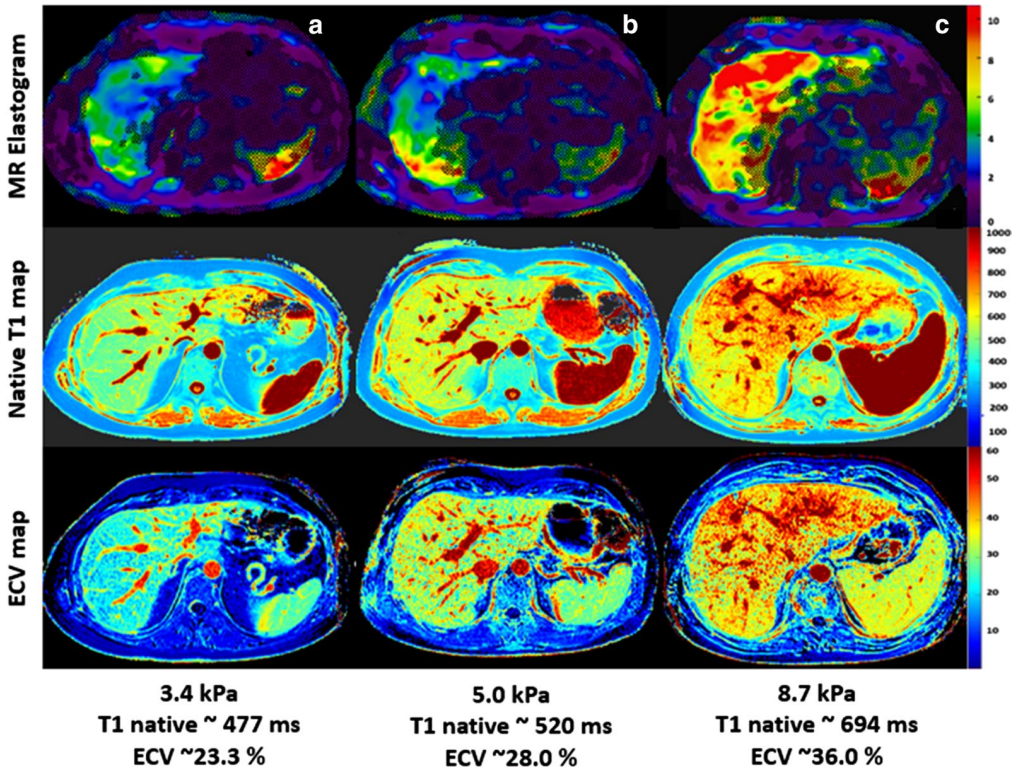

Fig. 1 Representative images of hepatic native T1 and extracellular volume (ECV) maps and magnetic resonance elastogram (MRE) from patient without significant fibrosis (< F2, **a**) and patients with significant fibrosis (≥ F2, **b** and **c**). Figure exemplarily illustrates alterations in quantitative hepatic parameters found in our study. ECV: extracellular volume fraction, F: fibrosis stage

both groups (48.9 ± 3.2 ms vs. 52.8 ± 7.9 ms; $P = 0.108$). Also, fat fraction differed not significantly between both groups (4.6 ± 3.5% vs. 3.1 ± 1.9%, $P = 0.153$). All MRI parameters are given in Table 2. A parameter correlation matrix is given in Table 3.

Diagnostic performance of MRI-derived mapping parameters

Analysis of the diagnostic performance of MRI-derived mapping parameters for diagnosing significant fibrosis (≥ F2) was performed. According to the ROC analysis among all mapping parameters, hepatic ECV and native T1 demonstrated the best diagnostic performances with an AUC of 0.858 and 0.711, respectively, which were also comparable ($P = 0.113$). Hepatic ECV provided a sensitivity of 84.2% (95% confidence interval (CI) 62.4–94.5%), and a specificity of 84.6% (CI 57.8–95.7%). Hepatic native T1 provided a sensitivity of 52.6% (CI 31.7–72.7%) and specificity of 100.0% (CI 77.2–100.0%). Diagnostic performance of hepatic ECV was significantly higher when

Table 2 Hepatic MRI characteristics of patients without (< F2) and with significant fibrosis (≥ F2)

Variable	PSC patients without significant fibrosis (< F2, n = 13)	PSC patients with significant fibrosis (≥ F2, n = 19)	*P* value
MRE-derived liver stiffness (kPa)	3.2 ± 0.3	5.4 ± 1.4	< 0.001
Hepatic native T1 relaxation time (ms)	522.8 ± 33.2	559.6 ± 56.3	0.043
Hepatic extracellular volume fraction (%)	26.3 ± 1.9	30.5 ± 4.4	0.003
Hepatic T2 relaxation time (ms)	48.9 ± 3.2	52.8 ± 7.9	0.108
Hepatic T2* relaxation time (ms)	30.6 ± 3.3	32.9 ± 8.4	0.370
Proton density fat fraction	4.6 ± 3.5	3.1 ± 1.9	0.153

Continuous data are means ± standard deviations

Table 3 Correlation matrix for quantitative MRI parameters and clinical fibrosis scores

Variable	Hepatic native T1		Hepatic T2		Hepatic ECV	
	r value	*P* value	r value	*p* value	r value	*p* value
MRE-derived liver stiffness	0.66	< 0.001	0.41	0.021	0.69	< 0.001
FIB-4	0.21	0.276	0.13	0.501	0.46	0.011
APRI	0.20	0.284	0.18	0.352	0.49	0.005
AST/ALT ratio (de-Ritis)	0.21	0.264	0.33	0.077	0.24	0.199
Mayo score	0.37	0.048	0.41	0.026	0.51	0.004

ECV, extracellular volume fraction. MRE, Magnetic resonance elastography, FIB-4, Fibrosis-4-Score; ASL/ALT ratio (de-Ritis), De-Ritis ratio, APRI, aspartate aminotransferase to platelet ratio index

Table 4 Diagnostic performance of different quantitative MRI parameters for and the assessment of liver fibrosis in patients without (< F2) and with significant (≥ F2) fibrosis

Variable	AUC	Cutoff value	Sensitivity (%)	Specificity (%)	PPV (%)	NPV (%)	Accuracy (%)
Hepatic native T1 (ms)	0.711	> 562.7	52.6 (31.7–72.7)	100.0 (77.2–100.0)	100.0 (72.2–100.0)	59.1 (38.7–76.7)	71.9 (54.6–84.4)
Hepatic extracellular volume fraction (%)	0.858	> 27.2	84.2 (62.4–94.5)	84.6 (57.8–95.7)	88.9 (67.2–96.9)	78.6 (52.4–92.4)	84.4 (68.2–93.1)
Hepatic T2 (ms)	0.686	> 52.0	57.9 (36.3–76.9)	92.3 (66.7–98.6)	91.7 (64.6–98.5)	60.0 (38.7–78.1)	71.9 (54.6–84.4)
APRI score	0.787	> 0.41	64.7 (41.3–82.7)	84.6 (57.8–95.7)	84.6 (57.8–95.7)	64.7 (41.3–82.7)	73.3 (55.6–85.8)
FIB-4 score	0.588	> 1.2	35.3 (17.3–58.7)	76.9 (49.7–91.8)	66.7 (35.4–87.9)	47.6 (28.3–67.6)	53.3 (36.1–69.8)
ALT/AST ratio (de-Ritis)	0.570	≤ 0.76	58.8 (36.6–78.4)	69.2 (42.4–87.3)	71.4 (45.4–88.3)	56.3 (33.2–76.9)	63.3 (45.5–78.1)
MELD score	0.680	> 6	52.6 (31.7–72.7)	84.6 (57.8–95.7)	83.3 (55.2–95.3)	55.0 (34.2–74.2)	65.6 (48.3–79.6)

Data in parentheses are 95% confidence interval

PPV, positive predictive value, NPV, negative predictive value, MELD, Score Model of End Stage Liver Disease; APRI, aspartate aminotransferase to platelet ratio index; FIB-4, Fibrosis-4-Score; ASL/ALT ratio (de-Ritis), De-Ritis ratio

compared to the evaluated fibrosis scores FIB-4 and de-Ritis ratio (*P* values: 0.028 and 0.016, respectively) and equal when compared to the APRI and MELD scores (*P* values: 0.523 and 0.123, respectively). Furthermore, in contrast to ECV, diagnostic performance of hepatic native T1 was comparable with that of all evaluated serological fibrosis scores: APRI (0.711 vs. 0.787, $P=0.336$), FIB-4 (0.711 vs. 0.588, $P=0.475$), de-Ritis ratio (0.711 vs. 0.570, $P=0.370$). Hepatic T2 also performed well, however, with diagnostic performance expressed as AUC significantly lower when compared to hepatic ECV (AUC 0.686 vs. 0.858, $P=0.006$) and equal when compared to hepatic native T1 (0.686 vs. 0.711, $P=0.196$). Hepatic T2 provided a sensitivity of 57.9% (CI 36.3–76.9%) and a specificity of 92.3% (CI 66.7–98.6%). All values of diagnostic performance statistics for evaluated laboratory and mapping parameters are presented in Table 4, see also Fig. 2.

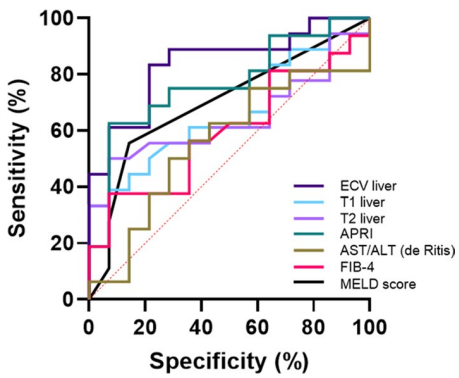

Fig. 2 Graphs show receiver operating characteristic curves of different MRI and laboratory markers for diagnosis of significant fibrosis in patients with primary sclerosing cholangitis (≥ F2). Curves are given for hepatic T1 relaxation times (area under curve [AUC]: 0.711), hepatic ECV (AUC: 0.858), hepatic T2 relaxation times (AUC: 0.686), APRI (AUC: 0.787), FIB-4 score (AUC: 0.588), ALT/AST ratio (de-Ritis) (AUC: 0.570), and MELD score (AUC: 0.680). APRI: AST-to-Platelet Ratio Index, FIB-4 score: Fibrosis-4 score, MELD: Model of End Stage Liver Disease

Discussion

The study aimed to investigate the diagnostic value of different MRI mapping parameters including ECV for the evaluation of liver fibrosis using MRE-derived liver stiffness as a reference standard in PSC patients. The

main findings of the present study are: (1) hepatic ECV and native T1 correlated strong with MRE-derived liver stiffness and, (2) for the diagnosis of significant fibrosis (≥ F2), hepatic ECV and native T1 revealed the highest diagnostic performance in patients with PSC.

According to both, the AASLD and EASL guidelines [5, 6, 33], imaging plays a fundamental role in the management of PSC patients, since it is essential for confirming the diagnosis of PSC in the majority of patients and aids in assessment of disease progression and identification of possible complications and associated diseases, especially cholangiocarcinoma. MRI as a modality of choice for liver parenchyma characterization may possibly replace both invasive procedures and non-specific clinical scores. Another modality, which has proven to be effective in detecting significant fibrosis in patients with PSC is TE. Liver stiffness measurements derived by TE also showed correlations with hepatic ECV in our study. Considering the fact that MRE has proved to be a more accurate method for liver fibrosis assessment in patients with chronic liver disease compared to TE and the fact that TE was not performed in all patients at the time of MRI examination, we chose MRE-derived liver stiffness measurements as the main reference standard in our study [34]. In a previous study including 38 patients with PSC, the authors demonstrated high sensitivity and specificity of apparent diffusion coefficient (ADC) values in the detection of early (75% and 75%, respectively) and advanced (80% and 85%, respectively) liver fibrosis [35]. However, the usefulness of diffusion-weighted imaging for assessment and staging of liver fibrosis is still controversial due to existing limitations in MRI protocols and also standardization and ADC value reproducibility [33, 36]. Another promising MRI technique is relaxometry including ECV calculation. Significant correlations between hepatic T1, T2 as well as ECV with liver fibrosis have been already sufficiently described in the previous studies [17, 20, 21, 37–39]. Liver fibrosis is defined as the accumulation of extracellular matrix proteins produced by fibrogenic cell populations in response to tissue injury. As a consequence, this process leads to extension of extracellular space and increased accumulation of extracellular MRI contrast agent, which is reflected by prolonged T1 relaxation times and increased ECV of liver [21]. However, there is still no sufficient data proving correlations between MRE-derived liver stiffness and mapping parameters in patients with PSC. Using MRE-derived liver stiffness as a reference standard, we found strong correlations between hepatic ECV and liver stiffness ($r = 0.69$, $P < 0.001$) in patients with PSC (see also Fig. 3). Moreover, hepatic ECV showed a high diagnostic performance to diagnose significant fibrosis (F ≥ 2) in patients with PSC (AUC of 0.858). The diagnostic performance of ECV was higher than that of all non-invasive laboratory tests under investigation. One of the most important drawbacks of all laboratory tests and clinical scores is that they are not liver-specific. As a result, fibrotic and inflammatory changes outside of the liver contribute to bias. This is of particular importance in the PSC group where the prevalence of comorbidities is commonly high. In particular, in cases with accompanying diseases, which are typical in patients with PSC. In contrast, quantitative mapping parameters reflect the changes in the liver parenchyma itself. Moreover, one of the main advantages of ECV calculation is that compared to conventional T1 and T2 mapping, ECV is

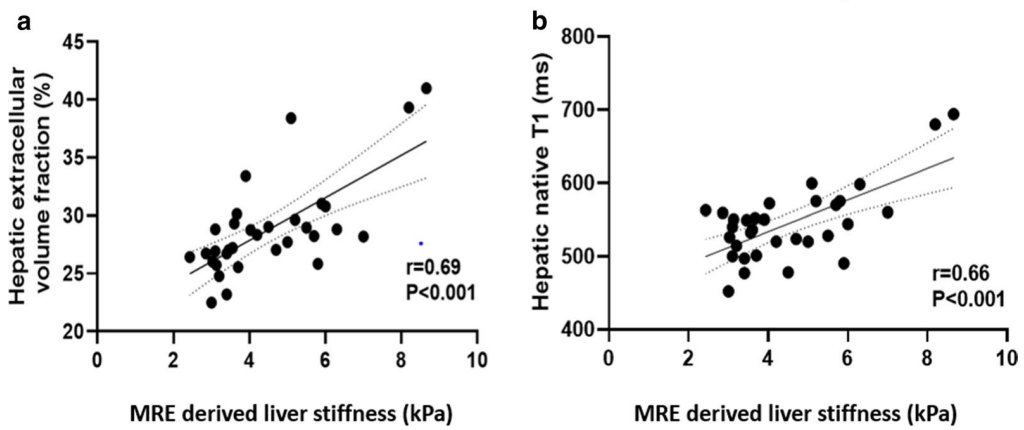

Fig. 3 Scatter plots shows correlations between magnetic resonance elastography (MRE) derived liver stiffness and hepatic extracellular volume fraction (**a**) and hepatic native T1 (**b**). Regression lines are given with 95% confidence intervals

relatively independent of field strength and acquisition parameters, and, thus, can be considered as a physiologically normalized measure.

Native hepatic T1 also demonstrated high diagnostic performance in diagnosing significant fibrosis ($r = 0.66$, $P < 0.001$, see also Fig. 3). For the same reasons as ECV, T1 mapping is more liver specific and reflects the changes in liver parenchyma itself. However, in contrast to ECV, T1 parameters are less sensitive (84.2% vs. 52.6%), which could be explained by the dependency on technical aspects, as mentioned previously, and by heterogeneous nature of hepatic fibrosis in patients with PSC.

Our study has several limitations. The main drawback of our study is the absence of liver biopsy as a "gold standard". Liver biopsy is an invasive procedure, which carries risks of periprocedural complications, and is also limited by sampling error due to disease heterogeneity in PSC. Thus, liver biopsy is no longer performed routinely for PSC and cannot be employed as a reference standard for PSC studies. Thus, we used MRE-derived liver stiffness as a reference standard for liver fibrosis assessment in our study. Another limitation is that we did not obtain full coverage of the liver parenchyma. Only a single transverse section for acquisition of T1 and T2 maps at the level of portal vein bifurcation was performed, which may have missed other significant changes, potentially occurring in other planes. As we additionally excluded the patients with iron overload and/or steatosis, our T1 measurements were not corrected for that. Moreover, similar to MRE, T1 and T2 mapping overestimate the degree of liver fibrosis in patients with inflammation or vascular congestion, highlighting these other factors that might affect T1 and T2 relaxation times. Additionally, the small sample size and the fact that most patients in our study cohort had fibrosis stage F4 might also limit the applicability of our results. Further studies with large patient cohorts using a liver biopsy as the main reference standard as well as other serological fibrosis scores (e.g. enhanced liver fibrosis test) are needed to establish the results of this study and confirm the accuracy and usefulness of MRI mapping in patients with chronic liver disease.

Conclusions

In our observational prospective study, MRI mapping parameters, including ECV calculation showed strong correlations with MRE-derived liver stiffness. Especially, T1 mapping techniques with estimation of ECV have a potential to be a new non-invasive biomarker for assessment and early detection of significant fibrosis in patients with PSC by providing additional information, without adding costs to examination.

Abbreviations

PSC: Primary sclerosing cholangitis; MRI: Magnetic resonance imaging; MRE: Magnetic resonance elastography; ECV: Extracellular volume fraction; AUC: Area under the curve.

Authors' contributions

J.A.L. and N.M. guarantors of integrity of entire study, contributed substantially to data acquisition, analysis, and interpretation; N.M. wrote the main manuscript text and prepared the figures and tables; all authors manuscript drafting or manuscript revision for important intellectual content; all authors approval of final version of submitted manuscript; J.A.L. and N.M. literature research; J.A.L. and N.M. manuscript editing.

Funding

Open Access funding enabled and organized by Projekt DEAL.

Availability of data and materials

The datasets generated and/or analysed during the current study are not publicly available due to privacy and ethical restriction but are available from the corresponding author on reasonable request.

Declarations

Ethics approval and consent to participate

The presented study was approved by the institutional review board of the University of Bonn and hence all methods were performed in compliance with the ethical standards set in the 1964 Declaration of Helsinki as well as its later amendments. Written informed consent was obtained prior to examination from all participants.

Consent for publication

Not applicable.

Competing interests

The authors declare that they have no competing interests.

Author details

[1] Department of Diagnostic and Interventional Radiology, University Hospital Bonn, Venusberg-Campus 1, 53127 Bonn, Germany. [2] Department of Radiology, Kantonsspital Graubünden, Chur, Switzerland. [3] Department of Internal Medicine I, University Hospital Bonn, Venusberg-Campus 1, 53127 Bonn, Germany.

Received: 1 January 2021 Accepted: 24 March 2021
Published online: 07 April 2021

References

1. Weismüller TJ, Trivedi PJ, Bergquist A, Imam M, Lenzen H, Ponsioen CY, et al. Patient age, sex, and inflammatory bowel disease phenotype associate with course of primary sclerosing cholangitis. Gastroenterology. 2017;152(1975–1984):e8. https://doi.org/10.1053/j.gastro.2017.02.038.
2. Hirschfield GM, Karlsen TH, Lindor KD, Adams DH. Primary sclerosing cholangitis. Lancet. 2013;382:1587–99. https://doi.org/10.1016/S0140-6736(13)60096-3.
3. Hildebrand T, Pannicke N, Dechene A, Gotthardt DN, Kirchner G, Reiter FP, et al. Biliary strictures and recurrence after liver transplantation for primary sclerosing cholangitis: a retrospective multicenter analysis. Liver Transpl. 2016;22:42–52. https://doi.org/10.1002/lt.24350.
4. Dyson JK, Beuers U, Jones DEJ, Lohse AW, Hudson M. Primary sclerosing cholangitis. Lancet. 2018;391:2547–59. https://doi.org/10.1016/S0140-6736(18)30300-3.
5. Chapman R, Fevery J, Kalloo A, Nagorney DM, Boberg KM, Shneider B, Gores GJ. Diagnosis and management of primary sclerosing cholangitis. Hepatology. 2010;51:660–78. https://doi.org/10.1002/hep.23294.
6. EASL Clinical Practice Guidelines. management of cholestatic liver diseases. J Hepatol. 2009;51:237–67. https://doi.org/10.1016/j.jhep.2009.04.009.

7. Ruiz A, Lemoinne S, Carrat F, Corpechot C, Chazouillères O, Arrivé L. Radiologic course of primary sclerosing cholangitis: assessment by three-dimensional magnetic resonance cholangiography and predictive features of progression. Hepatology. 2014;59:242–50. https://doi.org/10.1002/hep.26620.
8. Cazzagon N, Lemoinne S, El Mouhadi S, Trivedi PJ, Gaouar F, Kemgang A, et al. The complementary value of magnetic resonance imaging and vibration-controlled transient elastography for risk stratification in primary sclerosing cholangitis. Am J Gastroenterol. 2019;114:1878–85. https://doi.org/10.14309/ajg.0000000000000461.
9. Faria SC, Ganesan K, Mwangi I, Shiehmorteza M, Viamonte B, Mazhar S, et al. MR imaging of liver fibrosis: current state of the art. Radiographics. 2009;29:1615–35. https://doi.org/10.1148/rg.296095512.
10. Jhaveri KS, Hosseini-Nik H, Sadoughi N, Janssen H, Feld JJ, Fischer S, et al. The development and validation of magnetic resonance elastography for fibrosis staging in primary sclerosing cholangitis. Eur Radiol. 2019;29:1039–47. https://doi.org/10.1007/s00330-018-5619-4.
11. Hoodeshenas S, Welle CL, Navin PJ, Dzyubak B, Eaton JE, Ehman RL, Venkatesh SK. Magnetic resonance elastography in primary sclerosing cholangitis: interobserver agreement for liver stiffness measurement with manual and automated methods. Acad Radiol. 2019;26:1625–32. https://doi.org/10.1016/j.acra.2019.02.004.
12. Hoodeshenas S, Yin M, Venkatesh SK. Magnetic resonance elastography of liver: current update. Top Magn Reson Imaging. 2018;27:319–33. https://doi.org/10.1097/RMR.0000000000000177.
13. Eaton JE, Dzyubak B, Venkatesh SK, Smyrk TC, Gores GJ, Ehman RL, et al. Performance of magnetic resonance elastography in primary sclerosing cholangitis. J Gastroenterol Hepatol. 2016;31:1184–90. https://doi.org/10.1111/jgh.13263.
14. Radenkovic D, Weingärtner S, Ricketts L, Moon JC, Captur G. T1 mapping in cardiac MRI. Heart Fail Rev. 2017;22:415–30. https://doi.org/10.1007/s10741-017-9627-2.
15. Li Z, Sun J, Hu X, Huang N, Han G, Chen L, et al. Assessment of liver fibrosis by variable flip angle T1 mapping at 3.0T. J Magn Reson Imaging. 2016;43:698–703. https://doi.org/10.1002/jmri.25030.
16. Guimaraes AR, Siqueira L, Uppal R, Alford J, Fuchs BC, Yamada S, et al. T2 relaxation time is related to liver fibrosis severity. Quant Imaging Med Surg. 2016;6:103–14. https://doi.org/10.21037/qims.2016.03.02.
17. Luetkens JA, Klein S, Träber F, Schmeel FC, Sprinkart AM, Kuetting DLR, et al. Quantification of liver fibrosis at T1 and T2 mapping with extracellular volume fraction MRI: preclinical results. Radiology. 2018;288:748–54. https://doi.org/10.1148/radiol.2018180051.
18. Moon JC, Messroghli DR, Kellman P, Piechnik SK, Robson MD, Ugander M, et al. Myocardial T1 mapping and extracellular volume quantification: a society for cardiovascular magnetic resonance (SCMR) and CMR Working Group of the European Society of Cardiology consensus statement. J Cardiovasc Magn Reson. 2013;15:92. https://doi.org/10.1186/1532-429X-15-92.
19. Flett AS, Hayward MP, Ashworth MT, Hansen MS, Taylor AM, Elliott PM, et al. Equilibrium contrast cardiovascular magnetic resonance for the measurement of diffuse myocardial fibrosis: preliminary validation in humans. Circulation. 2010;122:138–44. https://doi.org/10.1161/CIRCULATIONAHA.109.930636.
20. Mesropyan N, Kupczyk P, Dold L, Weismüller TJ, Sprinkart AM, Mädler B, et al. Non-invasive assessment of liver fibrosis in autoimmune hepatitis: Diagnostic value of liver magnetic resonance parametric mapping including extracellular volume fraction. Abdom Radiol (NY). 2020. https://doi.org/10.1007/s00261-020-02822-x.
21. Mesropyan N, Isaak A, Faron A, Praktiknjo M, Jansen C, Kuetting D, et al. Magnetic resonance parametric mapping of the spleen for non-invasive assessment of portal hypertension. Eur Radiol. 2020. https://doi.org/10.1007/s00330-020-07080-5.
22. Wang H-Q, Jin K-P, Zeng M-S, Chen C-Z, Rao S-X, Ji Y, et al. Assessing liver fibrosis in chronic hepatitis B using MR extracellular volume measurements: comparison with serum fibrosis indices. Magn Reson Imaging. 2019;59:39–45. https://doi.org/10.1016/j.mri.2019.03.002.
23. Luetkens JA, Klein S, Traeber F, Schmeel FC, Sprinkart AM, Kuetting DLR, et al. Quantitative liver MRI including extracellular volume fraction for non-invasive quantification of liver fibrosis: a prospective proof-of-concept study. Gut. 2018;67:593–4. https://doi.org/10.1136/gutjnl-2017-314561.
24. Corpechot C, Gaouar F, El Naggar A, Kemgang A, Wendum D, Poupon R, et al. Baseline values and changes in liver stiffness measured by transient elastography are associated with severity of fibrosis and outcomes of patients with primary sclerosing cholangitis. Gastroenterology. 2014;146:970–9; quiz e15–6. https://doi.org/10.1053/j.gastro.2013.12.030.
25. Imperiale TF, Born LJ. Clinical utility of the AST/ALT ratio in chronic hepatitis C. Am J Gastroenterol. 2001;96:919–20. https://doi.org/10.1111/j.1572-0241.2001.03647.x.
26. Sterling RK, Lissen E, Clumeck N, Sola R, Correa MC, Montaner J, et al. Development of a simple noninvasive index to predict significant fibrosis in patients with HIV/HCV coinfection. Hepatology. 2006;43:1317–25. https://doi.org/10.1002/hep.21178.
27. Li J, Gordon SC, Rupp LB, Zhang T, Boscarino JA, Vijayadeva V, et al. The validity of serum markers for fibrosis staging in chronic hepatitis B and C. J Viral Hepat. 2014;21:930–7. https://doi.org/10.1111/jvh.12224.
28. Messroghli DR, Radjenovic A, Kozerke S, Higgins DM, Sivananthan MU, Ridgway JP. Modified look-locker inversion recovery (MOLLI) for high-resolution T1 mapping of the heart. Magn Reson Med. 2004;52:141–6. https://doi.org/10.1002/mrm.20110.
29. Sprinkart AM, Luetkens JA, Träber F, Doerner J, Gieseke J, Schnackenburg B, et al. Gradient Spin Echo (GraSE) imaging for fast myocardial T2 mapping. J Cardiovasc Magn Reson. 2015;17:12. https://doi.org/10.1186/s12968-015-0127-z.
30. Schelbert EB, Messroghli DR. State of the art: clinical applications of cardiac T1 mapping. Radiology. 2016;278:658–76. https://doi.org/10.1148/radiol.2016141802.
31. Singh S, Venkatesh SK, Wang Z, Miller FH, Motosugi U, Low RN, et al. Diagnostic performance of magnetic resonance elastography in staging liver fibrosis: a systematic review and meta-analysis of individual participant data. Clin Gastroenterol Hepatol. 2015;13(440–451):e6. https://doi.org/10.1016/j.cgh.2014.09.046.
32. DeLong ER, DeLong DM, Clarke-Pearson DL. Comparing the areas under two or more correlated receiver operating characteristic curves: a nonparametric approach. Biometrics. 1988;44:837–45.
33. Khoshpouri P, Habibabadi RR, Hazhirkarzar B, Ameli S, Ghadimi M, Ghasabeh MA, et al. Imaging features of primary sclerosing cholangitis: from diagnosis to liver transplant follow-up. Radiographics. 2019;39:1938–64. https://doi.org/10.1148/rg.2019180213.
34. Kennedy P, Wagner M, Castéra L, Hong CW, Johnson CL, Sirlin CB, Taouli B. Quantitative elastography methods in liver disease: current evidence and future directions. Radiology. 2018;286:738–63. https://doi.org/10.1148/radiol.2018170601.
35. Kovač JD, Ješić R, Stanisavljević D, Kovač B, Maksimovic R. MR imaging of primary sclerosing cholangitis: additional value of diffusion-weighted imaging and ADC measurement. Acta Radiol. 2013;54:242–8. https://doi.org/10.1177/0284185112471792.
36. Tokgöz Ö, Unal I, Turgut GG, Yildiz S. The value of liver and spleen ADC measurements in the diagnosis and follow up of hepatic fibrosis in chronic liver disease. Acta Clin Belg. 2014;69:426–32. https://doi.org/10.1179/2295333714Y.0000000062.
37. Müller A, Hochrath K, Stroeder J, Hittatiya K, Schneider G, Lammert F, et al. Effects of liver fibrosis progression on tissue relaxation times in different mouse models assessed by ultrahigh field magnetic resonance imaging. Biomed Res Int. 2017;2017:8720367. https://doi.org/10.1155/2017/8720367.
38. McDonald N, Eddowes PJ, Hodson J, Semple SIK, Davies NP, Kelly CJ, et al. Multiparametric magnetic resonance imaging for quantitation of liver disease: a two-centre cross-sectional observational study. Sci Rep. 2018;8:9189. https://doi.org/10.1038/s41598-018-27560-5.
39. Hoy AM, McDonald N, Lennen RJ, Milanesi M, Herlihy AH, Kendall TJ, et al. Non-invasive assessment of liver disease in rats using multiparametric magnetic resonance imaging: a feasibility study. Biol Open. 2018. https://doi.org/10.1242/bio.033910.

Publisher's Note

3.3 Extracellular volume fraction for the assessment of liver cirrhosis severity. *Scientific Reports 2022*

"*Assessment of liver cirrhosis severity with extracellular volume fraction MRI"*
Mesropyan N*, Kupczyk P*, Dold L, Praktiknjo M, Chang J, Isaak A, Endler C, Kravchenko D, Bischoff LM, Sprinkart AM, Pieper CC, Kuetting D, Jansen C, Attenberger UI, Luetkens JA.
Published in *Scientific Reports* 2022 Jun 12(1):9422

Purpose -The aim of this study was to investigate the diagnostic utility of MRI extracellular volume fraction (ECV) for the assessment of liver cirrhosis severity as defined by Child–Pugh class.

Methods - In this retrospective study, 90 patients (68 cirrhotic patients and 22 controls), who underwent multiparametric liver MRI, were identified. Hepatic T1 relaxation times and ECV were assessed. Clinical scores of liver disease severity were calculated. One-way analysis of variance (ANOVA) followed by Tukey's multiple comparison test, Spearman's correlation coefficient, and receiver operating characteristic (ROC) analysis were used for statistical analysis.

Results -In cirrhotic patients, hepatic native T1 increased depending on Child–Pugh class (620.5 ± 78.9 ms (Child A) vs. 666.6 ± 73.4 ms (Child B) vs. 828.4 ± 91.2 ms (Child C), $P < 0.001$). ECV was higher in cirrhotic patients compared to the controls (40.1 ± 11.9% vs. 25.9 ± 4.5%, $P < 0.001$) and increased depending on Child–Pugh class (33.3 ± 6.0% (Child A) vs. 39.6 ± 4.9% (Child B) vs. 52.8 ± 1.2% (Child C), $P < 0.001$). ECV correlated with Child–Pugh score ($r = 0.64$, $P < 0.001$). ECV allowed differentiating between Child–Pugh classes A and B, and B and C with an AUC of 0.785 and 0.944 ($P < 0.001$, respectively). The diagnostic performance of ECV for differentiating between Child–Pugh classes A and B, and B and C was higher compared to hepatic native T1 (AUC: 0.651 and 0.910) and MELD score (AUC: 0.740 and 0.795) ($P < 0.05$, respectively).

Conclusions - MRI-derived ECV correlated with Child–Pugh score and had a high diagnostic performance for the discrimination of different Child–Pugh classes. ECV might become a valuable non-invasive biomarker for the assessment of liver cirrhosis severity.

scientific reports

Check for updates

OPEN

Assessment of liver cirrhosis severity with extracellular volume fraction MRI

Narine Mesropyan[1,3], Patrick A. Kupczyk[1,3], Leona Dold[2], Michael Praktiknjo[2], Johannes Chang[2], Alexander Isaak[1], Christoph Endler[1], Dmitrij Kravchenko[1], Leon M. Bischoff[1], Alois M. Sprinkart[1], Claus C. Pieper[1], Daniel Kuetting[1], Christian Jansen[2], Ulrike I. Attenberger[1] & Julian A. Luetkens[1]✉

We aimed to investigate the diagnostic utility of MRI extracellular volume fraction (ECV) for the assessment of liver cirrhosis severity as defined by Child–Pugh class. In this retrospective study, 90 patients (68 cirrhotic patients and 22 controls), who underwent multiparametric liver MRI, were identified. Hepatic T1 relaxation times and ECV were assessed. Clinical scores of liver disease severity were calculated. One-way analysis of variance (ANOVA) followed by Tukey's multiple comparison test, Spearman's correlation coefficient, and receiver operating characteristic (ROC) analysis were used for statistical analysis. In cirrhotic patients, hepatic native T1 increased depending on Child–Pugh class (620.5 ± 78.9 ms (Child A) vs. 666.6 ± 73.4 ms (Child B) vs. 828.4 ± 91.2 ms (Child C), $P < 0.001$). ECV was higher in cirrhotic patients compared to the controls (40.1 ± 11.9% vs. 25.9 ± 4.5%, $P < 0.001$) and increased depending of Child–Pugh class (33.3 ± 6.0% (Child A) vs. 39.6 ± 4.9% (Child B) vs. 52.8 ± 1.2% (Child C), $P < 0.001$). ECV correlated with Child–Pugh score ($r = 0.64$, $P < 0.001$). ECV allowed differentiating between Child–Pugh classes A and B, and B and C with an AUC of 0.785 and 0.944 ($P < 0.001$, respectively). The diagnostic performance of ECV for differentiating between Child–Pugh classes A and B, and B and C was higher compared to hepatic native T1 (AUC: 0.651 and 0.910) and MELD score (AUC: 0.740 and 0.795) ($P < 0.05$, respectively). MRI-derived ECV correlated with Child–Pugh score and had a high diagnostic performance for the discrimination of different Child–Pugh classes. ECV might become a valuable non-invasive biomarker for the assessment of liver cirrhosis severity.

Although the burden and underlying causes of chronic liver disease (CLD) and cirrhosis vary worldwide, they are—with an increasing incidence—a major cause of morbidity and mortality[1–3]. Regardless of the pattern and underlying etiology, liver cirrhosis is characterized by severe scarring of the liver tissue with collagen deposition, architecture distortion and failed function, and is related to life-threatening complications such as portal hypertension, spontaneous bacterial peritonitis, ascites, variceal bleeding, hepatic encephalopathy, and hepatorenal syndrome. Outcome prediction of cirrhotic patients, who undergo surgery/interventions as well as overall mortality risk estimation are of great clinical importance. Therefore, different scores for the assessment of short- or long-term mortality, also for a specific etiology of chronic liver disease have been developed and proposed (e.g., MELD score or CLIF-C ACLF score). One of the most validated and widely used scoring systems, however, the Child–Pugh score, is simple to calculate and suitable for various etiologies of liver disease[4]. For instance, patients with a Child–Pugh A class have a generally good prognosis, and are considered for elective surgery. Patients with a Child–Pugh B class have an increased risk and commonly have to undergo medical optimization before surgery. For patients with a Child–Pugh C class elective surgery is contraindicated, as they have a mortality risk up to 82%[4–6].

Imaging plays an important role for prognosis estimation and complication assessment in patients with CLD and cirrhosis. In this regard, magnetic resonance imaging (MRI) has experienced a steady evolution and is considered today the clinical standard in patients with CLD and cirrhosis, mainly for malignancy exclusion.

[1]Department of Diagnostic and Interventional Radiology and Quantitative Imaging Lab Bonn (QILaB), University Hospital Bonn, Venusberg-Campus 1, 53127 Bonn, Germany. [2]Department of Internal Medicine I and Center for Cirrhosis and Portal Hypertension Bonn (CCB), University Hospital Bonn, Venusberg-Campus 1, 53127 Bonn, Germany. [3]These authors contributed equally: Narine Mesropyan and Patrick A. Kupczyk. ✉email: julian.luetkens@ukbonn.de

Furthermore, current state-of-the art MRI techniques allow not only for morphological liver parenchyma assessment, but also for the assessment of liver function. Particularly, several MRI techniques such as diffusion-weighted imaging (DWI), as well as contrast-enhanced MRI have already been described in previous studies[7–11]. Another promising technique is quantitative T1 mapping with calculation of the extracellular volume fraction (ECV). The ability of T1 mapping with ECV calculation in liver fibrosis assessment has already been sufficiently described in patients with CLD of different etiologies as well as in animal models[12–16]. However, to our knowledge, the ability of MRI-derived ECV to assess liver cirrhosis severity has not been under investigation yet. The implementation of new non-invasive imaging-based biomarkers, which allows for comprehensive liver assessment beyond morphology (e.g., fibrosis quantification and possibly also liver function) and, at the same time, reproducible and simple to estimate, are highly desirable.

Therefore, the aim of this study was to investigate the diagnostic utility of MRI-derived ECV for the assessment of cirrhosis severity as well as to differentiate between different Child–Pugh classes in patients with CLD of various etiologies.

Materials and methods

This retrospective study was approved by the local institutional review board that waived informed consent. Between January 2019 and September 2020 patients with confirmed diagnosis of liver cirrhosis, who underwent multiparametric liver MRI, were identified. The diagnosis of liver cirrhosis was established based on previous medical history, clinical examinations, liver biopsy as well as imaging according to the current guidelines[17]. Additionally, all patients with liver cirrhosis were categorized into three groups based on Child–Pugh classes of cirrhosis severity: A, B and C. Child–Pugh classes were calculated as a sum of individual points of clinical and laboratory criteria as previously published[18]. For patients with cholestatic liver disease, a modified Child–Pugh score was used. Patients with no history of chronic liver disease, who underwent clinical MRI examinations, were also enrolled into this study as a control group. The absence of chronic liver disease was based on previous medical history, clinical and laboratory tests. Exclusion criteria were contraindications to contrast-enhanced MRI and insufficient imaging quality. Laboratory markers were retrieved from the patients´ charts. Model of End-Stage Liver Disease (MELD) was also calculated.

Magnetic resonance imaging. All MRI examinations were conducted on a clinical whole-body 1.5 Tesla MR-system (Ingenia, Philips Healthcare). A 32-channel body coil with digital interface was used for signal reception. Besides morphological sequences, hepatic T1 mapping before and 10 min after contrast media application was performed in the same slice position in end-expiration[19]. For T1 mapping, a heart rate independent 10-(2)-7-(2)-5-(2)-3-(2) modified Look-Locker inversion recovery (MOLLI) acquisition scheme with internal triggering was applied. Technical parameters were as follows: TR/TE 1.92/0.84 ms, FA 20°, parallel imaging factor 2, acquired voxel size $1.98 \times 2.45 \times 10.00$ mm^3, reconstructed voxel size $1.13 \times 1.13 \times 100.00$ mm^3, scan duration/breath hold 14 s. A gadolinium-based extracellular contrast agent in a dose of 1.0 mmol/ml solution with 0.1 mmol per kilogram of body weight (gadobutrol, Gadovist, Bayer Healthcare Pharmaceuticals) was administered as a single bolus with an injection rate of 1.5 ml/s.

Image analysis. Image analysis was performed in consensus by two board-certified radiologists with 9 (J.A.L.) and 10 (P.K.) years of experience in abdominal radiology. The radiologists were blinded to the clinical data. The mean relaxation time of at least three representative regions of interest (ROI) drawn centrally in the right and left lobe at the level of portal vein bifurcation was used for the final analysis as previously described[13,14]. T1 values of the blood pool were obtained from the abdominal aorta from the same level. Calculation of ECV was performed with ROI-based values using following equation[20]: $ECV = (1 - \text{hematocrit}) \times (\Delta R1_{liver}/\Delta R1_{blood})$, where R1 = 1/T1. Hematocrit was retrieved at the same day of MRI.

Statistical analysis. Prism 8 (GraphPad Software) and SPSS Statistics (Version 25, IBM) were used for statistical analysis. Data were checked for normal distribution using the Shapiro–Wilk test. Data are given as mean ± standard deviation or absolute frequencies, as appropriate. Spearman's correlation coefficient was used for a correlation analysis. One-way analysis of variance (ANOVA) followed by Tukey´s multiple comparison tests was performed to compare variables between groups of patients with liver cirrhosis of different Child–Pugh classes and control subjects. Dichotomous variables were compared by using the χ^2 test. Receiver operating analysis (ROC) was used to determine the cut-offs with the highest combined sensitivity and specificity, positive predictive values (PPV), negative predictive values (NPV) and accuracy to differentiate between Child–Pugh classes A and B as well as Child–Pugh classes B and C. The level of statistical significance was set to $P < 0.05$.

Ethical approval and informed consent. The presented study was approved by the institutional review board of the University of Bonn and hence all methods were performed in compliance with the ethical standards set in the 1964 Declaration of Helsinki as well as its later amendments. The requirement for written informed consent was waived by the institutional review board of the University of Bonn.

Results

Cohort characteristics. Sixty-eight patients (mean age: 55 ± 13 years; body mass index: 24.3 ± 3.8 kg/m^2; 27 female) with liver cirrhosis were analyzed. N = 27 (39.7%), n = 32 (47.1%), and n = 9 (13.2%) of patients with liver cirrhosis had Child–Pugh class A, B and C, respectively. The etiologies of CLD and cirrhosis in the whole study cohort were as follows: alcoholic liver disease (n = 26, 38.2%); autoimmune liver diseases, including autoimmune

Variable	Controls (n = 22)	Child–Pugh A (n = 27)	Child–Pugh B (n = 32)	Child–Pugh C (n = 9)	*P* value
Clinical parameters					
Age (years)	44.7 ± 16.3†	48.4 ± 13.5†	60.6 ± 9.7*‡	57.9 ± 13.1	< 0.001
Body mass index (kg/m^2)	25.6 ± 5.0	24.7 ± 2.9	23.6 ± 3.9	25.7 ± 5.4	0.271
Sex					0.102
Male	14 (64%)	18 (67%)	18 (56%)	5 (56%)	
Female	8 (36%)	9 (33%)	14 (44%)	4 (44%)	
Underlying liver disease					**0.005**
Autoimmune liver disease	0 (0%)	10 (37%)	5 (16%)	1 (11%)	
Alcoholic liver disease	0 (0%)	5 (18%)	17 (53%)	4 (44%)	
Viral hepatitis	0 (0%)	4 (15%)	4 (12%)	0 (0%)	
Non-alcoholic fatty liver disease	0 (0%)	0 (0%)	1 (3%)	2 (22%)	
Unknown	0 (0%)	7 (26%)	5 (16%)	2 (22%)	
Budd-Chiari syndrome	0 (0%)	1 (4%)	0 (0%)	0 (0%)	
Laboratory parameters					
Blood hematocrit level (%)	41.6 ± 3.9$^{\dagger\|}$	37.9 ± 0.7$^{\dagger\|}$	30.7 ± 0.5*‡	27.6 ± 0.8*‡	< 0.001
Bilirubin (mg/dl)	0.78 ± 0.51$^{\dagger\|}$	1.02 ± 0.49$^{\|}$	1.89 ± 2.64*	2.97 ± 2.25*‡	< 0.001
ALT (U/l)	35.0 ± 11.2	49.1 ± 40.4	35.8 ± 26.9	31.6 ± 15.9	0.276
AST (U/l)	27.9 ± 15.4$^{\ddagger\dagger\|}$	62.6 ± 44.7*	65.7 ± 41.3*	60.6 ± 9.7*	< 0.001
GGT (U/l)	33.5 ± 19.0$^{\ddagger\dagger\|}$	198.2 ± 184.9*	178.5 ± 252.9*	148.7 ± 145.7*	< 0.001
AP (U/l)	50.5 ± 21.5$^{\ddagger\dagger\|}$	161.6 ± 118.3*	161.0 ± 182.1*	166.0 ± 99.6*	< 0.001
Albumin (g/l)	49.2 ± 19.2	40.7 ± 5.9$^{\dagger\|}$	30.3 ± 9.7‡	26.8 ± 11.6‡	< 0.001
Platelets cells × 10^9/l	282.7 ± 107.2$^{\ddagger\dagger\|}$	174.9 ± 107.7*	151.4 ± 108.1*	113.0 ± 67.2*	< 0.001
International normalized ratio	1.03 ± 0.12$^{\dagger\|}$	1.12 ± 0.12$^{\|}$	1.2 ± 0.2*	1.54 ± 0.64*‡	< 0.001
Creatinine (mg/dl)	0.86 ± 1.18$^{\|}$	1.07 ± 0.95$^{\|}$	1.13 ± 0.54	1.5 ± 0.6*‡	0.019
C-reactive protein level (mg/l)	1.4 ± 1.6$^{\ddagger\dagger\|}$	7.3 ± 7.6*	12.6 ± 14.5*	15.3 ± 11.4*	< 0.001
MELD	6.3 ± 0.7$^{\ddagger\dagger\|}$	9.3 ± 4.1$^{*\dagger\|}$	11.9 ± 4.2*‡	17.9 ± 6.1*‡	< 0.001
FIB-4	0.73 ± 0.47$^{\ddagger\dagger\|}$	3.51 ± 3.68*†	6.15 ± 4.06*‡	6.53 ± 2.08*	< 0.001
APRI	0.22 ± 0.07$^{\ddagger\dagger\|}$	1.18 ± 1.28*	1.36 ± 1.01*	1.56 ± 0.64*	< 0.001
MRI parameters					
Hepatic native T1 relaxation time (ms)	518.6 ± 47.9$^{\ddagger\dagger\|}$	620.5 ± 78.9$^{*\|}$	666.6 ± 73.4$^{*\|}$	828.4 ± 91.2*‡†	< 0.001
Extracellular volume fraction (%)	25.9 ± 4.5$^{\ddagger\dagger\|}$	33.3 ± 6.0$^{*\dagger\|}$	39.6 ± 4.9$^{*\ddagger\|}$	52.8 ± 1.2*‡†	< 0.001

Table 1. Clinical, laboratory and quantitative magnetic resonance imaging (MRI) parameters of control subjects and patients with liver cirrhosis of different Child–Pugh classes. Continuous variables are given as means ± standard deviations. Nominal data are absolute frequencies with percentages in parentheses. *P* values were obtained using ANOVA test followed by Turkey's multiple comparison test. *MELD* score model of end-stage liver disease, *ALT* alanine aminotransferase, *AST* aspartate aminotransferase, *AP* alkaline phosphatase, *GGT* gamma-glutamyltransferase, *APRI* aspartate aminotransferase to platelet ratio index, *FIB-4* fibrosis-4-score. $^{*}P < 0.05$ versus controls. $^{\ddagger}P < 0.05$ versus Child–Pugh A. $^{\dagger}P < 0.05$ versus Child–Pugh B. $^{\|}P < 0.05$ versus Child–Pugh C.

hepatitis, primary sclerosing cholangitis, overlap syndromes, and primary biliary cirrhosis (n = 16, 23.5%); viral hepatitis (n = 8, 11.8%); non-alcoholic fatty liver disease (n = 3, 4.4%), and other unknown and/or rare etiologies (n = 15, 22.1%). Twenty-two patients (mean age: 46 ± 16 years ; body mass index: 25.6 ± 5.0 kg/m^2; 8 female) without history of chronic liver disease, who had normal liver function tests were included as control subjects. The group of patients consisted of patients with clinical indications for liver MRI such as non-specific abdominal pain (9/22, 41%) and benign liver lesion characterization/follow-up (13/22, 59%). Clinical scores for the assessment of liver fibrosis and disease severity differed significantly between control subjects and patients with liver cirrhosis of all Child–Pugh classes (e.g., MELD score: 6.3 ± 0.7 in control subjects vs. 11.5 ± 4.9 in cirrhotic patients, $P < 0.001$). Detailed clinical characteristics of patients with liver cirrhosis and control subjects are given in Table 1.

MRI results. Hepatic T1 relaxation times were significantly higher in cirrhotic patients than in control subjects (518.6 ± 47.9 ms) and also increased depending on Child–Pugh class: 620.5 ± 78.9 ms (Child–Pugh A) vs. 666.6 ± 74.3 ms (Child–Pugh B) vs. 828.4 ± 91.2 ms (Child–Pugh C) ($P < 0.001$). Hepatic ECV values were also significantly higher in cirrhotic patients compared to control subjects (25.9 ± 4.5%) and increased depending on Child–Pugh class: 33.3 ± 6.0% (Child–Pugh A) vs. 39.6 ± 4.9% (Child–Pugh B) vs. 52.8 ± 1.2% (Child–Pugh

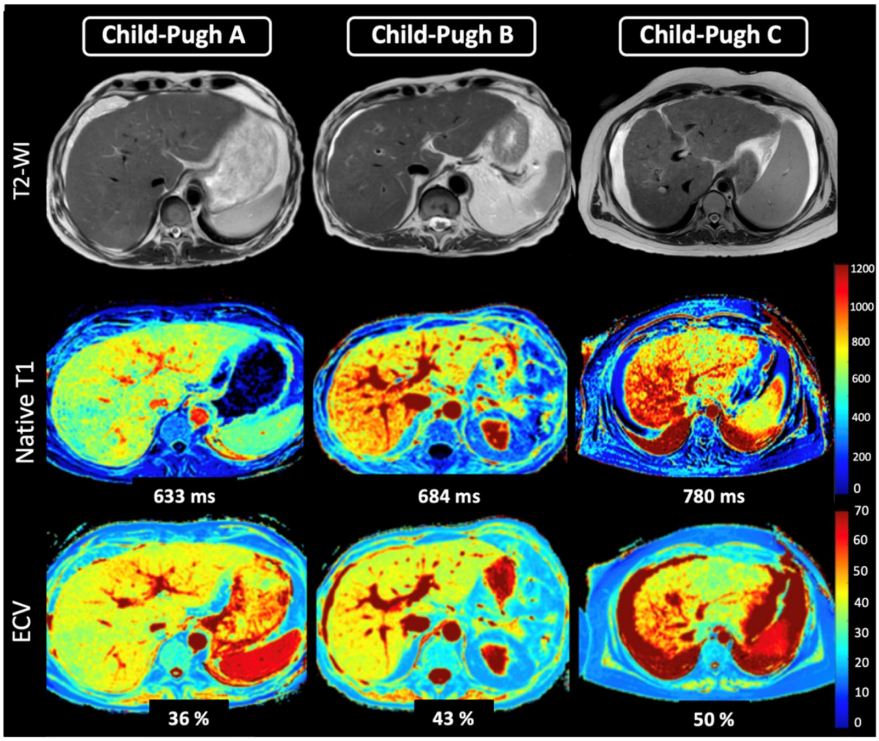

Figure 1. Representative images of T2-weighted images, hepatic native T1 and extracellular volume fraction (ECV) maps from a 54-years-old male patient with liver cirrhosis Child–Pugh class A, from a 61-year-old female patient with Child–Pugh class B, and a 41-year-old female patient with Child–Pugh class C. T1 relaxation times and ECV show increased values depending on Child–Pugh class. *T2-WI* T2-weighted image, *ECV* extracellular volume fraction.

C) ($P<0.001$). There were also significant differences in hepatic ECV between patients with liver cirrhosis of different Child–Pugh classes: Child–Pugh A vs. B (33.3 ± 6.0% vs. 39.6 ± 4.9%, $P<0.001$), A vs. C (33.3 ± 6.0% vs. 52.8 ± 1.2%, $P<0.001$), and B vs. C (39.6 ± 4.9% vs. 52.8 ± 1.2%, $P<0.001$) (see also Fig. 1). Hepatic MRI parameters of all included patients are given in Table 1, see also Fig. 2. According to correlation analysis, hepatic native T1 ($r=0.45$, $P<0.001$) and ECV ($r=0.64$, $P<0.001$) correlated with Child–Pugh score. A correlation matrix is given in Fig. 3.

Diagnostic performance of MRI-derived mapping parameters. MRI-derived mapping parameters, as well as clinical scores of liver disease severity, were evaluated regarding their diagnostic performance to discriminate between different Child–Pugh classes. In general, the diagnostic performance of mapping parameters and MELD score were higher in discriminating between Child–Pugh classes B and C, than between Child–Pugh classes A and B (see also Tables 2, 3, and Fig. 4). Hepatic ECV revealed the highest diagnostic performance for differentiation between Child–Pugh classes A and B, as well as B and C, with an AUC of 0.785 (cutoff value: > 36.2%, sensitivity of 86.2%, specificity of 55.6%) and 0.944 (cutoff value: > 46.9%, sensitivity of 88.9%, specificity of 90%), respectively. The diagnostic performance of hepatic native T1 relaxation times was lower than that of ECV for differentiating between Child–Pugh scores A and B as well as between Child–Pugh score B and C with an AUC of 0.651 (cutoff: > 620.3 ms, sensitivity of 86.2%, specificity of 55.6%) and 0.910 (cutoff: > 722 ms, sensitivity of 100%, specificity of 82.8%) ($P<0.05$, respectively). Furthermore, the diagnostic performance of native hepatic T1 relaxation times was higher than that of MELD score in differentiating between Child–Pugh classes B and C (0.910 vs. 0.795), but lower than that of MELD in differentiating between classes Child–Pugh A and B (0.651 vs. 0.740) ($P<0.05$, respectively). Detailed parameters of diagnostic performance statistics are given in Tables 2 and 3.

Discussion

The aim of this study was to evaluate the diagnostic utility of MRI-derived hepatic ECV for the assessment of cirrhosis severity as well discrimination of different Child–Pugh classes in patients with liver cirrhosis of various etiologies. The main findings of our study are: (1) hepatic native T1, as well as MRI-derived ECV, showed

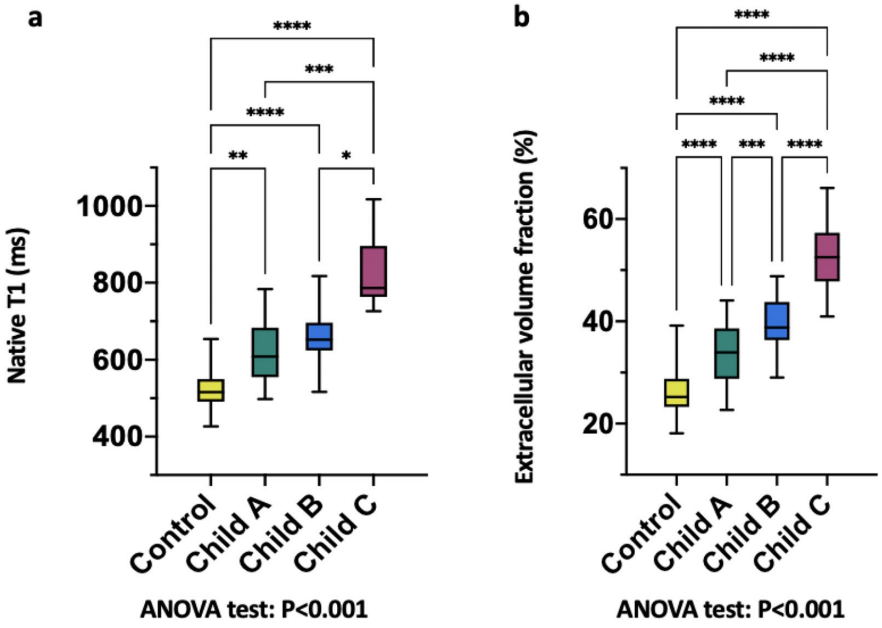

Figure 2. Column graphs with values distribution of hepatic native T1 (**a**) and MRI-derived extracellular volume fraction (**b**) in the control group and in the clinically subclassified cirrhosis groups (Child–Pugh classes A, B, and C). Mean of data is represented by horizontal line. *, **, ***, **** represents significance levels of pairwise comparisons with *P* values of ≤ 0.05, ≤ 0.01, ≤ 0.001, ≤ 0.0001 respectively. *P* values were obtained using ANOVA test followed by Turkey's multiple comparison test.

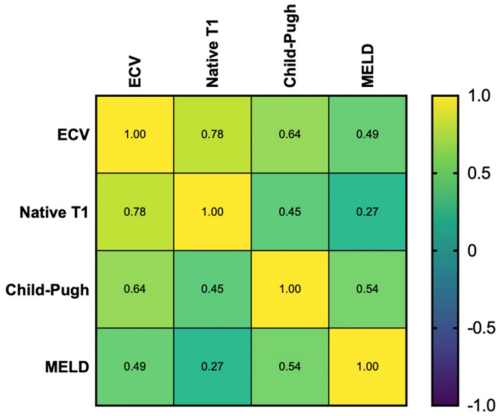

P values	Hepatic native T1	MRI-derived ECV
Child-Pugh	<0.001	<0.001
MELD	0.031	<0.001

Figure 3. Heatmap shows correlations between hepatic native T1 and MRI-derived extracellular volume fraction (ECV) and clinical scores of liver disease severity. *ECV* extracellular volume fraction, *MELD* model for end-stage liver disease.

	AUC	Cutoff value	Sensitivity (%)	Specificity (%)	PPV (%)	NPV (%)	Accuracy (%)
Native T1	0.651	> 620.3 ms	86.2 (69.4–94.5)	55.6 (37.3–72.4)	67.6 (51.5–80.4)	78.9 (56.7–91.5)	71.4 (58.5–81.6)
ECV	0.785	> 36.18%	80.6 (63.7–90.8)	68.0 (48.4–82.8)	75.8 (59.0–87.2)	73.9 (53.5–87.5)	75.0 (62.3–84.5)
MELD score	0.740	> 8.5	75.0 (57.9–86.7)	59.3 (40.7–75.5)	68.6 (55.1–78.3)	66.7 (46.7–82.0)	67.8 (55.1–78.3)
APRI score	0.618	> 0.786	68.8 (51.4–82.0)	51.9 (34.0–69.3)	62.9 (46.3–76.8)	58.3 (38.8–75.5)	61.0 (48.3–72.4)
FIB-4 score	0.760	> 3.242	84.4 (68.2–93.1)	63.0 (44.2–78.5)	73.0 (57.0–84.6)	77.3 (56.6–89.9)	74.6 (62.2–83.9)

Table 2. Diagnostic performance of hepatic native T1 and MRI-derived extracellular volume fraction as well as clinical scores of liver disease severity for the differentiation between patients with liver cirrhosis of Child–Pugh classes A and B. *ECV* extracellular volume fraction, *MELD* model of end-stage liver disease, *APRI score* aspartate aminotransferase to platelet ratio index, *FIB-4 score* fibrosis 4 score, *AUC* area under the curve, *PPV* positive predictive value, *NPV* negative predictive value.

	AUC	Cutoff value	Sensitivity (%)	Specificity (%)	PPV (%)	NPV (%)	Accuracy (%)
Native T1	0.910	> 722 ms	100.0 (72.2–100.0)	82.8 (65.5–94.2)	66.7 (41.7–84.8)	100 (86.2–100.0)	87.2 (73.3–94.4)
ECV	0.944	> 46.85%	88.9 (56.5–98.0)	90.0 (74.4–96.5)	72.7 (43.4–90.3)	96.4 (82.3–99.4)	89.7 (76.4–95.9)
MELD score	0.795	> 10.5	100.0 (64.6–100.0)	50.0 (33.6–66.4)	30.4 (15.6–50.9)	100.0 (80.6–100.0)	59.0 (43.4–72.9)
APRI score	0.634	> 1.176	71.4 (35.9–91.8)	56.3 (39.3–71.8)	26.3 (11.8–48.8)	90.0 (69.9–97.2)	59.0 (43.4–72.9)
FIB-4 score	0.607	> 5.208	85.7 (48.7–97.4)	59.4 (42.3–74.5)	31.6 (15.4–54.0)	95.0 (76.4–99.1)	64.1 (48.4–77.3)

Table 3. Diagnostic performance of hepatic native T1 and MRI-derived extracellular volume fraction as well as clinical scores of liver disease severity for the differentiation between patients with liver cirrhosis of Child–Pugh classes B and C. *ECV* extracellular volume fraction, *MELD* model of end-stage liver disease, *APRI score* aspartate aminotransferase to platelet ratio index, *FIB-4 score* fibrosis 4 score, *AUC* area under the curve, *PPV* positive predictive value, *NPV* negative predictive value.

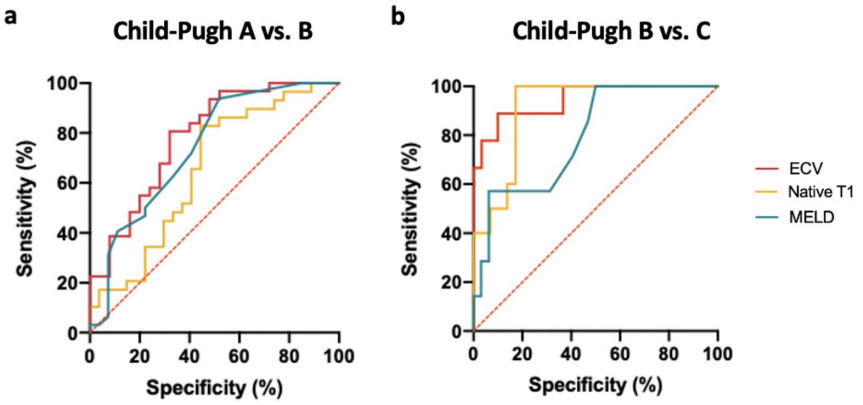

Figure 4. Graphs show receiver operating characteristic curves of hepatic native T1 and MRI-derived extracellular volume fraction (ECV) as well as clinical scores of liver disease severity for differentiation between different Child–Pugh A and B classes (**a**) and Child–Pugh B and C classes (**b**). (**a**) Curves are given for hepatic native T1 (area under the curve [AUC]: 0.651), hepatic ECV (AUC: 0.785), MELD (AUC: 0.740). (**b**) Curves are given for hepatic native T1 (AUC: 0.910), hepatic ECV (AUC: 0.944), MELD (AUC: 0.795). *ECV* extracellular volume fraction, *MELD* model of end-stage liver disease.

significant correlations with the Child–Pugh score and, (2) MRI-derived hepatic ECV revealed a high diagnostic performance for the discrimination of different Child–Pugh classes, which was higher than that of hepatic native T1 and MELD score.

The assessment of liver cirrhosis severity is currently based mainly on clinical and laboratory examinations with calculation of different scores, including the Child–Pugh score, as the most established one. In the past decade, different imaging modalities, including MRI, experienced a fast evolution and now represent an important pillar in terms of clinical management, risk stratification, prognosis estimation, and procedural planning in patients with CLD and cirrhosis. Elastography methods, including ultrasound- and MR-based elastography

have become important diagnostic tools in patients with CLD, mainly for the assessment of fibrosis stage[21]. However, as the stage of liver fibrosis in cirrhotic patients is already final, the assessment of the fibrosis stage alone seems to be insufficient to draw conclusions about the liver function and disease severity. There are also studies demonstrating the ability of baseline liver stiffness measurements, as well as the dynamic of liver stiffness changes, for the prediction of hepatic decompensation[22–24]. In a cross-sectional setting, several MRI techniques have been tried out to assess the functional aspect of liver cirrhosis/disease, e.g., using DWI extended to intravoxel incoherent motion, contrast-enhanced T1 techniques using different techniques and contrast media (e.g., hepatocyte-specific vs. extracellular), and even T1 rho mapping. However, these techniques suffer from lack of standardization (e.g., DWI and contrast-enhanced MRI) and availability across institutions (e.g., T1 rho mapping). Quantitative MRI mapping using T1 mapping techniques with calculation of ECV may potentially overcome these limitations and allow for assessment of liver function and disease severity. A representative hepatic T1 map can be acquired during a single breath-hold and T1 values can be fast and directly obtained from the parametric map. Therefore, the technique can be implemented cost-effectively into clinical routine. It is known that fibrosis is associated with prolongation of T1 relaxation times (which can be also caused due to intra- and extracellular edema in inflammatory settings). Also, fibrosis is associated with an expansion of extracellular space and, as a consequence, with an increased accumulation of extracellular contrast in the extracellular space, which is reflected in increased ECV values[13–16].

In our study we extended the applicability of mapping techniques to the assessment of liver cirrhosis severity. We found a significant correlation between hepatic native T1 and Child–Pugh score ($r = 0.45$). This is consistent with some previous studies, showing that cirrhotic changes lead to prolongation of T1 relaxation times compared to healthy subjects and increase with the increasing stage of liver cirrhosis from patients with Child–Pugh A up to C[25,26]. However, there are other studies, showing no significant differences in native T1 relaxation times between healthy volunteers and cirrhotic patients[11,27]. These conflicting results have been discussed controversially. On the one hand, prolongation of hepatic native T1 relaxation times could be explained by the tissue remodeling, on the other hand, shortening of the T1 relaxation times in patients with liver cirrhosis may be explained by the presence of paramagnetic molecules (e.g. iron) as well as the presence of macromolecules with increased amounts of bound water[11,25,26,28–32]. Liver function might also be correlated with post-contrast hepatic T1 relaxation times in patients with liver cirrhosis. However, post-contrast T1 relaxation times of the liver are highly variable as they depend on time and flow rate of contrast agent application, as well as the applied contrast agent (e.g. hepatocyte-specific vs. extracellular). Furthermore, post-contrast values may vary depending on contrast agent dose, renal clearance rate, time, as well as hematocrit level. These factors would limit the general applicability and a comparability of study results.

Unlike native and post-contrast T1 relaxation times, ECV seems to be a physiologically normalized and a more robust parameter as it does not depend on magnetic field and acquisition parameters. Expansion of the extracellular matrix caused by chronic liver injury leads to enlargement of the extracellular space and, consequently to increased ECV values[15,16,33]. According to histopathological studies, collagen proportionate area increases proportionately across all stages of cirrhosis, which can be explained by the fact that thicker cirrhotic septa contain more collagen[34]. Increased hepatic ECV values in liver cirrhosis, may reflect increased extracellular matrix protein synthesis and deposition, which is higher in advanced stages. For the same reason, ECV is well-known parameter in cardiac MRI and can be employed for non-invasive assessment of myocardial fibrosis[35–37]. There are also studies in animal and humans, demonstrating that ECV correlates better with portal pressure measurements than native T1[16,38]. In our study, we demonstrated significant differences in ECV values between all Child–Pugh classes, which was also different to that in the healthy subjects. ECV correlated stronger with Child–Pugh score than hepatic native T1 ($r = 0.64$ vs. 0.45). Our study results also support previous data in terms of diagnostic utility of ECV to diagnose liver cirrhosis[12–14,39,40]. However, none of the previous study focused exclusively on cirrhotic patients, nor on the ability of MRI-derived ECV to differentiate between different cirrhosis classes.

Finally, we demonstrated a high diagnostic performance of mapping parameters to discriminate between different cirrhosis classes, which was also higher than that of the MELD score. This might be explained by the fact that for the calculation of clinical scores of liver disease severity different laboratory and clinical markers are used. On the one hand, it may decrease the specificity of these markers, as changes outside the liver and also comorbidities, which are not primary related to liver disease, contribute to the final score. On the other hand, ECV seems to be especially more liver-specific as all variables for ECV calculation are obtained from liver parenchyma directly[41] and then normalized for hematocrit. Moreover, approaches for automated calculation of ECV even without hematocrit sampling already exist and can be further developed with the use of machine learning[41,42]. However, because clinical information and laboratory markers are crucial for the assessment of liver function and disease severity, the intention of this study was not to discourage the use of clinical scores and laboratory markers but instead to demonstrate the potential diagnostic value of a quantitative imaging approach.

Despite the advantages of MRI-derived ECV as a potential non-invasive biomarker of liver cirrhosis severity, our study has several limitations. First, the small sample size with a limited number of controls and patients with Child–Pugh class C limit the generalizability of the the study results. Second, we included patients with CLD and cirrhosis of different etiologies. This may have an influence on hepatic T1 values, as the pattern of liver fibrosis and cirrhosis depends on underlying etiology of CLD. Another limitation is the absence of liver biopsy as the reference standard at the time of MRI examination. Larger prospective studies focusing on the etiology of liver disease in correlation with histopathological findings are needed to further investigate the diagnostic utility of MRI-derived ECV.

In conclusion, this is the first study investigating the diagnostic utility of MRI-derived ECV for the assessment of cirrhosis severity. MRI-derived ECV can provide valuable diagnostic information beyond standard morphological imaging for liver fibrosis assessment and might represents a new non-invasive imaging-based biomarker

for the assessment and follow-up of liver cirrhosis severity. Our study results might also motivate future studies to evaluate whether quantitative liver MRI can be used in combination with clinical scoring to improve severity assessment and outcome prediction in patients with liver cirrhosis.

Data availability

The datasets generated during and/or analyzed during the current study are available from the corresponding author on reasonable request.

Received: 19 December 2021; Accepted: 23 May 2022
Published online: 08 June 2022

References

1. Blachier, M., Leleu, H., Peck-Radosavljevic, M., Valla, D.-C. & Roudot-Thoraval, F. The burden of liver disease in Europe: A review of available epidemiological data. *J. Hepatol.* **58**, 593–608 (2013).
2. D'Amico, G., Garcia-Tsao, G. & Pagliaro, L. Natural history and prognostic indicators of survival in cirrhosis: A systematic review of 118 studies. *J. Hepatol.* **44**, 217–231 (2006).
3. Asrani, S. K., Devarbhavi, H., Eaton, J. & Kamath, P. S. Burden of liver diseases in the world. *J. Hepatol.* **70**, 151–171 (2019).
4. Peng, Y., Qi, X. & Guo, X. Child–Pugh versus MELD score for the assessment of prognosis in liver cirrhosis: A systematic review and meta-analysis of observational studies. *Medicine* **95**, e2877 (2016).
5. Lopez-Delgado, J. C. *et al.* Outcomes of abdominal surgery in patients with liver cirrhosis. *World J. Gastroenterol.* **22**, 2657–2667 (2016).
6. Garrison, R. N., Cryer, H. M., Howard, D. A. & Polk, H. C. Clarification of risk factors for abdominal operations in patients with hepatic cirrhosis. *Ann. Surg.* **199**, 648–655 (1984).
7. Chen, W. *et al.* Quantitative assessment of liver function with whole-liver T1rho mapping at 3.0T. *Magn. Reson. Imaging* **46**, 75–80 (2018).
8. Lee, S., Choi, D. & Jeong, W. K. Hepatic enhancement of Gd-EOB-DTPA-enhanced 3 Tesla MR imaging: Assessing severity of liver cirrhosis. *J. Magn. Reson. Imaging JMRI* **44**, 1339–1345 (2016).
9. Yoon, J. H., Lee, J. M., Paek, M., Han, J. K. & Choi, B. I. Quantitative assessment of hepatic function: Modified look-locker inversion recovery (MOLLI) sequence for T1 mapping on Gd-EOB-DTPA-enhanced liver MR imaging. *Eur. Radiol.* **26**, 1775–1782 (2016).
10. Zhang, J. *et al.* MRI-based estimation of liver function by intravoxel incoherent motion diffusion-weighted imaging. *Magn. Reson. Imaging* **34**, 1220–1225 (2016).
11. Haimerl, M. *et al.* Assessment of clinical signs of liver cirrhosis using T1 mapping on Gd-EOB-DTPA-enhanced 3T MRI. *PLoS ONE* **8**, e85658 (2013).
12. Kupczyk, P. A. *et al.* Quantitative MRI of the liver: Evaluation of extracellular volume fraction and other quantitative parameters in comparison to MR elastography for the assessment of hepatopathy. *Magn. Reson. Imaging* **77**, 7–13 (2021).
13. Mesropyan, N. *et al.* Non-invasive assessment of liver fibrosis in autoimmune hepatitis: Diagnostic value of liver magnetic resonance parametric mapping including extracellular volume fraction. *Abdom. Radiol.* **46**, 2458–2466 (2021).
14. Mesropyan, N. *et al.* Diagnostic value of magnetic resonance parametric mapping for non-invasive assessment of liver fibrosis in patients with primary sclerosing cholangitis. *BMC Med. Imaging* **21**, 65 (2021).
15. Luetkens, J. A. *et al.* Quantitative liver MRI including extracellular volume fraction for non-invasive quantification of liver fibrosis: A prospective proof-of-concept study. *Gut* **67**, 593–594 (2018).
16. Luetkens, J. A. *et al.* Quantification of liver fibrosis at T1 and T2 mapping with extracellular volume fraction MRI: Preclinical results. *Radiology* **288**, 748–754 (2018).
17. Angeli, P. *et al.* EASL Clinical Practice Guidelines for the management of patients with decompensated cirrhosis. *J. Hepatol.* **69**, 406–460 (2018).
18. Garcia-Tsao, G. The Child–Turcotte classification: from gestalt to sophisticated statistics and back. *Dig. Dis. Sci.* **61**, 3102–3104 (2016).
19. Vu, K.-N., Haldipur, A. G., Roh, A.T.-H., Lindholm, P. & Loening, A. M. Comparison of end-expiration versus end-inspiration breath-holds with respect to respiratory motion artifacts on T1-weighted abdominal MRI. *AJR Am. J. Roentgenol.* **212**, 1–6 (2019).
20. Schelbert, E. B. & Messroghli, D. R. State of the art: Clinical applications of cardiac T1 mapping. *Radiology* **278**, 658–676 (2016).
21. Kennedy, P. *et al.* Quantitative elastography methods in liver disease: Current evidence and future directions. *Radiology* **286**, 738–763 (2018).
22. Robic, M. A. *et al.* Liver stiffness accurately predicts portal hypertension related complications in patients with chronic liver disease: A prospective study. *J. Hepatol.* **55**, 1017–1024 (2011).
23. Vizzutti, F. *et al.* Liver stiffness measurement predicts severe portal hypertension in patients with HCV-related cirrhosis. *Hepatology (Baltimore, MD)* **45**, 1290–1297 (2007).
24. Macías, J. *et al.* Liver stiffness measurement versus liver biopsy to predict survival and decompensations of cirrhosis among HIV/hepatitis C virus-coinfected patients. *AIDS (London, England)* **27**, 2541–2549 (2013).
25. Katsube, T. *et al.* Estimation of liver function using T1 mapping on Gd-EOB-DTPA-enhanced magnetic resonance imaging. *Investig. Radiol.* **46**, 277–283 (2011).
26. Heye, T. *et al.* MR relaxometry of the liver: Significant elevation of T1 relaxation time in patients with liver cirrhosis. *Eur. Radiol.* **22**, 1224–1232 (2012).
27. Goldberg, H. I. *et al.* Hepatic cirrhosis: Magnetic resonance imaging. *Radiology* **153**, 737–739 (1984).
28. Thomsen, C., Christoffersen, P., Henriksen, O. & Juhl, E. Prolonged T1 in patients with liver cirrhosis: An in vivo MRI study. *Magn. Reson. Imaging* **8**, 599–604 (1990).
29. Ito, K. *et al.* Hepatocellular carcinoma: Association with increased iron deposition in the cirrhotic liver at MR imaging. *Radiology* **212**, 235–240 (1999).
30. Bataller, R. & Brenner, D. A. Liver fibrosis. *J. Clin. Investig.* **115**, 209–218 (2005).
31. Kim, K. A. *et al.* Quantitative evaluation of liver cirrhosis using T1 relaxation time with 3 tesla MRI before and after oxygen inhalation. *J. Magn. Reson. Imaging JMRI* **36**, 405–410 (2012).
32. Eddowes, P. J. *et al.* Utility and cost evaluation of multiparametric magnetic resonance imaging for the assessment of non-alcoholic fatty liver disease. *Aliment. Pharmacol. Ther.* **47**, 631–644 (2018).
33. Luetkens, J. A. *et al.* Quantification of liver fibrosis: Extracellular volume fraction using an MRI bolus-only technique in a rat animal model. *Eur. Radiol. Exp.* **3**, 22 (2019).
34. Tsochatzis, E. *et al.* Collagen proportionate area is superior to other histological methods for sub-classifying cirrhosis and determining prognosis. *J. Hepatol.* **60**, 948–954 (2014).
35. Radenkovic, D., Weingärtner, S., Ricketts, L., Moon, J. C. & Captur, G. T1 mapping in cardiac MRI. *Heart Fail. Rev.* **22**, 415–430 (2017).

36. Moon, J. C. *et al.* Myocardial T1 mapping and extracellular volume quantification: A Society for Cardiovascular Magnetic Resonance (SCMR) and CMR Working Group of the European Society of Cardiology consensus statement. *J. Cardiovasc. Magn. Reson. Off. J. Soc. Cardiovasc. Magn. Reson.* **15**, 92 (2013).
37. Flett, A. S. *et al.* Equilibrium contrast cardiovascular magnetic resonance for the measurement of diffuse myocardial fibrosis: Preliminary validation in humans. *Circulation* **122**, 138–144 (2010).
38. Mesropyan, N. *et al.* Magnetic resonance parametric mapping of the spleen for non-invasive assessment of portal hypertension. *Eur. Radiol.* **31**, 85–93 (2021).
39. Guo, S. L. *et al.* The clinical value of hepatic extracellular volume fraction using routine multiphasic contrast-enhanced liver CT for staging liver fibrosis. *Clin. Radiol.* **72**, 242–246 (2017).
40. Yoon, J. H. *et al.* Estimation of hepatic extracellular volume fraction using multiphasic liver computed tomography for hepatic fibrosis grading. *Investig. Radiol.* **50**, 290–296 (2015).
41. Mesropyan, N. *et al.* Synthetic extracellular volume fraction without hematocrit sampling for hepatic applications. *Abdom. Radiol.* https://doi.org/10.1007/s00261-021-03140-6 (2021).
42. Spottiswoode, B. S., Ugander, M. & Kellman, P. Automated inline extracellular volume (ECV) mapping. *J.. Cardiovasc. Magn. Reson.* **17**, 1–2 (2015).

Author contributions

N.M., J.A.L. and P.A.K. guarantors of integrity of entire study, contributed substantially to data acquisition, analysis, and interpretation; N.M. wrote the main manuscript text and prepared the figures and tables; all authors manuscript drafting or manuscript revision for important intellectual content; all authors approval of final version of submitted manuscript; N.M., J.A.L. and P.A.K. literature research; N.M., J.A.L., P.A.K. manuscript editing.

Funding

Open Access funding enabled and organized by Projekt DEAL.

Competing interests

The authors declare no competing interests.

Additional information

Correspondence and requests for materials should be addressed to J.A.L.

Reprints and permissions information is available at www.nature.com/reprints.

Publisher's note Springer Nature remains neutral with regard to jurisdictional claims in published maps and institutional affiliations.

3.4 Quantitative mapping for the assessment of the severity of portal hypertension. *European Radiology 2021*

"Magnetic resonance parametric mapping of the spleen for non-invasive assessment of portal hypertension"
Mesropyan N, Isaak A, Faron A, Praktiknjo M, Jansen C, Kuetting D, Meyer C, Sprinkart AM Chang J, Maedler B, Thomas D, Kupczyk P, Attenberger UI, Luetkens A.
Published in *European Radiology* 2021 31: 85–93

Purpose - This study aimed to determine the diagnostic value of T1 and T2 mapping and extracellular volume fraction (ECV) for the non-invasive assessment of portal hypertension.

Methods – In this prospective study, 50 participants (33 patients with indication for trans-jugular intrahepatic portosystemic shunt (TIPS) and 17 healthy volunteers) underwent MRI. The derivation and validation cohorts included 40 and 10 participants, respectively. T1 and T2 relaxation times and ECV of the liver and the spleen were assessed using quantitative mapping techniques. Direct hepatic venous pressure gradient (HVPG) and portal pressure measurements were performed during TIPS procedure. ROC analysis was performed to compare diagnostic performance.

Results - Splenic ECV correlated with portal pressure ($r = 0.72$; $p < 0.001$) and direct HVPG ($r = 0.50$; $p = 0.003$). No significant correlations were found between native splenic T1 and T2 relaxation times with portal pressure measurements ($p > 0.05$, respectively). In the derivation cohort, splenic ECV revealed a perfect diagnostic performance with an AUC of 1.000 for the identification of clinically significant portal hypertension (direct HVPG ≥ 10 mmHg) and outperformed other parameters: hepatic T2 (AUC, 0.731), splenic T2 (AUC, 0.736), and splenic native T1 (AUC, 0.806) ($p < 0.05$, respectively). The diagnostic performance of mapping parameters was comparable in the validation cohort.

Conclusions - Splenic ECV was associated with portal pressure measurements in patients with advanced liver disease. Future studies should explore the diagnostic value of parametric mapping across a broader range of pressure values.

European Radiology (2021) 31:85–93
https://doi.org/10.1007/s00330-020-07080-5

MAGNETIC RESONANCE

Magnetic resonance parametric mapping of the spleen for non-invasive assessment of portal hypertension

Narine Mesropyan[1] · Alexander Isaak[1] · Anton Faron[1] · Michael Praktiknjo[2] · Christian Jansen[2] · Daniel Kuetting[1] · Carsten Meyer[1] · Claus C. Pieper[1] · Alois M. Sprinkart[1] · Johannes Chang[2] · Burkhard Maedler[3] · Daniel Thomas[1] · Patrick Kupczyk[1] · Ulrike Attenberger[1] · Julian A. Luetkens[1]

Received: 6 May 2020 / Revised: 25 June 2020 / Accepted: 16 July 2020 / Published online: 4 August 2020

Abstract

Objectives In patients with advanced liver disease, portal hypertension is an important risk factor, leading to complications such as esophageal variceal bleeding, ascites, and hepatic encephalopathy. This study aimed to determine the diagnostic value of T1 and T2 mapping and extracellular volume fraction (ECV) for the non-invasive assessment of portal hypertension.

Methods In this prospective study, 50 participants (33 patients with indication for trans-jugular intrahepatic portosystemic shunt (TIPS) and 17 healthy volunteers) underwent MRI. The derivation and validation cohorts included 40 and 10 participants, respectively. T1 and T2 relaxation times and ECV of the liver and the spleen were assessed using quantitative mapping techniques. Direct hepatic venous pressure gradient (HVPG) and portal pressure measurements were performed during TIPS procedure. ROC analysis was performed to compare diagnostic performance.

Results Splenic ECV correlated with portal pressure ($r = 0.72$; $p < 0.001$) and direct HVPG ($r = 0.50$; $p = 0.003$). No significant correlations were found between native splenic T1 and T2 relaxation times with portal pressure measurements ($p > 0.05$, respectively). In the derivation cohort, splenic ECV revealed a perfect diagnostic performance with an AUC of 1.000 for the identification of clinically significant portal hypertension (direct HVPG ≥ 10 mmHg) and outperformed other parameters: hepatic T2 (AUC, 0.731), splenic T2 (AUC, 0.736), and splenic native T1 (AUC, 0.806) ($p < 0.05$, respectively). The diagnostic performance of mapping parameters was comparable in the validation cohort.

Conclusion Splenic ECV was associated with portal pressure measurements in patients with advanced liver disease. Future studies should explore the diagnostic value of parametric mapping accross a broader range of pressure values.

Key Points

- *Non-invasive assessment and monitoring of portal hypertension is an area of unmet interest.*
- *Splenic extracellular volume fraction is strongly associated with portal pressure in patients with end-stage liver disease.*
- *Quantitative splenic and hepatic MRI-derived parameters have a potential to become a new non-invasive diagnostic parameter to assess and monitor portal pressure.*

Keywords Liver cirrhosis · Portal · Hypertension · Magnetic resonance imaging

✉ Julian A. Luetkens
julian.luetkens@ukbonn.de

[1] Department of Diagnostic and Interventional Radiology and Quantitative Imaging Lab Bonn (QILaB), University Hospital Bonn, Venusberg-Campus 1, 53127 Bonn, Germany

[2] Department of Internal Medicine I, University Hospital Bonn, Venusberg-Campus 1, 53127 Bonn, Germany

[3] Philips GmbH Germany, Roentgenstrasse 22, 22335 Hamburg, Germany

Abbreviations

BMI	Body mass index
CHILD	Child-Pugh score
ECV	Extracellular volume fraction
GraSE	Gradient spin echo sequence
HVPG	Hepatic venous pressure gradient
IAC	International Ascites Club
MELD	Model for end-stage liver disease
MOLLI	Modified Look-Locker inversion recovery
MRE	Magnetic resonance elastography

NAFLD Non-alcoholic fatty liver disease
TIPS Trans-jugular intrahepatic portosystemic shunt

Introduction

Any chronic liver disease may lead to liver fibrosis, which distorts normal liver architecture by the expansion of the extracellular space, and impairs hepatic function [1]. Liver cirrhosis is tightly linked to the occurrence of portal hypertension [2]. Portal hypertension may lead to life-threatening complications such as esophageal variceal bleeding, ascites, and hepatic encephalopathy. Therapy refractory ascites is associated with significantly increased mortality 6–12 months after diagnosis [3]. Therefore, precise diagnosis of portal hypertension plays an important role in clinical decision-making and early interventions may prevent severe complications. Currently, the hepatic venous pressure gradient (HVPG) is considered the reference standard for the assessment of portal hypertension [4]. The HVPG is the difference between the wedged portal vein pressure and the free hepatic venous pressure. Portal hypertension is defined as HVPG > 5 mmHg. Clinically significant portal hypertension is defined as an increase in HVPG to ≥ 10 mmHg [5, 6]. The invasive procedure of HVPG has clear disadvantages because it may be associated with procedural complications and, therefore, cannot be used as a follow-up method. HVPG measurements also require high clinical expertise and are costly. Therefore, alternative non-invasive techniques are needed for the assessment and monitoring of portal pressure.

Recently, quantitative T1 and T2 mapping techniques have been applied to the liver and spleen and might be used for tissue characterization and for the staging of liver fibrosis [7, 8]. Furthermore, T1 relaxation times can also be measured before and after the administration of an extracellular contrast agent, which allows the additional calculation of the extracellular volume (ECV). ECV values are calculated from the change in relaxation rate (R1 = 1/T1) of blood and parenchyma corrected for the hematocrit [9]. ECV is a measure of the extracellular space and represents the tissue volume, which is not taken by cells [10]. Also, ECV is a physiologically intuitive unit of measurement and is independent of field strength. ECV was initially developed for quantifying the myocardial extracellular fractional distribution volume and has been validated in histopathological studies as a measurement of diffuse myocardial fibrosis [11]. Besides the evaluation of myocardial tissue composition, this technique can also be used as a new tool for the non-invasive assessment of liver fibrosis [7, 8]. Furthermore, animal studies suggest that abdominal ECV measures might be correlated with portal pressure measurements [8]. Also, splenic post contrast T1 measurements showed correlations with HVPG in humans [12]. Therefore, the assessment of splenic ECV might be advantageous for non-invasive assessment of portal pressure, as splenomegaly in portal hypertension is not only caused by congestion but also by tissue hyperplasia and fibrosis [13, 14]. The purpose of our study was to find a possible correlation between different parametric magnetic resonance imaging (MRI) parameters (T1, T2, and ECV mapping) of liver and spleen and to evaluate their diagnostic performance for the assessment of portal hypertension.

Material and methods

This prospective, proof-of-concept study was approved by the institutional review committee. All study participants provided written informed consent prior to MRI examination. From November 2018 to September 2019, patients with advanced liver disease and portal hypertension scheduled for trans-jugular intrahepatic portosystemic shunt (TIPS) implantation were consecutively included in this study. All patients completed MRI before TIPS implantation. Healthy volunteers underwent MRI as controls. Diagnosis of refractory ascites was based on the diagnostic criteria recommended by the International Ascites Club (IAC) [15]. Clinical data and laboratory markers were retrieved from the institutional medical information system. The control group consisted of healthy volunteers with no previous medical history of liver disease. All control participants had normal liver MRI and normal laboratory results and were defined to have normal portal pressure.

Magnetic resonance imaging

All imaging was performed on a clinical whole-body 1.5-T MRI system (Ingenia, Philips Healthcare) equipped with 32-channel abdominal coil with digital interface for signal reception. Besides morphological sequences, patients underwent parametric mapping MRI of the liver and the spleen: For splenic and hepatic T1 mapping, a heart rate independent10-(2)-7-(2)-5-(2)-3-(2) modified Look-Locker inversion recovery (MOLLI) acquisition scheme [16] with internal triggering was implemented. The following technical parameters were applied: time of repetition (TR) 1.92 ms, time of echo (TE) 0.84 ms, flip angle (FA) 20°, parallel imaging factor 2, acquired voxel size 1.98 × 2.45 × 10 mm, reconstructed voxel size 1.13 × 1.13 × 10 mm, scan duration/breath-hold 14.0 s. Using the same technique, post-contrast T1 maps were performed in the same positions as pre-contrast examinations. As ECV measurements in the liver are constant from 5 to 25 min according to the experimental data, post-contrast T1 mapping was performed 10 min after contrast administration [17]. For contrast enhancement, the extracellular contrast agent Gadobutrol (0.2 mmol per kilogram of body weight, Gadovist, Bayer Healthcare Pharmaceuticals) was injected at a rate of 1.5 ml/s. T2 mapping was performed before contrast administration using a six-echo gradient spin echo sequence (GraSE) [18]. The following scan parameters were applied: TR 450 ms, inter-echo spacing 16 ms, FA 90°, parallel

imaging factor 2.5, acquired voxel size 1.98 × 2.01 × 10 mm, reconstructed voxel size 0.88 × 0.88 × 10 mm, scan duration/breath-hold 15/3 × 5 s. Parametric maps were acquired in a single transverse section at the level of the bifurcation of portal vein covering the liver and the spleen. T1 and T2 relaxation maps were reconstructed at the scanner console.

HVPG measurements by trans-jugular intrahepatic portosystemic shunt implantation

TIPS procedures establish an artificial connection between the portal and systemic circulation. It is applied in patients with end-stage liver disease for reduction of the portal pressure [15]. TIPS procedure was performed in aseptic conditions under fluoroscopic guidance by experienced interventional radiologists. After puncture of the right portal vein branch, a guidewire was advanced through the TIPS needle and advanced into the portal vein. Afterward, an angiographic 5-French pigtail was advanced into the portal vein for direct portal pressure measurement. No wedged portal vein pressure was measured in this study. Central vein pressure was in inferior vena cava. Direct HVPG was calculated as a difference between portal vein pressure and free inferior vena cava pressure. Also, absolute portal vein pressure was recorded. Significant portal hypertension was defined as a direct HVPG of ≥ 10 mmHg. No invasive portal pressure measurements were performed in the control group. Healthy controls were defined to have no portal hypertension.

Image analysis

Image analyses were performed by an experienced board-certified radiologist, blinded to the clinical information and portal vein pressure measurements. Three regions of interest (ROIs) were respectively drawn within the liver and the spleen parenchyma, away from confounding factors like vessels, biliary structures, and organ boundaries. Minimum ROI size was ≥ 1 cm^2. The ROIs were firstly placed into the native T1 map. Afterward, the ROIs were copied on all other relaxation maps for the same patient. Mean T1 and T2 relaxation times were used for analysis. T1 values of the blood pool were obtained from the abdominal aorta. ECV values were normalized for hematocrit and calculated from pre- and post-contrast T1 values using the following equation [9]: ECV = (1 − hematocrit)*(1/T1 parenchyma post-contrast −1/T1 parenchyma pre-contrast)/(1/T1 aortic post-contrast −1/T1 aortic pre-contrast). For this explorative study, we assumed that for abdominal ECV calculations, a bolus-only contrast injection technique leads to a dynamic equilibrium 10 min after contrast administration [17]. Blood hematocrit levels were obtained before MRI investigations.

Statistical analysis

Statistical analysis was performed using SPSS Statistics (Version 22, IBM) and MedCalc (version 19.1.3, MedCalc Software). Patient characteristics are presented as mean ± standard deviation or as absolute frequency. Continuous variables between the two groups were compared by using the Student *t* test. Dichotomous variables were compared by using the $\chi 2$ test. Pearson correlation coefficient (r) was used for correlation analyses. In the derivation cohort, the diagnostic performance of MRI parameters was analyzed by plotting receiver operating characteristics and comparing the area under the curve (AUC). Youden's index was used to determine the optimal cutoff of the ROC curve providing the highest combination of sensitivity and specificity. The presence of clinically significant portal hypertension (direct HVPG ≥ 10 mmHg) was the reference standard against which the diagnostic performance of MRI-derived mapping parameters of spleen and liver was tested. AUCs were compared by using the method proposed by DeLong et al [19]. Using the cutoff values of the derivation cohort, sensitivity, specificity, accuracy, and predictive values were calculated for the validation cohort. The level of statistical significance was set to $p < 0.05$.

Results

Cohort characteristics

A total of 33 patients with liver cirrhosis and refractory ascites/esophageal variceal bleeding and 17 healthy volunteers were included. The first 40 participants (28 patients with liver cirrhosis and 12 healthy volunteers) were used as a derivation cohort to establish the cutoff values of mapping parameters. The next 10 participants that were included constituted our validation cohort (5 patients with liver cirrhosis and 5 healthy volunteers). The mean interval between pre-interventional MRI and TIPS implantation was 9.66 ± 11.87 days. All patients had clinically significant portal hypertension (direct HVPG ≥ 10 mmHg). There were no peri- or post-procedural complications related to TIPS implantation.

Derivation cohort

Etiologies of liver disease included alcoholic liver disease ($n = 14$, 50.00%), non-alcoholic fatty liver disease (NAFLD, $n = 2$, 7.14%), virus-related liver cirrhosis ($n = 1$, 3.57%), toxic liver disease ($n = 3$, 10.71%), unknown etiology ($n = 5$, 17.85%), and sinusoidal liver disease ($n = 2$, 7.14%). Indications for TIPS implantation were refractory ascites ($n = 21/28$, 75.00%) and esophageal variceal bleeding ($n = 7/28$, 25.00%).

Validation cohort

Etiologies of liver disease included alcoholic liver disease ($n = 4$, 80.00%) and unknown etiology ($n = 1$, 20.00%). Indications for TIPS implantation were refractory ascites ($n = 4/5$, 80.00%) and esophageal variceal bleeding ($n = 1/5$, 20.00%). The clinical characteristics of the derivation and validation cohorts are summarized in Table 1.

MRI results

Portal vein pressure ($r = 0.72$, $p < 0.001$) and direct HVPG ($r = 0.50$, $p = 0.003$) were significantly correlated with splenic ECV in cirrhotic patients (see Fig. 1). A correlation matrix is given in Table 2.

Derivation cohort

Compared with healthy controls, patients with liver cirrhosis had significant increased splenic native T1 relaxation times (1010.17 ± 49.13 ms vs. 1100.52 ± 95.76 ms; $p < 0.001$), T2 relaxation times (98.83 ± 11.69 ms vs. 113.17 ± 18.72 ms, $p = 0.007$), and splenic ECV values (25.82 ± 2.40% vs. 42.53 ± 6.29%; $p < 0.001$). There were significant differences in hepatic MRI parameters between controls and patients: native T1 relaxation time (544.78 ± 41.25 ms vs. 681.03 ± 83.93 ms; $p < 0.001$) and ECV (26.14 ± 2.31% vs. 45 ± 18.55%; $p < 0.001$). No significant differences in hepatic T2 relaxation times were present between both groups (48.58 ± 8.41 ms vs. 53.72 ± 7.56 ms; $p = 0.062$).

Validation cohort

Splenic and hepatic MRI results of the validation cohort are given in Table 3.

Diagnostic performance of parametric mapping parameters

Several parametric mapping parameters were evaluated regarding the diagnostic performance to diagnose clinically significant portal hypertension.

Derivation cohort

Splenic ECV revealed a perfect diagnostic performance with an area under the curve (AUC) of 1.000, a sensitivity of 100%, and a specificity of 100% (see Fig. 2, Fig. 3, and Table 4). There were no significant differences in the diagnostic performance of splenic and hepatic ECV (AUC, 1.000 vs. 0.954; $p = 0.116$). The diagnostic performance of splenic ECV was also not significantly higher compared with that of hepatic

Table 1 Clinical characteristics of the derivation and validation cohort for patients with clinically significant portal hypertension and healthy control participants

Variable	Derivation cohort ($n = 40$)			Validation cohort ($n = 10$)		
	Healthy controls ($n = 12$)	Portal hypertension ($n = 28$)	p value	Healthy controls ($n = 5$)	Portal hypertension ($n = 5$)	p value
Age (years)	43.58 ± 17.42	58.32 ± 11.66	0.017	52.40 ± 20.26	55.60 ± 4.50	0.739
Body mass index (kg/m^2)	22.53 ± 4.57	24.58 ± 5.42	0.281	22.72 ± 2.22	25.88 ± 8.71	0.454
Sex			0.722			0.350
Male	8 (66.66%)	21 (75.00%)		1 (20.00%)	3 (60.00%)	
Female	4 (33.33%)	7 (25.00%)		4 (80.00%)	2 (40.00%)	
Hematocrit level (%)	45.25 ± 3.71	29.46 ± 5.90	< 0.001	41.00 ± 2.55	33.00 ± 3.31	0.003
MELD	6.8 ± 1.4	12.92 ± 5.46	< 0.001	6.20 ± 0.44	13.50 ± 5.00	0.013
CHILD			< 0.001			0.007
A	0 (0.00%)	7 (25.00%)		0 (0.00%)	2 (40.00%)	
B	0 (0.00%)	17 (60.71%)		0 (0.00%)	3 (60.00%)	
C	0 (0.00%)	4 (14.28%)		0 (0.00%)	0 (0.00%)	
Bilirubin (mg/dl)	0.69 ± 0.26	0.137 ± 1.36	0.017	0.39 ± 0.18	1.25 ± 0.71	0.031
ALT (U/l)	35.00 ± 12.67	25.93 ± 9.90	0.041	35.60 ± 30.22	39.40 ± 24.70	0.833
AST (U/l)	23.66 ± 4.57	47.14 ± 27.19	< 0.001	26.00 ± 12.58	61.20 ± 27.39	0.031
GGT (U/l)	36.16 ± 20.78	140.53 ± 240.42	0.031	69.20 ± 94.05	235.20 ± 235.62	0.182
Platelets cells×10^9/l	281.25 ± 85.24	153.04 ± 112.11	0.001	287.40 ± 39.91	172.50 ± 90.98	0.037
C-reactive protein level (mg/l)	1.09 ± 1.94	10.65 ± 11.82	< 0.001	1.12 ± 0.68	15.68 ± 4.90	0.003
AP (U/l)	49.20 ± 20.42	121.64 ± 102.18	0,035	83.60 ± 27.71	139.40 ± 60.85	0.099
Creatinine (mg/dl)	0.88 ± 0.21	1.14 ± 0.54	0.042	0.78 ± 0.13	2.25 ± 2.18	0.170
Albumin (g/l)	Not available	31.90	–	Not available	32.98 ± 6.91	–
International normalized ratio	1.01 ± 0.04	1.15 ± 0.09	< 0.001	1.26 ± 0.58	1.30 ± 0.18	0.887

Continuous data are means ± standard deviations. Nominal data are absolute frequencies with percentages in parentheses. *Abbreviations*: *MELD*, score model of end-stage liver disease; *CHILD*, Child-Pugh score; *ALT*, alanine aminotransferase; *AST*, aspartate aminotransferase; *AP*, alkaline phosphatase; *GGT*, gamma-glutamyltransferase

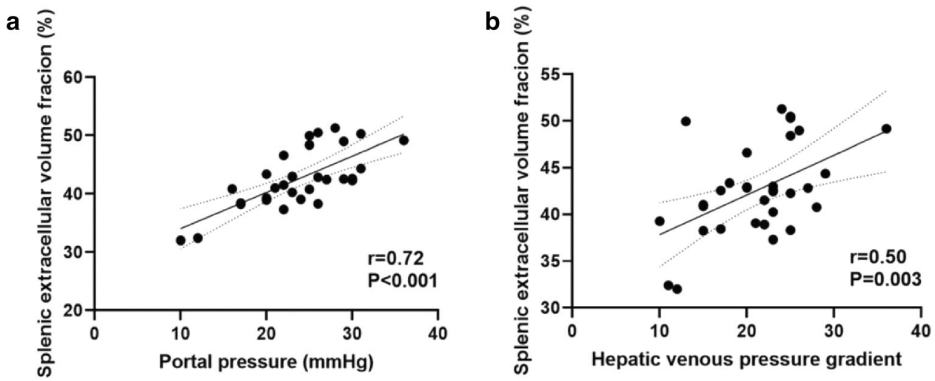

Fig. 1 Scatter plots shows correlations between splenic extracellular volume fraction and portal vein pressure (**a**) and direct hepatic venous pressure gradient (**b**) in the patients with liver cirrhosis ($n = 33$). Regression line is given with 95% confidence interval

native T1 (AUC, 1.000 vs. 0.926; $p = 0.105$) but significantly higher than that of splenic native T1 (AUC, 1.000 vs. 0.806; $p = 0.005$). There were no significant differences in the diagnostic performance of native splenic and hepatic T1 (AUC, 0.806 vs. 0.926, $p = 0.058$). Hepatic ECV showed a higher diagnostic performance compared with native splenic T1 (AUC, 0.954 vs. 0.806, $p = 0.038$). Between hepatic ECV and hepatic native T1, no significant differences in diagnostic performance were observed. The diagnostic performance of hepatic and splenic T2 was significantly lower than that of the splenic and hepatic native T1 and ECV parameters.

Validation cohort

The parameters of the diagnostic performance of the validation cohort are given in Table 4. The 95% confidence intervals of diagnostic performance were comparable between the derivation and the validation cohort.

Discussion

In our proof-of-principle study, we evaluated different parametric MRI parameters for non-invasive assessment of portal hypertension. The main findings of our study are that (1) splenic ECV showed a statistically significant correlation with portal pressure and direct HVPG and, (2) splenic and hepatic ECV showed a high diagnostic performance to diagnose clinically significant portal hypertension and performed better than native T1 and T2 mapping parameters.

Hepatocyte injury in chronic liver disease leads can activate potentially fibrogenic cells and promote the occurrence of liver fibrosis. The formation of liver fibrosis leads to an increased deposition of abnormal extracellular matrix components [20]. Liver fibrosis also leads to an increased accumulation of extracellular MRI contrast agents in the extracellular space, which can be measured via ECV assessment. Histopathological studies show correlations between hepatic T1, T2, and ECV with liver fibrosis, as well as hepatic ECV and portal pressure in both animal and human models [8, 13, 14, 21–23]. There are also studies mentioning positive correlations between mapping parameters and magnetic resonance elastography (MRE) [22, 24, 25].

Portal hypertension initially develops because of increased intrahepatic resistance to the passage of blood flow through the liver as a consequence of hepatic fibrotic changes. In this regard, splenomegaly in liver disease is likely to be a consequence of portal congestion with blood pooling as well as pulp hyperplasia and fibrosis [26]. All these changes lead to an expansion of the extracellular space, which is reflected in increased splenic ECV, as shown in our data. In our study, splenic ECV values were also significantly correlated with portal pressure and with direct HVPG.

To our knowledge, there are still no studies directly showing correlations between invasive measured direct HVPG in patients with end-stage liver disease and clinically significant portal hypertension and splenic ECV as a

Table 2 Correlation matrix for quantitative MRI parameters and parameters of portal pressure of the patients with liver cirrhosis

	Splenic native T1		Splenic post-contrast T1		Splenic T2		Splenic ECV		Hepatic native T1		Hepatic T2		Hepatic ECV	
Variable	*r* value	*p* value	*r* value	*p* value	*r* value	*p* value	*r* value	*p* value	*r* value	*p* value	*r* value	*p* value	*r* value	*p* value
Portal vein pressure	0.31	0.091	−0.300	0.101	0.19	0.294	0.72	< 0.001	0.025	0.894	0.02	0.925	0.07	0.714
Direct HVPG	0.28	0.122	−0.076	0.679	0.17	0.361	0.50	0.003	−0.19	0.918	−0.83	0.648	−0.12	0.945

Abbreviations: *ECV*, extracellular volume fraction; *HVPG*, hepatic venous pressure gradient

Table 3 Splenic and hepatic MRI characteristics of the derivation and validation cohort for patients with portal hypertension and healthy participants

Variable	Derivation cohort ($n = 40$)			Validation cohort ($n = 10$)		
	Healthy controls ($n = 12$)	Portal hypertension ($n = 28$)	p value	Healthy controls ($n = 5$)	Portal hypertension ($n = 5$)	p value
Hepatic venous pressure gradient	Not available	20.71 ± 5.49	–	Not available	22.40 ± 7.83	–
Portal pressure (mmHg)	Not available	23.07 ± 5.47	–	Not available	26.00 ± 7.17	–
Splenic native T1 relaxation time (ms)	1010.17 ± 49.13	1100.52 ± 95.76	< 0.001	1016 ± 45.05	1116 ± 23.02	0.002
Splenic contrast T1 relaxation time (ms)	360.92 ± 51.41	291.44 ± 56.89	0.001	483.00 ± 76.34	333.00 ± 78.36	0.002
Splenic extracellular volume fraction (%)	25.82 ± 2.40	42.53 ± 6.29	< 0.001	28.94 ± 1.53	42.89 ± 3.92	< 0.001
Splenic T2 relaxation time (ms)	98.83 ± 11.69	113.17 ± 18.72	0.007	103.00 ± 5.19	116 ± 13.21	0.062
Hepatic native T1 relaxation time (ms)	544.78 ± 41.25	681.03 ± 83.93	< 0.001	535.60 ± 20.88	705.60 ± 59.18	< 0.001
Hepatic extracellular volume fraction (%)	26.14 ± 2.31	45.00 ± 18.55	< 0.001	27.35 ± 4.22	35.42 ± 6.99	< 0.001
Hepatic T2 relaxation time (ms)	48.58 ± 8.41	53.72 ± 7.56	0.062	47.60 ± 2.07	54.66 ± 3.51	0.005

Continuous data are means ± standard deviations

non-invasive marker of portal pressure. Splenic ECV showed a perfect diagnostic performance for clinically significant portal hypertension with an AUC of 1.000 in the derivation cohort. Moreover, although not statistically significant, the diagnostic performance of splenic ECV was superior to that of the liver, possibly because liver fibrosis reflects only one element of pathophysiological changes in portal hypertension, while splenic ECV directly reflects all consequences of portal hypertension (congestion, tissue hyperplasia, and fibrosis). ECV measurements also showed a higher diagnostic performance compared with T1 and T2 mapping parameters, probably because ECV is a physiologically normalized measure and reflects changes of splenic parenchyma more accurately. Therefore, ECV seems to be a stable and biologically significant biomarker for non-invasive assessment of portal hypertension.

Splenic post-contrast T1 has also been recognized as a potential biomarker for diagnosing portal hypertension as well

Table 4 Diagnostic performance of different quantitative MRI parameters of the derivation and validation cohort for assessment of clinically significant portal hypertension in patients with advanced liver disease

Variable	Cutoff value	Sensitivity (%)	Specificity (%)	PPV (%)	NPV (%)	Accuracy (%)
Derivation cohort ($n = 40$)						
Splenic extracellular volume fraction (%)	> 30.42%	100.0 (87.5–100.0)	100 (75.8–100.0)	100.0 (87.5–100.0)	100.0 (75.8–100.0)	100.0 (91.0–100.0)
Splenic native T1 (ms)	> 1060 ms	74.07 (55.3–86.8)	91.67 (64.6–98.5)	95.2 (77.3-99.2)	61.1 (38.6–79.7	79.5 (64.5–89.2)
Splenic T2 (ms)	> 115 ms	46.4 (29.5–64.2)	100 (75.8–100)	100.0 (77.2–100.0)	44.4 (27.6–62.7)	62.5 (47.0–75.8)
Hepatic extracellular volume fraction (%)	> 29%	89.29 (72.8–96.3)	91.67 (64.6–98.5)	96.2 (81.1–99.3)	78.6 (52.4–92.4)	90.0 (76.9–96.0)
Hepatic native T1 (ms)	> 569 ms	92.86 (77.4–98.0)	91.67 (64.6–98.5)	96.3 (81.7–99.3)	84.6 (57.8–95.7)	92.5 (80.1–97.4)
Hepatic T2 (ms)	> 47.60 ms	85.71 (68.5–94.3)	58.33 (32.0–80.7)	82.8 (65.5–92.4)	63.6 (35.4–84.8)	77.5 (62.5–87.7)
Validation cohort ($n = 10$)						
Splenic extracellular volume fraction (%)	> 30.42%	100 (56.6–100.0)	80.00 (37.6–96.4)	83.3 (43.6–97.0)	100 (51.0–100.0)	90.0 (59.6–98.2)
Splenic native T1 (ms)	> 1060 ms	100.0 (56.6–100.0)	80.00 (37.6–96.4)	83.3 (43.6–97.0)	100 (51.0–100.0)	90.0 (59.6–98.2)
Splenic T2 (ms)	> 115 ms	40.0 (11.8–76.9)	100 (56.6–100.0)	100 (34.2–100.0)	62.5 (30.6–86.3)	70.0 (39.7–89.2)
Hepatic extracellular volume fraction (%)	> 29%	80.0 (37.6–96.4)	60.0 (23.1–88.2)	66.7 (30.0–90.3)	75.0 (30.1–95.4)	70.0 (39.7–89.2)
Hepatic native T1 (ms)	> 569 ms	100.0 (56.6–100.0)	100.0 (56.6–100.0)	100.0 (56.6–100.0)	100.0 (56.6–100.0)	100.0 (72.2–100.0)
Hepatic T2 (ms)	> 47.60 ms	100 (56.6–100.0)	40.0 (11.8–76.9)	62.5 (30.6–86.3)	100.0 (34.2–100.0)	70.0 (39.7–89.2)

Cutoff values of the derivation cohort were used to calculate sensitivity, specificity, PPV, NPV, and accuracy of the validation cohort. *Abbreviations*: *PPV*, positive predictive value; *NPV*, negative predictive value. Data in parentheses are 95% confidence interval

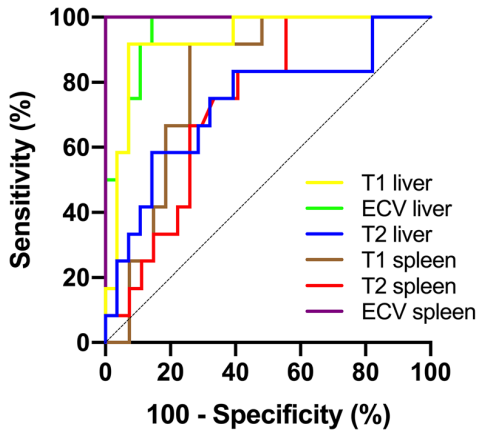

Fig. 2 Graphs show receiver operating characteristic curves for diagnosis of clinically significant portal hypertension (direct hepatic venous pressure gradient, ≥ 10 mmHg) in the derivation cohort. Curves are given for hepatic T1 relaxation times (area under curve [AUC], 0.926), hepatic ECV (AUC, 0.954), hepatic T2 relaxation times (AUC, 0.731), splenic T1 relaxation times (AUC, 0.806), splenic T2 relaxation times (AUC, 0.736), and splenic ECV (AUC, 1.000)

as for treatment monitoring and prognosis [12]. In contrast to the previous study, in which post-contrast splenic T1 values showed a significant correlation with HVPG ($r = 0.69$, $p = 0.001$), we did not found significant correlations between the post-contrast splenic T1 and direct HVPG measures. This might be explained due to our very homogeneous patient collective with end-stage liver disease and clinically significant portal hypertension (mean direct HVPG 20.71 ± 5.49 mmHg). In the previous study, only half of the patients (47%) had clinically significant portal hypertension [12], which might have led to an artificial increase in the correlation coefficient. On the other hand, post-contrast T1 values are known to vary depending on the gadolinium dose, renal clearance rate, scanning time, body composition, and hematocrit levels. The above factors might have contributed to the fact that no significant correlation in post-contrast splenic T1 values was revealed in our study.

Unlike ECV, native hepatic T1 (AUC 0.926) performed better than native splenic T1 (AUC 0.806) in the derivation cohort. This might be explained by a higher contribution of fibrosis to changes in T1 values, as fibrotic changes are more remarkable in hepatic than in splenic parenchyma. Splenic and hepatic T2 mapping parameters had a similar diagnostic performance to patients diagnosed with clinically significant portal hypertension with AUCs of 0.736 and 0.731, respectively. According to previous cardiac studies, increased T2 relaxation times are mainly driven due to myocardial edema or inflammation [27]. Therefore, increased T2 relaxation times in abdominal mapping probably reflect the coexistence of inflammatory or edematous changes in regions of fibrosis [28, 29], which does not correlate well with measures of portal hypertension.

However, hepatic and splenic mapping is a rapidly evolving field and standardized protocols are still being established. Unlike CT, MRI techniques have the advantages that they do not require radiation dose for the assessment of portal hypertension [30]. Also, in contrast to other techniques like MR elastography, which can also be used for the prediction of esophageal varices and, therefore, the severity of portal hypertension [31], the proposed mapping techniques do not require additional equipment. Multiparametric MRI with T1 mapping techniques may reduce the need for invasive and expensive procedures, such as HVPG measurements, in clinical practice. Our findings suggest that MRI-derived ECV values may be a potential new biomarker to assess and monitor portal pressure.

Despite the advantages of ECV measurements as a potential non-invasive parameter, our study has several limitations. First, only patients with end-stage liver disease and significant portal hypertension were included in our explorative study. Therefore, only a small homogenous population with HVPG ≥ 10 mmHg was observed and no conclusion about a broader range of portal pressure measurement can be drawn. As direct portal pressure measurements in patients without indication for TIPS procedure are not clinical routine in our clinic, diagnostic

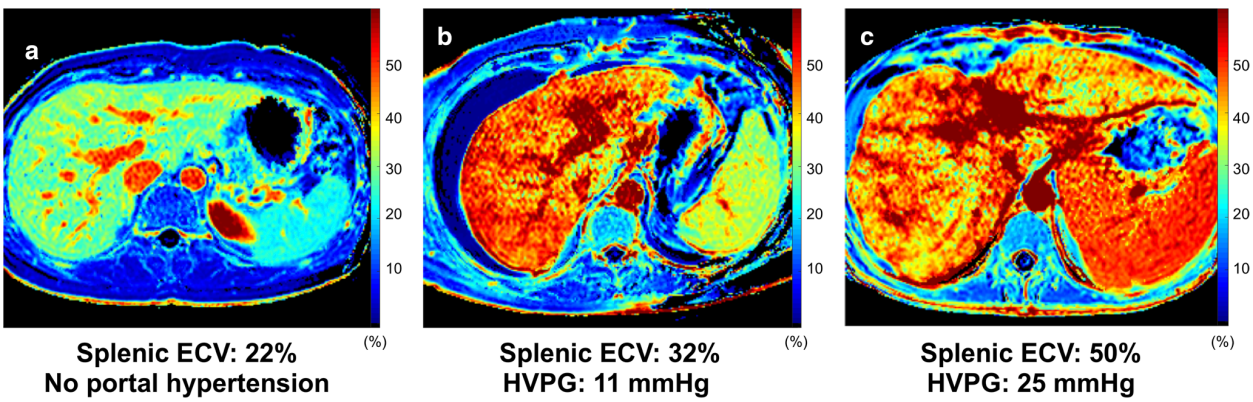

Fig. 3 Representative images of splenic extracellular volume (ECV) maps from a healthy volunteer (**a**) and patients with clinically significant portal hypertension (**b**, **c**). *Abbreviations*: ECV, extracellular volume fraction; HVPG, hepatic venous pressure gradient

performance of mapping parameters was tested against a control group and not against a patient group without a significant portal hypertension. Therefore, the selected study design does not represent a real-life setting and reported parameters of diagnostic performance have to be regarded as study specific. T1 and T2 maps were acquired in a single transverse section at the level of the bifurcation of portal vein and, therefore, may have missed other significant changes, which probably occurred in other planes. Furthermore, our T1 measurements were not corrected for hepatic steatosis or hepatic/splenic iron overload, which might impair the correct assessment of T1 values [29, 30]. Another limitation of our study was that the reading of all cases was performed only by one experienced radiologist. We used a double-contrast bolus for ECV calculations, as commonly used for cardiac applications. However, as contrast dosage might influence ECV calculation, attention should be paid to standardized contrast protocols, when introducing this technique into clinical routine. The study results have to be considered preliminary and further prospective studies are necessary to establish the results of this study and confirm the accuracy and usefulness of ECV and other MRI parameters for the assessment and follow-up in patients with portal hypertension in routine clinical practice.

In conclusion, in our prospective proof-of-principle study, quantitative splenic and hepatic MRI-derived parameters including ECV appear to be a new valuable, non-invasive diagnostic parameter for the assessment of portal pressure in patients with advanced liver disease. Especially, splenic ECV might provide important information about the presence of clinically significant portal hypertension.

Funding information Open Access funding provided by Projekt DEAL.

Compliance with ethical standards

Guarantor The scientific guarantor of this publication is Julian A. Luetkens.

Conflict of interest The authors of this manuscript declare no relationships with any companies, whose products or services may be related to the subject matter of the article.

Statistics and biometry One of the authors (Julian A. Luetkens) has significant statistical expertise.

Informed consent Written informed consent was obtained from all subjects (patients) in this study.

Ethical approval Institutional Review Board approval was obtained.

Methodology
- retrospective
- observational
- performed at one institution

References

1. Bandula S, Punwani S, Rosenberg WM et al (2015) Equilibrium contrast-enhanced CT imaging to evaluate hepatic fibrosis: initial validation by comparison with histopathologic sampling. Radiology 275(1):136–143
2. Ekstedt M, Franzén LE, Mathiesen UL et al (2006) Long-term follow-up of patients with NAFLD and elevated liver enzymes. Hepatology 44(4):865–873
3. Siqueira F, Kelly T, Saab S (2009) Refractory ascites: pathogenesis, clinical impact, and management. Gastroenterol Hepatol (N Y) 5(9):647–656
4. La Mura V, Nicolini A, Tosetti G, Primignani M (2015) Cirrhosis and portal hypertension: the importance of risk stratification, the role of hepatic venous pressure gradient measurement. World J Hepatol 7(4):688–695
5. Kamath PS, Mookerjee RP (2015) Individualized care for portal hypertension: not quite yet. J Hepatol 63(3):543–545
6. Ripoll C, Groszmann R, Garcia-Tsao G et al (2007) Hepatic venous pressure gradient predicts clinical decompensation in patients with compensated cirrhosis. Gastroenterology 133(2):481–488
7. Luetkens JA, Klein S, Traeber F et al (2018) Quantitative liver MRI including extracellular volume fraction for non-invasive quantification of liver fibrosis: a prospective proof-of-concept study. Gut 67(3):593–594
8. Luetkens JA, Klein S, Träber F et al (2018) Quantification of liver fibrosis at T1 and T2 mapping with extracellular volume fraction MRI: preclinical results. Radiology 288(3):748–754
9. Schelbert EB, Messroghli DR (2016) State of the art: clinical applications of cardiac T1 mapping. Radiology 278(3):658–676
10. Moon JC, Messroghli DR, Kellman P et al (2013) Myocardial T1 mapping and extracellular volume quantification: a Society for Cardiovascular Magnetic Resonance (SCMR) and CMR Working Group of the European Society of Cardiology consensus statement. J Cardiovasc Magn Reson 15:92
11. Flett AS, Hayward MP, Ashworth MT et al (2010) Equilibrium contrast cardiovascular magnetic resonance for the measurement of diffuse myocardial fibrosis: preliminary validation in humans. Circulation 122(2):138–144
12. Levick C, Phillips-Hughes J, Collier J et al (2019) Non-invasive assessment of portal hypertension by multi-parametric magnetic resonance imaging of the spleen: a proof of concept study. PLoS One 14(8):e0221066
13. McDonald N, Eddowes PJ, Hodson J et al (2018) Multiparametric magnetic resonance imaging for quantitation of liver disease: a two-centre cross-sectional observational study. Sci Rep 8(1):9189
14. Hoy AM, McDonald N, Lennen RJ et al (2018) Non-invasive assessment of liver disease in rats using multiparametric magnetic

resonance imaging: a feasibility study. Biol Open. https://doi.org/10.1242/bio.033910
15. Moore KP, Wong F, Gines P et al (2003) The management of ascites in cirrhosis: report on the consensus conference of the International Ascites Club. Hepatology 38(1):258–266
16. Messroghli DR, Radjenovic A, Kozerke S, Higgins DM, Sivananthan MU, Ridgway JP (2004) Modified Look-Locker inversion recovery (MOLLI) for high-resolution T1 mapping of the heart. Magn Reson Med 52(1):141–146
17. Luetkens JA, Klein S, Träber F et al (2019) Quantification of liver fibrosis: extracellular volume fraction using an MRI bolus-only technique in a rat animal model. Eur Radiol Exp 3(1):22
18. Sprinkart AM, Luetkens JA, Träber F et al (2015) Gradient spin echo (GraSE) imaging for fast myocardial T2 mapping. J Cardiovasc Magn Reson 17:12
19. DeLong ER, DeLong DM, Clarke-Pearson DL (1988) Comparing the areas under two or more correlated receiver operating characteristic curves: a nonparametric approach. Biometrics 44(3):837–845
20. Wells RG (2008) Cellular sources of extracellular matrix in hepatic fibrosis. Clin Liver Dis 12(4):759–768
21. Müller A, Hochrath K, Stroeder J et al (2017) Effects of liver fibrosis progression on tissue relaxation times in different mouse models assessed by ultrahigh field magnetic resonance imaging. Biomed Res Int 2017:8720367
22. Hoffman DH, Ayoola A, Nickel D, Han F, Chandarana H, Shanbhogue KP (2020) T1 mapping, T2 mapping and MR elastography of the liver for detection and staging of liver fibrosis. Abdom Radiol (NY) 45(3):692–700
23. Wang H-Q, Jin K-P, Zeng M-S et al (2019) Assessing liver fibrosis in chronic hepatitis B using MR extracellular volume measurements: comparison with serum fibrosis indices. Magn Reson Imaging 59:39–45
24. Hoffman DH, Ayoola A, Nickel D et al (2020) MR elastography, T1 and T2 relaxometry of liver: role in noninvasive assessment of liver function and portal hypertension. Abdom Radiol (NY). https://doi.org/10.1007/s00261-020-02432-7
25. Ramachandran P, Serai SD, Veldtman GR et al (2019) Assessment of liver T1 mapping in fontan patients and its correlation with magnetic resonance elastography-derived liver stiffness. Abdom Radiol (NY) 44(7):2403–2408
26. Bolognesi M, Merkel C, Sacerdoti D, Nava V, Gatta A (2002) Role of spleen enlargement in cirrhosis with portal hypertension. Dig Liver Dis 34(2):144–150
27. Luetkens JA, Doerner J, Schwarze-Zander C et al (2016) Cardiac magnetic resonance reveals signs of subclinical myocardial inflammation in asymptomatic HIV-infected patients. Circ Cardiovasc Imaging 9(3):e004091
28. Guimaraes AR, Siqueira L, Uppal R et al (2016) T2 relaxation time is related to liver fibrosis severity. Quant Imaging Med Surg 6(2):103–114
29. Luetkens JA, von Landenberg C, Isaak A et al (2019) Comprehensive cardiac magnetic resonance for assessment of cardiac involvement in Myotonic muscular dystrophy type 1 and 2 without known cardiovascular disease. Circ Cardiovasc Imaging 12(6):e009100
30. Han X, An W, Cao Q, Liu C, Shang S, Zhao L (2020) Noninvasive evaluation of esophageal varices in cirrhotic patients based on spleen hemodynamics: a dual-energy CT study. Eur Radiol 30:3210–3216
31. Abe H, Midorikawa Y, Matsumoto N et al (2019) Prediction of esophageal varices by liver and spleen MR elastography. Eur Radiol 29:6611–6619

3.5 Synthetic extracellular volume fraction calculation for hepatic applications. *Abdominal Radiology (NY) 2021*

"Synthetic extracellular volume fraction without hematocrit sampling for hepatic applications"
Mesropyan N, Kupczyk P, Isaak A, Endler C, Faron A, Dold L, Sprinkart AM, Pieper CC, Kuetting D, Attenberger UI, Luetkens JA.
Published in *Abdominal Radiology (NY)* 2021 Oct 46(10):4637-4646

Purpose - The aim of this study was to generate synthetic ECV for hepatic applications without the need for hematocrit sampling.

Methods - In this prospective study participants underwent liver MRI. T1 mapping was performed before and after contrast administration. Blood hematocrit was obtained prior to MRI. We hypothesized that the relationship between hematocrit and longitudinal relaxation rate of blood (R1 = 1/T1blood) could be calibrated and used to generate the equation for synthetic hematocrit and ECV calculation. Conventional and synthetic ECV were calculated. Pearson correlation, linear regression and Bland-Altman method were used for statistical analysis.

Results - 180 consecutive patients were divided into derivation (n = 90) and validation (n = 90) cohorts. In the derivation cohort, native R1blood and hematocrit showed a linear relationship (HctMOLLI = 98.04 × (1/T1blood) - 33.17, R2 = 0.75, P < 0.001), which was used to calculate synthetic ECV in the validation and whole study cohorts. Synthetic and conventional ECV showed significant correlations in the derivation, validation and in the whole study cohorts (r = 0.99, 0.97 and 0.99, respectively, P < 0.001, respectively) with minimal bias according to the Bland-Altman analysis.

Conclusions - Synthetic ECV seems to offer an alternative method for non-invasive quantification of the hepatic ECV. It may potentially overcome an important barrier to clinical implementation of ECV and thus, enable broader use of hepatic ECV in routine clinical practice.

Abdominal Radiology (2021) 46:4637–4646
https://doi.org/10.1007/s00261-021-03140-6

SPECIAL SECTION: DIFFUSE LIVER DISEASE

Synthetic extracellular volume fraction without hematocrit sampling for hepatic applications

Narine Mesropyan[1,2] · Patrick Kupczyk[1,2] · Alexander Isaak[1,2] · Christoph Endler[1,2] · Anton Faron[1,2] · Leona Dold[3] · Alois M. Sprinkart[1,2] · Claus C. Pieper[1] · Daniel Kuetting[1,2] · Ulrike Attenberger[1] · Julian A. Luetkens[1,2]

Received: 3 January 2021 / Revised: 3 May 2021 / Accepted: 22 May 2021 / Published online: 10 June 2021

Abstract

Purpose Calculation of extracellular volume fraction (ECV) currently receives increasing interest as a potential biomarker for non-invasive assessment of liver fibrosis. ECV calculation requires hematocrit (Hct) sampling, which might be difficult to obtain in a high-throughput radiology department. The aim of this study was to generate synthetic ECV for hepatic applications without the need for Hct sampling.

Methods In this prospective study participants underwent liver MRI. T1 mapping was performed before and after contrast administration. Blood Hct was obtained prior to MRI. We hypothesized that the relationship between Hct and longitudinal relaxation rate of blood ($R1 = 1/T1_{blood}$) could be calibrated and used to generate the equation for synthetic Htc and ECV calculation. Conventional and synthetic ECV were calculated. Pearson correlation, linear regression and Bland–Altman method were used for statistical analysis.

Results 180 consecutive patients were divided into derivation ($n = 90$) and validation ($n = 90$) cohorts. In the derivation cohort, native $R1_{blood}$ and Hct showed a linear relationship ($Hct_{MOLLI} = 98.04 \times (1/T1_{blood}) - 33.17$, $R^2 = 0.75$, $P < 0.001$), which was used to calculate synthetic ECV in the validation and whole study cohorts. Synthetic and conventional ECV showed significant correlations in the derivation, validation and in the whole study cohorts ($r = 0.99$, 0.97 and 0.99, respectively, $P < 0.001$, respectively) with minimal bias according to the Bland–Altman analysis.

Conclusion Synthetic ECV seems to offer an alternative method for non-invasive quantification of the hepatic ECV. It may potentially overcome an important barrier to clinical implementation of ECV and thus, enable broader use of hepatic ECV in routine clinical practice.

Keywords Magnetic resonance imaging · Extracellular volume fraction · Liver fibrosis · Hematocrit

Abbreviations

MRI	Magnetic resonance imaging
ECV	Extracellular volume fraction
Htc	Hematocrit

Introduction

Chronic liver disease is a global public health concern and accounts for approximately 2 million deaths per year worldwide [1]. Liver cirrhosis as a consequence of chronic liver disease is currently the 11th most common cause of death globally and within the top 20 causes of disability-adjusted life years and years of life lost [2]. The detection and staging of liver fibrosis is of great clinical importance for treatment decisions and prognosis estimation, therefore, reliable tools are necessary in these patients. Although considered the gold standard, liver biopsy has its clear drawbacks and, therefore, is no longer routinely performed for staging and monitoring of liver fibrosis. Consequently, non-invasive techniques such as transient elastography and magnetic resonance elastography (MR-elastography) are increasingly preferred in order to diagnose and grade liver fibrosis. Especially MR-elastography

✉ Julian A. Luetkens
julian.luetkens@ukbonn.de

1 Department of Diagnostic and Interventional Radiology, University Hospital Bonn, Venusberg-Campus 1, 53127 Bonn, Germany

2 Quantitative Imaging Lab (QILab), Venusberg-Campus 1, 53127 Bonn, Germany

3 Department of Internal Medicine I, University Hospital Bonn, Venusberg-Campus 1, 53127 Bonn, Germany

is considered one of the most accurate non-invasive technique for liver fibrosis assessment with accuracies varying from 89 to 95% depending on fibrosis stage and underlying liver disease [3, 4]. However, it can be associated with a high technical failure rate, i.e., in patients with massive ascites, obesity or iron deposition [5, 6].

In differentiating between normal and diseased liver parenchyma, the concept of evaluating the T1 relaxation times was first mentioned in the 1980s. Hepatic fibrosis increases the T1 relaxation time of liver parenchyma due to an increase of extracellular matrix and protein concentration. T1 mapping techniques also allow the estimation of extracellular volume fraction (ECV) from native and post-contrast T1. ECV values are calculated from the change in relaxation rate (R1 = 1/T1) of blood and parenchyma corrected for the hematocrit (Hct) [7]. Therefore, calculation of ECV requires Hct sampling. MRI-derived ECV using T1 mapping techniques is currently of increased interest as a new non-invasive tool for liver fibrosis assessment [7–12]. There are already studies, demonstrating a high diagnostic performance of ECV in liver fibrosis assessment in both, animal and human models [7, 9]. ECV correlates with histological markers of liver fibrosis and has a high diagnostic performance for liver fibrosis assessment with accuracies up to 85% depending on underlying liver disease and fibrosis stage [7, 9, 13–15]. Furthermore, the longitudinal reflexivity (R1 = 1/T1) of blood is known to be in a linear relationship with blood Hct. It is determined by the water fractions of plasma and the erythrocyte cytoplasm, which undergo fast water exchange [16–21]. Previous cardiac MRI studies showed that ECV quantification without blood sampling, assuming a linear relationship between blood Hct and longitudinal T1 relaxation times ($1/T1_{blood}$), is feasible [22, 23]. But there are still no studies showing whether it is also applicable for calculation of hepatic ECV. A synthetic ECV calculation would be beneficial considering the fact that liver fibrosis assessment and staging using T1 mapping techniques could be performed non-invasively and time-efficient directly after the MRI examination.

The hypothesis of our study was that a linear relationship between blood Hct and longitudinal T1 relaxation times ($1/T1_{blood}$) could be used for synthetic Hct estimation, which permits synthetic ECV calculation without Hct sampling. The aim of this study was (1) to create a synthetic Hct regression model and (2) to investigate whether synthetic Hct can be used for reliable and valid calculation of synthetic ECV compared to conventional ECV.

Materials and methods

This study was approved by the institutional review board. Written informed consent was obtained from all participants prior to MRI examination. From March 2019 to November 2020, consecutive patients with clinical indications for liver MRI examination were included in this study. Patients with and without chronic liver disease were included. Diagnosis of chronic liver disease was based on past medical history (including liver biopsy, clinical and laboratory examinations) and MRI (including MR-elastography). When necessary, the presence of significant fibrosis at MRI was assessed by MR-elastography as a reference standard using previous published cutoffs [3, 4]. Exclusion criteria were contraindications for contrast-enhanced MRI. Hematocrit samples were derived directly prior to MRI examination. According to the underlying liver disease, all patients were randomly split into the derivation and validation cohort. Clinical data and additional laboratory markers were recorded from the patient charts. Biochemical blood analyses were performed using standard tests and non-invasive scoring systems based on laboratory tests for assessment of liver fibrosis (aspartate aminotransferase-to-platelet ratio index (ARPI), fibrosis index based on the 4 factor (FIB-4), MELD score (Model of End Stage Liver Disease) and aspartate aminotransferase and alanine aminotransferase ratio (AST/ALT ratio (de-Ritis)) were calculated [24–26].

Magnetic resonance imaging

All participants underwent MRI examination on a clinical whole-body 1.5-T system (Ingenia, Philips Healthcare) equipped with 32-channel abdominal coil with digital interface for signal reception. In addition to morphological sequences, patients underwent hepatic T1 mapping with a heart rate independent 10-(2)-7-(2)-5-(2)-3-(2) modified Look-Locker inversion recovery (MOLLI) acquisition scheme with internal triggering [27]. Technical parameters were as follows: time of repetition/time of echo 1.92/0.84 ms, flip angle 20°, parallel imaging factor 2, acquired voxel size 1.98 × 2.45 × 10 mm, reconstructed voxel size 1.13 × 1.13 × 10 mm, scan duration/breath-hold 14.0 s. For the post-contrast T1 maps, the same technique was used after 10 min of contrast agent application in the same positions as pre-contrast examinations. T1 maps were acquired in end-expiration [28]. For contrast-enhanced T1 mapping, a gadolinium-based contrast agent (Gadobutrol, 1.0 mmol/ml solution with 0.1 mmol per kilogram of body weight, Gadovist, Bayer Healthcare Pharmaceuticals) was administered as a single bolus with an injection rate of 1.5 ml/s. Hepatic quantitative maps were acquired in a single transversal slice at the level of the bifurcation of portal vein. Relaxation maps were reconstructed directly at the scanner console. Liver MR-elastography was performed with a 2D gradient-recalled echo sequence to acquire liver elasticity maps with motion-encoding gradients. MR-elastography measurements were performed as previously described [8].

Image analysis

An experienced board-certified radiologist (J.A.L, 8 years of experience in abdominal MRI) performed image analyses, blinded to the clinical data. For the assessment of T1 relaxation times, the mean relaxation time of three representative regions of interest (ROI) (≥ 1 cm^2), drawn centrally in the hepatic segments II, IVa and VII, were calculated (see also Fig. 1). Blood pool T1 values were derived from the abdominal aorta. In the derivation cohort as well as whole study cohort conventional ECV values were normalized for blood Hct and calculated with ROI-based on pre- and post-contrast T1 values according to the previously published equation [29]: ECV = (1 − hematocrit) × (1/T1 parenchyma post-contrast − 1/T1 parenchyma pre-contrast)/(1/T1 aortic post-contrast − 1/T1 aortic pre-contrast).

Proof-of-concept: synthetic hepatic ECV calculation

The longitudinal relaxivity of blood (R1 = 1/T1) demonstrate a linear relationship with blood Htc, and is determined by the relaxivity of the water fractions of plasma ($R1_P$) and the erythrocyte cytoplasm ($R1_{RBC}$) [17]: $R1_{blood} = R1_p \times (1 - Hct) + R1_{RBC} \times Hct$. Hence, synthetic Hct was derived from the linear relationship between Hct and $R1_{blood}$ and used to calculate synthetic ECV. Synthetic ECV was normalized for synthetic Hct and calculated using the same equation as conventional ECV. Synthetic and conventional ECV were then compared.

Statistical analysis

Statistical analysis was performed using software (SPSS Statistics, version 25, IBM; Prism 8, GraphPad Software). Patient characteristics are presented as mean ± standard deviation or as absolute frequency, as appropriate. Student t test was used for comparison of continuous variables between two different groups. Dichotomous variables were compared using the χ^2 test (with the cell count > 5) and Fisher test (with a cell count ≤ 5). A locally derived synthetic ECV was created from the longitudinal relaxivity of blood (R1, or 1/T1). This model was created using linear regression, where R1 is the predictor variable and the measured Hct is the outcome. The bivariate Pearson correlation coefficient (r) was used for a correlation analysis between synthetic and blood Hct as well as synthetic and conventional ECV. Agreement between individual sets of blood and synthetic Hct as well as conventional and synthetic ECV was analyzed and represented graphically using the Bland–Altman method. The level of statistical significance was set to $P < 0.05$.

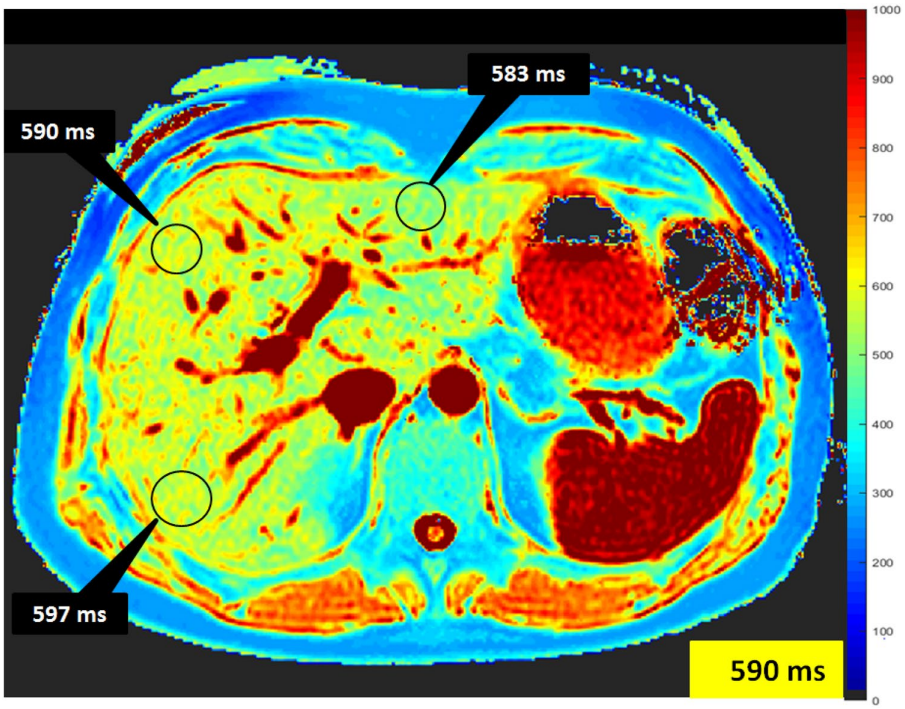

Fig. 1 Representative image demonstrating assessment of T1 relaxation times derived from T1 maps. The mean relaxation time of three representative regions of interest drawn centrally in the hepatic segments II, IVa and VII was assessed calculated

Results

Cohort characteristics

A total of 180 consecutive patients were included. In the whole study cohort, 87.8% (158/180) of patients had diffuse liver disease and 12.2% (22/180) of patients did not have diffuse liver disease based on past medical history, clinical and laboratory examinations as well as MR-elastography. The mean MR-elastography derived liver stiffness in the group of patients without chronic and/or fibrotic liver disease was 2.1 ± 0.5 kPa. This group of patients consisted of patients with indications for liver MRI examinations as follows: non-specific abdominal symptoms, e.g., non-specific abdominal pain (11/22, 50.0%) or liver lesions detection or/and characterization (11/22, 50.0%). Indications for all MRI examinations in patients with diffuse liver disease were follow-up and/or malignancy exclusion by known chronic liver disease. Etiologies of liver diseases included: alcoholic liver disease ($n = 27$, 15.0%); autoimmune liver diseases, including autoimmune hepatitis, primary sclerosing cholangitis, and primary biliary cirrhosis ($n = 80$, 44.4%); non-alcoholic fatty liver disease ($n = 12$, 6.7%); viral hepatitis ($n = 13$, 7.2%) and other rare etiologies such as portal sinusoidal disease, Budd–Chiari syndrome and Fontan-associated hepatopathy ($n = 5$/180, 2.8%) as well as cryptogenic hepatopathy ($n = 21$, 11.7%). All patients were randomly divided into the derivation ($n = 90$) and validation ($n = 90$) cohorts. The derivation cohort was used to establish the linear regression equation for calculation of synthetic Htc and ECV. The clinical characteristics of the derivation and validation cohorts are presented in Table 1.

MRI results

Derivation cohort

For the applied hepatic T1 MOLLI mapping sequence, the regression line between hematocrit and $R1_{blood}$ was linear with $R^2 = 0.75$, $P < 0.001$. The regression equation for Htc was: Synthetic $Hct_{MOLLI} = 98.04 \times (1/T1_{blood}) - 33.17$, where Hct is hematocrit (1 to 100%) and $R1_{blood} = 1/T1_{blood}$ in 10^{-3} s (see also Fig. 2). No significant differences in blood and synthetic Hct (38.5 ± 6.1% vs. 38.5 ± 5.3%, $P > 0.05$) as well as between conventional and synthetic ECV (32.7 ± 8.5% vs. 32.6 ± 7.9%, $P > 0.05$) were found using the above-mentioned equation. Moreover, we found significant correlations between synthetic and blood Htc ($r = 0.87$) as well as synthetic and conventional ECV ($r = 0.99$), in each case $P < 0.001$ (see also Fig. 3).

Validation cohort

Using above-named equation derived from derivation cohort in the validation cohort, we found no significant differences between blood and synthetic Htc values (39.6 ± 5.1% vs. 38.6 ± 4.8%, $P > 0.05$) as well as conventional and synthetic ECV (30.0 ± 6.7% vs. 30.6 ± 6.9%, $P > 0.05$). Moreover, synthetic and conventional ECV were highly correlated ($r = 0.97$, $P < 0.001$). Synthetic and blood Hct also correlated well ($r = 0.81$, $P < 0.001$). Bland–Altman analysis demonstrated minimal bias for both Hct (− 0.97 ± 3.25%, 95% limits of agreement: − 7.4% to 5.4%) as well as ECV (0.53 ± 1.67, 95% limits of agreement: − 2.75% to − 3.82%) (see also Figs. 4, 5 and 6). MRI characteristics of patients in the derivation and validation cohorts are presented in Table 2.

Moreover, we found also strong correlation between conventional and synthetic ECV in patients with chronic liver disease in the whole study cohort with a Pearson's correlation coefficient of 0.98 ($P < 0.001$).

Discussion

The purpose of our study was to (1) create locally derived synthetic Hct values from the linear relationship between blood Hct and the longitudinal relaxivity (R1) of the blood and (2) investigate whether synthetic Hct can be used for reliable and valid calculation of synthetic hepatic ECV compared to conventional hepatic ECV. The main findings of our study are that: (1) synthetic Hct derived from linear regression modeling showed a strong correlation with blood Hct and, (2) synthetic ECV showed a strong correlation with conventional ECV and minimal bias according to the Bland–Altman analysis and, therefore, has a potential to be used as a reliable valid biomarker in routine clinical practice alternatively to conventional ECV.

Liver fibrogenesis in patients with chronic liver disease is a consequence of cellular damage and following regeneration processes, leading to increased production of connective tissue with extracellular matrix components. This process leads to the extension of extracellular space and an increased accumulation of extracellular contrast agents, which is reflected by prolonged native T1 relaxation times and increased ECV of the liver. Therefore, with a growing body of evidence, calculation of ECV is considered a new promising potential biomarker for non-invasive assessment of liver fibrosis [7–9]. Therefore, parametric MRI mapping including ECV requires routine clinical use of mapping beyond morphological sequences. However, calculation of ECV requires hematocrit sampling, which may limit the application and availability of these techniques in routine clinical practice. As a result, attempts have been made to

Table 1 Clinical characteristics of patients in the validation and derivation cohorts

Variable	Derivation cohort ($n=90$)	Validation cohort ($n=90$)	P value
Age (years)	47.7 ± 16.7	48.6 ± 15.4	0.71
Body mass index (kg/m^2)	25.6 ± 4.8	25.3 ± 5.3	0.71
Sex			0.88
Male	48	47	
Female	42	43	
Blood hematocrit level (%)	38.5 ± 6.1	39.6 ± 5.1	0.21
Underlying liver disease			
Primary sclerosing cholangitis (PSC)	22 (24.4%)	21 (23.3%)	0.88
Autoimmune hepatitis (AIH)	8 (8.9%)	9 (15%)	0.88
AIH/PSC overlap syndrome	8 (8.9%)	8 (8.9%)	1.00
Primary biliary cirrhosis	2 (22.2%)	2 (22.2%)	1.00
Alcoholic liver disease	14 (15.5%)	13 (7.2%)	0.88
Viral hepatitis	6 (6.7%)	7 (3.9%)	0.88
Non-alcoholic fatty liver disease (NASH)	6 (6.7%)	6 (6.7%)	1.00
Portal sinusoid disease	1 (1.1%)	1 (1.1%)	1.00
Unknown	11 (15.0%)	10 (8.9%)	0.88
Fontan-associated hepatopathy	1 (1.1%)	1 (1.1%)	1.00
Budd–Chiari syndrome	0 (0%)	1 (1.1%)	
No chronic liver disease	11 (12.2%)	11 (12.2%)	1.00
Laboratory parameters			
Bilirubin (mg/dl)	1.33 ± 1.9	1.0 ± 0.74	0.16
ALT (U/l)	77.0 ± 146.1	62.6 ± 87.7	0.43
AST (U/l)	69.7 ± 105.3	51.1 ± 48.5	0.14
GGT (U/l)	182.7 ± 230.5	121.9 ± 150.6	0.04
Platelets cells × 10^9/l	222.1 ± 109.7	228.1 ± 111.9	0.72
C-reactive protein level (mg/l)	11.6 ± 21.3	5.2 ± 7.7	0.01
AP (U/l)	178.2 ± 181.1	122.4 ± 84.6	0.01
Creatinine (mg/dl)	0.86 ± 0.29	0.90 ± 0.41	0.45
Albumin (g/l)	39.0 ± 10.4	41.2 ± 8.4	0.18
International normalized ratio	1.16 ± 0.36	1.09 ± 0.16	0.11
ASL/ALT (de-Ritis)	1.27 ± 0.9	1.07 ± 0.57	0.07
FIB-4	2.9 ± 3.5	2.3 ± 2.8	0.22
MELD	9.0 ± 4.5	8.43 ± 3.6	0.35
APRI	1.01 ± 1.57	0.76 ± 0.98	0.20

Continuous data are means ± standard deviations. Nominal data are absolute frequencies with percentages in parentheses

MELD Score Model of End Stage Liver Disease, *ALT* alanine aminotransferase, *AST* aspartate aminotransferase, *AP* alkaline phosphatase, *GGT* gamma-glutamyltransferase, *APRI* aspartate aminotransferase-to-platelet ratio index, *FIB-4* fibrosis-4 score, *ASL/ALT (de-Ritis)* De-Ritis ratio

eliminate the necessity for blood Htc through estimation of a synthetic Htc in order to calculate an ECV based on the observed linear relationship between Htc and blood R1 ($1/T1_{blood}$). However, the clinical validity of this approach for abdominal applications has not been established yet. A few recent studies in cardiac MRI already demonstrated that synthetic ECV quantification without blood sampling might be a reliable valid tool compared with conventional ECV [22, 23, 30]. However, to our knowledge, there are still no studies showing whether this is also applicable for calculation of hepatic ECV.

In our study we implemented a simple to obtain synthetic ECV measurement using Hct derived from pre-contrast blood T1. The linear relationship between Hct and $R1_{blood}$ has been sufficiently investigated [17, 19–21, 31, 32], and, therefore, we used R1 for curve fitting. We found strong correlations between blood and synthetic Hct with Pearson's correlation coefficient of 0.81 and 0.83 in the validation as

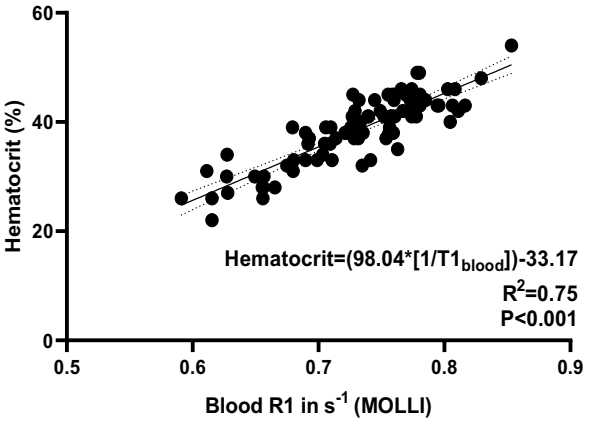

Fig. 2 Derivation cohort: Correlation $R1_{blood}$ versus hematocrit using abdominal T1 MOLLI mapping sequence. The regression line between hematocrit and pre-contrast $R1_{blood}$ was linear with $R^2 = 0.75$, $P < 0.001$ with regression equation as given in the graph. Regression line is given with 95% confidence interval. *MOLLI* modified Look-Locker Inversion Recovery

well as the whole study cohort, respectively ($P < 0.001$ in each case). There were also strong correlations between conventional and synthetic ECV in the validation as well as the whole study cohort with $r = 0.97$ and 0.99, respectively ($P < 0.001$ in each case). As far as the results of this study can be compared with the results of previous cardiac studies, these findings support previous data, demonstrating higher correlations between synthetic and conventional ECV compared to synthetic and blood Hct [22, 23]. On the one hand it could be explained by a considerable error in Htc laboratory tests. On the other hand, ECV has other dependencies and additional terms, making it a more stable and robust parameter [33, 34]. Therefore, there could be more inaccuracy as a result of Hct measurements than that as a result of variations in T1 mapping approaches [35, 36]. However, regardless of excellent linear regression fit and in general strong correlations between blood and synthetic Htc as well as conventional and synthetic ECV values, the main disadvantage of synthetic ECV application is that it might lead to considerable errors in individual cases. According to Bland–Altman analysis these variations in

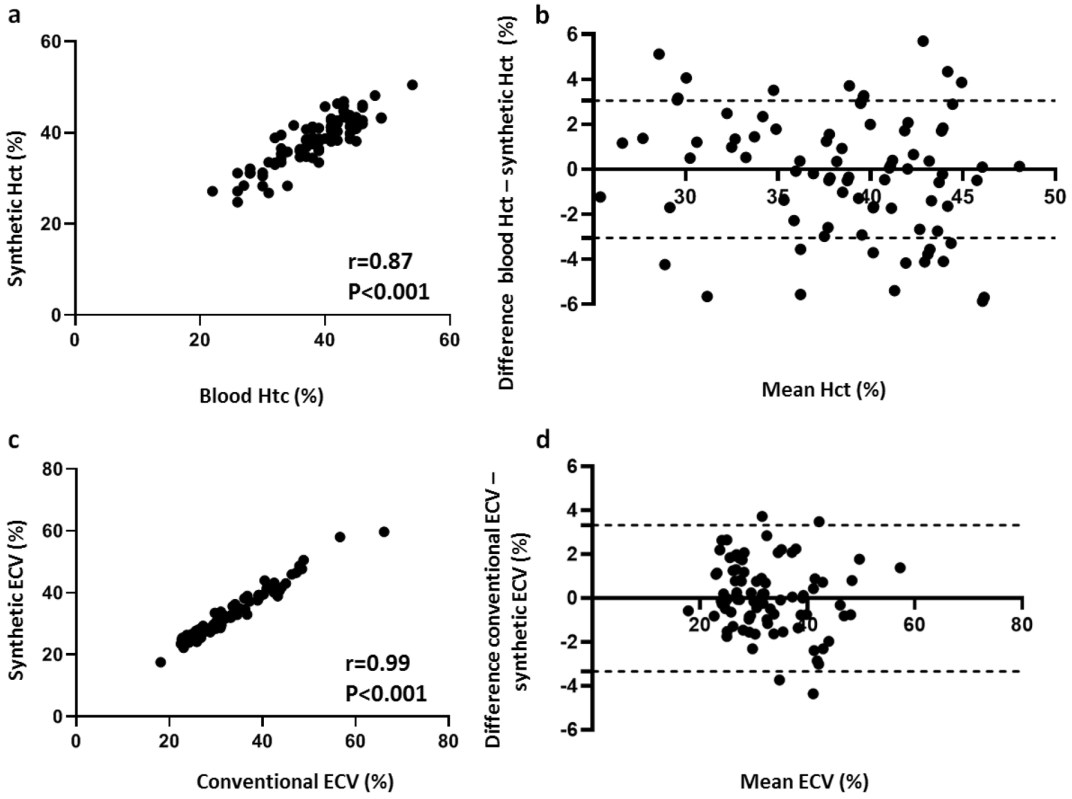

Fig. 3 Derivation cohort: synthetic versus blood hematocrit (**a**, **b**) as well as synthetic versus conventional ECV (**c**, **d**). Scatter plots shows correlations between synthetic and blood Hct as well as synthetic and conventional ECV ($n = 90$) (**a**, **c**). Bland–Altman plots of mean differences between blood and synthetic Htc as well as conventional and synthetic ECV. The mean value of measurements for both approaches is plotted on the *x*-axis and the difference between techniques is plotted on the *y*-axis. The solid black horizontal line plots the mean difference and the dotted black lines indicate the limits of agreement (differences from the mean of 1.96 SDs) for each parameter (**b**, **d**). *Htc* hematocrit, *ECV* extracellular volume fraction

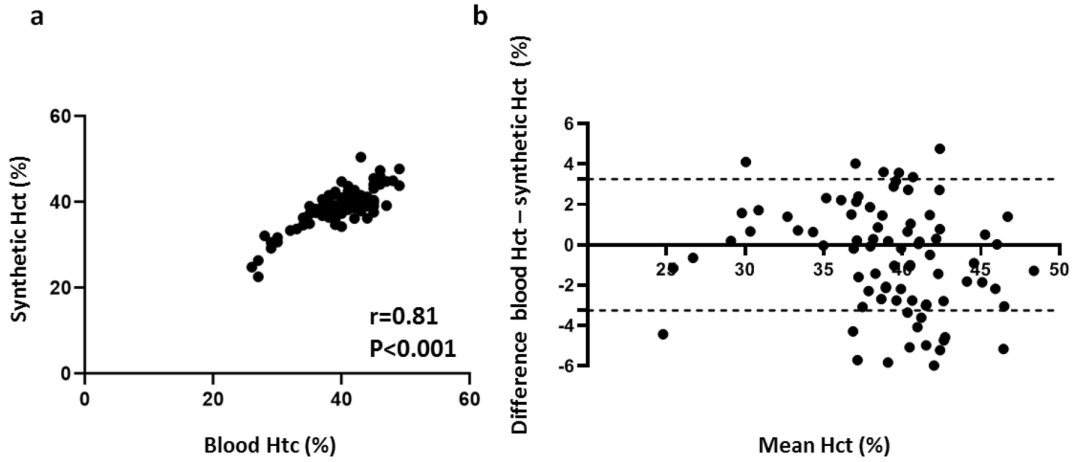

Fig. 4 Validation cohort: synthetic versus blood hematocrit. Scatter plots show correlations between synthetic and blood Hct ($n=90$) (**a**). Bland–Altman plots of mean differences between blood Hct and synthetic Hct. The mean value of measurements for both approaches is plotted on the x-axis and the difference between techniques is plotted on the *y*-axis. The solid black horizontal line plots the mean difference and the dotted black lines indicated the limits of agreement (differences from the mean of 1.96 SDs) for each parameter (**b**). *Htc* hematocrit

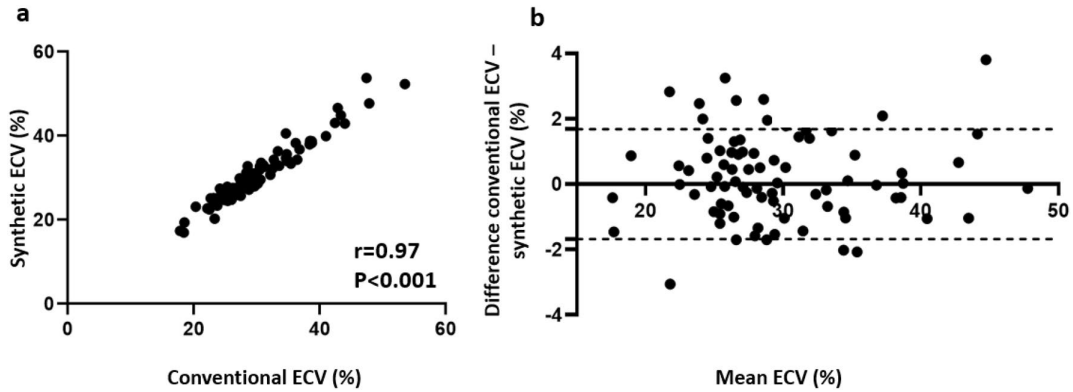

Fig. 5 Validation cohort: synthetic versus conventional ECV. Scatter plots show correlations between synthetic and conventional ECV ($n=90$) (**a**). Bland–Altman plots of mean differences between conventional and synthetic ECV. The mean value of measurements for both approaches is plotted on the *x*-axis and the difference between techniques is plotted on the *y*-axis. The solid black horizontal line plots the mean difference and the dotted black lines indicate the limits of agreement (differences from the mean of 1.96 SDs) for each parameter (**b**). *ECV* extracellular volume fraction

individual measurement sets may reach up to 6% between blood and synthetic Hct and up to 4% between conventional and synthetic ECV (see also Figs. 4 and 5). Although the variations between conventional and synthetic ECV were less than 2%, higher variations may have clinical importance for liver fibrosis staging. Patients could be misclassified in a wrong fibrosis stage, which is especially vital for the detection of significant fibrosis. The presence of even greater variabilities was also demonstrated in previous cardiac studies, with more pronounced differences in Htc than in ECV values [22, 23]. The variability in laboratory Htc and calibration of conventional ECV to blood Hct may also lead to miscategorization. Hence, precise clinical evaluation based on medical history, laboratory examinations as well as MRI (including, e.g., MR-elastography) in individual patients are needed to minimize the possible discrepancies between synthetic and conventional values and therefore its influence on clinical decision-making (Table 3).

There are several limitations in our study. The main limitation was that the sample size was modest and all examinations were performed in a single center. Furthermore, the fact that T1 mapping techniques vary across the institutions can additionally limit the applicability of our study results. Furthermore, synthetic Hct requires local

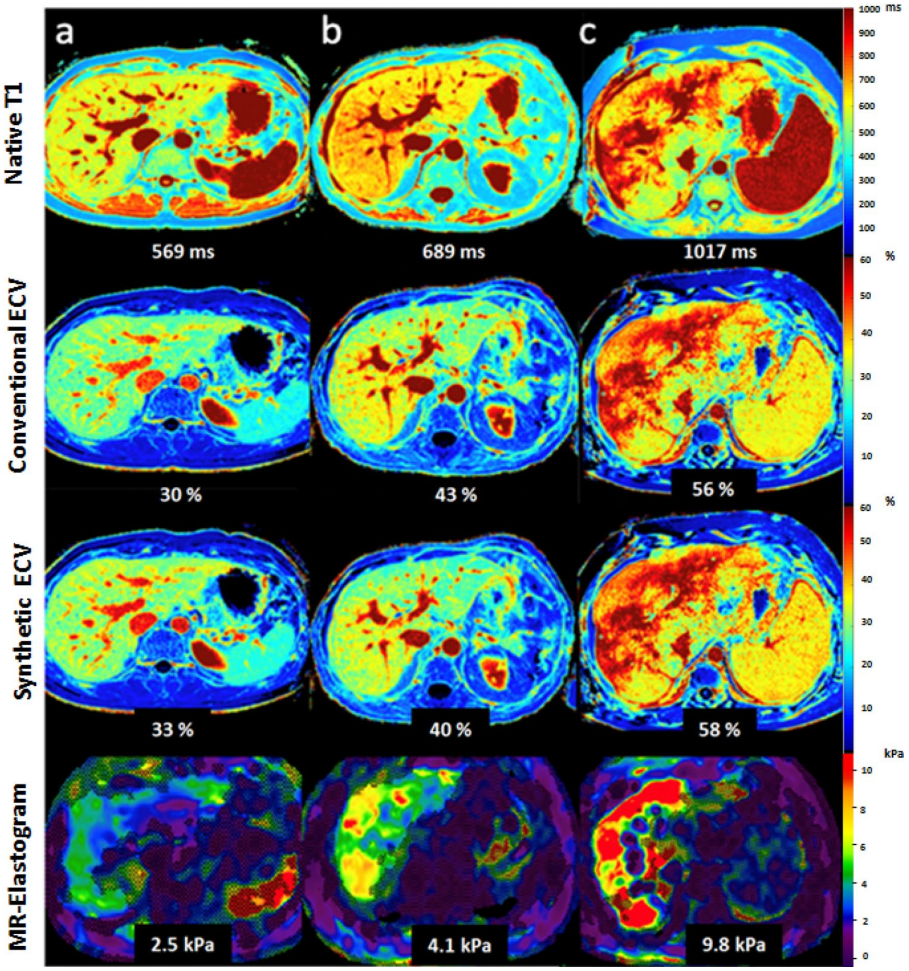

Fig. 6 Representative images of conventional and synthetic hepatic extracellular volume (ECV) maps from a 30-year-old male patient with no diffuse liver disease (**a**), from a 24-year-old female patient with autoimmune hepatitis and advanced fibrosis (fibrosis stage (F) 3, **b**) and a 49-year-old male patient with alcoholic liver disease and cirrhosis (F4, **c**) with corresponding MR elastograms. *ECV* extracellular volume fraction

Table 2 MRI characteristics of patients in the derivation and validation cohorts

Variable	Derivation cohort ($n=90$)	Validation cohort ($n=90$)	P value
Hepatic native T1 relaxation time (ms)	600.5 ± 108.3	571.5 ± 94.0	0.06
Native T1 relaxation time of blood (ms)	1376.6 ± 106.9	1372.3 ± 99.4	0.78
Conventional extracellular volume fraction (%)	32.7 ± 8.5	30.0 ± 6.7	0.02
Synthetic extracellular volume fraction (%)	32.6 ± 7.9	30.6 ± 6.9	0.06
Synthetic hematocrit (%)	38.5 ± 5.3	38.6 ± 4.8	0.83
MR-elastography derived liver stiffness	4.5 ± 1.6	4.2 ± 1.9	0.46

Continuous data are means ± standard deviations

calibration, unless MRI scanner, used T1 mapping parameters, and machine for Hct laboratory are the same. Moreover, as the accuracy of current T1 measurements method remains to be established, this study does not claim to report an accurate measure of T1, but that synthetic calculation of hepatic Hct derived from used T1 MOLLI sequence is a stable and reliable approach for routine clinical practice. Another significant limitation for clinical application of synthetic measurements is that equations for synthetic Hct calculation should be derived individually on each MRI scanner using the same acquisition scheme. Therefore, if synthetic ECV is to be used in routine clinical practice where blood Hct cannot be obtained, using a locally derived synthetic Hct regression model for the used T1 mapping sequence is preferred.

Table 3 Correlation values for synthetic hematocrit and ECV in the derivation, validation and the whole study cohorts

Variable	Derivation cohort		Validation cohort		Whole study cohort	
	R value	*P* value	*R* value	*P* value	*R* value	*P* value
Blood hematocrit vs. synthetic hematocrit	0.87	< 0.001	0.81	< 0.001	0.83	< 0.001
Conventional ECV vs. synthetic ECV	0.99	< 0.001	0.97	< 0.001	0.99	< 0.001

ECV extracellular volume fraction

In conclusion, this is the first study investigating the applicability of synthetic hepatic Hct derived from a regression model for ECV calculation without Htc sampling. Our findings suggest that ECV calculated from synthetic Hct may be a useful, valid and reliable tool compared with conventional ECV. Further multi-centric prospective studies on a larger population are needed to validate these findings across the centers, using different T1 mapping sequences to enable the further clinical implementation of ECV by liver examinations. The use of synthetic ECV may potentially overcome an important barrier for clinical implementation of hepatic ECV measurements.

Author contribution J.A.L. and N.M. guarantors of integrity of entire study, contributed substantially to data acquisition, analysis, and interpretation; N.M. wrote the main manuscript text and prepared the figures and tables; all authors manuscript drafting or manuscript revision for important intellectual content; all authors approval of final version of submitted manuscript; J.A.L. and N.M. literature research; J.A.L. and N.M. manuscript editing.

Funding Open Access funding enabled and organized by Projekt DEAL. The authors did not receive support from any organization for the submitted work.

Data Availability The datasets generated and/or analyzed during the current study are available from the corresponding author on reasonable request.

Declarations

Conflicts of interest The authors have no relevant financial or non-financial interests to disclose.

Ethical approval This study was performed in line with the principles of the Declaration of Helsinki. Institutional Review Board of University Hospital Bonn approval was obtained.

Consent to participate Written informed consent was obtained from all subjects (patients) in this study.

References

1. Moon AM, Singal AG, Tapper EB (2020) Contemporary Epidemiology of Chronic Liver Disease and Cirrhosis. Clin Gastroenterol Hepatol 18:2650–2666. https://doi.org/10.1016/j.cgh.2019.07.060
2. Asrani SK, Devarbhavi H, Eaton J et al. (2019) Burden of liver diseases in the world. Journal of Hepatology 70. https://doi.org/10.1016/j.jhep.2018.09.014
3. Singh S, Venkatesh SK, Wang Z, et al. (2015) Diagnostic performance of magnetic resonance elastography in staging liver fibrosis: a systematic review and meta-analysis of individual participant data. Clin Gastroenterol Hepatol 13:440–451.e6. https://doi.org/10.1016/j.cgh.2014.09.046
4. Hoodeshenas S, Yin M, Venkatesh SK (2018) Magnetic Resonance Elastography of Liver: Current Update. Top Magn Reson Imaging 27:319–333. https://doi.org/10.1097/RMR.0000000000000177
5. Guo Y, Parthasarathy S, Goyal P, et al. (2015) Magnetic resonance elastography and acoustic radiation force impulse for staging hepatic fibrosis: a meta-analysis. Abdom Imaging 40:818–834. https://doi.org/10.1007/s00261-014-0137-6
6. Wagner M, Corcuera-Solano I, Lo G, et al. (2017) Technical Failure of MR Elastography Examinations of the Liver: Experience from a Large Single-Center Study. Radiology 284:401–412. https://doi.org/10.1148/radiol.2016160863
7. Luetkens JA, Klein S, Träber F, et al. (2018) Quantification of Liver Fibrosis at T1 and T2 Mapping with Extracellular Volume Fraction MRI: Preclinical Results. Radiology 288:748–754. https://doi.org/10.1148/radiol.2018180051
8. Mesropyan N, Kupczyk P, Dold L, et al. (2020) Non-invasive assessment of liver fibrosis in autoimmune hepatitis: Diagnostic value of liver magnetic resonance parametric mapping including extracellular volume fraction. Abdom Radiol (NY) . https://doi.org/10.1007/s00261-020-02822-x
9. Luetkens JA, Klein S, Traeber F, et al. (2018) Quantitative liver MRI including extracellular volume fraction for non-invasive quantification of liver fibrosis: a prospective proof-of-concept study. Gut 67:593–594. https://doi.org/10.1136/gutjnl-2017-314561
10. Hoffman DH, Ayoola A, Nickel D, et al. (2020) MR elastography, T1 and T2 relaxometry of liver: role in noninvasive assessment

of liver function and portal hypertension. Abdom Radiol (NY) 45:2680–2687. https://doi.org/10.1007/s00261-020-02432-7
11. (1987) Magnetic resonance imaging of parenchymal liver disease: a comparison with ultrasound, radionuclide scintigraphy and X-ray computed tomography. Clinical Radiology 38:495–502. https://doi.org/10.1016/s0009-9260(87)80131-9
12. Thomsen C, Christoffersen P, Henriksen O, et al. (1990) Prolonged T1 in patients with liver cirrhosis: An in vivo MRI study. Magnetic Resonance Imaging 8:599–604. https://doi.org/10.1016/0730-725X(90)90137-Q
13. Kupczyk PA, Mesropyan N, Isaak A, et al. (2021) Quantitative MRI of the liver: Evaluation of extracellular volume fraction and other quantitative parameters in comparison to MR elastography for the assessment of hepatopathy. Magnetic Resonance Imaging 77:7–13. https://doi.org/10.1016/j.mri.2020.12.005
14. Mesropyan N, Kupczyk P, Kukuk GM, et al. (2021) Diagnostic value of magnetic resonance parametric mapping for non-invasive assessment of liver fibrosis in patients with primary sclerosing cholangitis. BMC Med Imaging 21:65. https://doi.org/10.1186/s12880-021-00598-0
15. Yoon JH, Lee JM, Kim JH, et al. (2021) Hepatic fibrosis grading with extracellular volume fraction from iodine mapping in spectral liver CT. Eur J Radiol 137: https://doi.org/10.1016/j.ejrad.2021.109604
16. Spees WM, Yablonskiy DA, Oswood MC, et al. (2001) Water proton MR properties of human blood at 1.5 Tesla: magnetic susceptibility, T(1), T(2), T*(2), and non-Lorentzian signal behavior. Magn Reson Med 45:533–542. https://doi.org/10.1002/mrm.1072
17. Li W, Grgac K, Huang A, et al. (2016) Quantitative theory for the longitudinal relaxation time of blood water. Magn Reson Med 76:270–281. https://doi.org/10.1002/mrm.25875
18. Shimada K, Nagasaka T, Shidahara M, et al. (2012) In vivo measurement of longitudinal relaxation time of human blood by inversion-recovery fast gradient-echo MR imaging at 3T. Magn Reson Med Sci 11:265–271. https://doi.org/10.2463/mrms.11.265
19. Lu H, Clingman C, Golay X, et al. (2004) Determining the longitudinal relaxation time (T1) of blood at 3.0 Tesla. Magn Reson Med 52:679–682. https://doi.org/10.1002/mrm.20178
20. Martin MA, Tatton WG, Lemaire C et al. (1990) Determination of extracellular/intracellular fluid ratios from magnetic resonance images: accuracy, feasibility, and implementation. Magn Reson Med 15. https://doi.org/10.1002/mrm.1910150107
21. Piechnik SK, Ferreira VM, Lewandowski AJ et al. (2013) Normal variation of magnetic resonance T1 relaxation times in the human population at 1.5 T using ShMOLLI. J Cardiovasc Magn Reson 15:13. https://doi.org/10.1186/1532-429x-15-13
22. Treibel TA, Fontana M, Maestrini V et al. (2016) Automatic Measurement of the Myocardial Interstitium: Synthetic Extracellular Volume Quantification Without Hematocrit Sampling. JACC. Cardiovascular imaging 9. https://doi.org/10.1016/j.jcmg.2015.11.008
23. Raucci FJ, Parra DA, Christensen JT, et al. (2017) Synthetic hematocrit derived from the longitudinal relaxation of blood can lead to clinically significant errors in measurement of extracellular volume fraction in pediatric and young adult patients. J Cardiovasc Magn Reson 19:58. https://doi.org/10.1186/s12968-017-0377-z
24. Li J, Gordon SC, Rupp LB et al. (2014) The validity of serum markers for fibrosis staging in chronic hepatitis B and C. Journal of viral hepatitis 21. https://doi.org/10.1111/jvh.12224
25. Sterling RK, Lissen E, Clumeck N, et al. (2006) Development of a simple noninvasive index to predict significant fibrosis in patients with HIV/HCV coinfection. Hepatology 43:1317–1325. https://doi.org/10.1002/hep.21178
26. Imperiale TF, Born LJ (2001) Clinical utility of the AST/ALT ratio in chronic hepatitis C. Am J Gastroenterol 96:919–920. https://doi.org/10.1111/j.1572-0241.2001.03647.x
27. Messroghli DR, Radjenovic A, Kozerke S, et al. (2004) Modified Look-Locker inversion recovery (MOLLI) for high-resolution T1 mapping of the heart. Magn Reson Med 52:141–146. https://doi.org/10.1002/mrm.20110
28. Vu K-N, Haldipur AG, Roh AT-H et al. (2019) Comparison of End-Expiration Versus End-Inspiration Breath-Holds With Respect to Respiratory Motion Artifacts on T1-Weighted Abdominal MRI. AJR Am J Roentgenol:1–6. https://doi.org/10.2214/ajr.18.20239
29. Schelbert EB, Messroghli DR (2016) State of the Art: Clinical Applications of Cardiac T1 Mapping. Radiology 278:658–676. https://doi.org/10.1148/radiol.2016141802
30. Robison S, Karur GR, Wald RM, et al. (2018) Noninvasive hematocrit assessment for cardiovascular magnetic resonance extracellular volume quantification using a point-of-care device and synthetic derivation. J Cardiovasc Magn Reson 20:19. https://doi.org/10.1186/s12968-018-0443-1
31. Fullerton GD, Potter JL, Dornbluth NC (1982) NMR relaxation of protons in tissues and other macromolecular water solutions. Magnetic Resonance Imaging 1:209–226. https://doi.org/10.1016/0730-725X(82)90172-2
32. Braunschweiger PG, Schiffer L, Furmanski P (1986) The measurement of extracellular water volumes in tissues by Gadolinium modification of 1H-NMR spin lattice (T1) relaxation. Magnetic Resonance Imaging 4:285–291. https://doi.org/10.1016/0730-725X(86)91038-6
33. Ugander M, Oki AJ, Hsu L-Y, et al. (2012) Extracellular volume imaging by magnetic resonance imaging provides insights into overt and sub-clinical myocardial pathology. Eur Heart J 33:1268–1278. https://doi.org/10.1093/eurheartj/ehr481
34. Wong TC, Piehler K, Meier CG, et al. (2012) Association between extracellular matrix expansion quantified by cardiovascular magnetic resonance and short-term mortality. Circulation 126:1206–1216. https://doi.org/10.1161/CIRCULATIONAHA.111.089409
35. Roujol S, Weingärtner S, Foppa M, et al. (2014) Accuracy, precision, and reproducibility of four T1 mapping sequences: a head-to-head comparison of MOLLI, ShMOLLI, SASHA, and SAPPHIRE. Radiology 272:683–689. https://doi.org/10.1148/radiol.14140296
36. Kellman P, Arai AE, Xue H (2013) T1 and extracellular volume mapping in the heart: estimation of error maps and the influence of noise on precision. J Cardiovasc Magn Reson 15:56. https://doi.org/10.1186/1532-429X-15-56

4 Discussion

The diagnostic value of MRI-derived quantitative mapping parameters for the assessment of liver fibrosis and disease severity was elaborated in this cumulative habilitation thesis. In particular, the diagnostic utility of MRI-derived quantitative mapping parameters for the non-invasive assessment of liver fibrosis severity in patients with autoimmune CLDs, such as AIH and PSC, was investigated. Non-invasive assessment and monitoring of liver fibrosis would allow for timely antifibrogenic therapies, monitoring of therapy response, and possibly prognosis estimation. Further, we explored the ability and diagnostic value of MRI-derived mapping parameters for the assessment of liver cirrhosis severity in CLDs of different etiologies. Quantitative mapping may play an important role in the clinical management of patients with liver cirrhosis due to non-invasive monitoring of liver cirrhosis severity, including the severity of portal hypertension. This approach could allow for timely interventions and prevention of life-threatening complications associated with portal hypertension. In general, the results of our studies expanded the clinical application of MRI-derived quantitative mapping parameters and demonstrated their potential value for non-invasive comprehensive characterization of liver fibrosis and disease severity.

Since the first introduction of quantitative mapping techniques for liver fibrosis assessment, there has been intensive research aimed at developing and establishing imaging-based biomarkers for the assessment of liver fibrosis. To date, numerous studies have focused on the diagnostic utility of various quantitative MRI mapping parameters for the non-invasive assessment of liver fibrosis in patients of CLDs of different etiologies (Wang et al., 2019; Ulmenstein et al., 2022; Thomsen et al., 1990; Obmann et al., 2021; Luetkens et al., 2018; Lu et al., 2022; Li et al., 2016b; Hoad et al., 2015). Considering the broad spectrum of CLDs, a separate investigation of mapping parameters in patients with specific etiologies of CLD is required. Following the concept of development and broader clinical implementation of non-invasive imaging-based, reliable, and accurate biomarkers, we could demonstrate the high diagnostic value of MRI-derived mapping parameters, even in specific etiologies of CLDs (i.e., AIH and PSC).

AIH is considered a relatively rare CLD and predominantly affects young and middle-aged females (5:1) (Puustinen et al., 2019). Autoimmune hepatitis remains a diagnosis of exclusion since there is no disease-specific test and one-third of patients present with advanced liver

disease. However, the epidemiological data on autoimmune hepatitis are likely to be underreported and underestimated. Based on European studies, the incidence of AIH is between 0.9. and 2 per 100,000 population per year with a prevalence rate of 11-25 cases per 100,000 population per year (Puustinen et al., 2019). Without timely therapy, AIH can lead to severe fibrosis and cirrhosis. Liver cirrhosis can develop in about 7% to 40% of treated patients (Pape et al., 2019). Furthermore, the development of cirrhosis in patients with AIH might be associated with incomplete response, treatment failure, and multiple relapses. The detection, accurate staging and life-long monitoring of the disease course are required (Heneghan et al., 2022).

Studies investigating the role of quantitative mapping in AIH patients are still insufficient or missing. Using MRE-based liver stiffness as the reference standard for liver fibrosis assessment, we found a strong correlation between hepatic ECV and liver stiffness measurements in patients with AIH with a correlation coefficient (r) of 0.80 ($P < 0.001$). Additionally, hepatic ECV showed high diagnostic performance for the detection of significant fibrosis ($F \geq 2$) in patients with AIH, with an AUC of 0.885. Although it is not statistically significant, the diagnostic performance of hepatic ECV was higher than that of all non-invasive serologic tests, probably because of liver-specific nature of mapping parameters compared to clinical scores. The results of this study support previous data and demonstrate that T1 mapping with ECV calculation correlates with the severity of liver fibrosis, also in patients with AIH (Hoffman et al., 2020). Interestingly, in contrast to previous data, we did not find significant correlations between T2 relaxation times and liver stiffness measurement (Hoffman et al., 2020). It might be explained by the fact that, similar to cardiac imaging, T2 relaxation times might be increased in regions of fibrosis with coexisting inflammation, due to increased water content. Therefore, the absence of significant differences in patients with AIH and different fibrosis stages can be explained by the same inflammatory activity in the liver at the time of MRI examination in our study.

PSC is another rare progressive autoimmune CLD, characterized by strictures in both intra- and extrahepatic ducts. Currently, PSC represents an important cause of morbidity and mortality in Western societies, with many patients ultimately requiring liver transplantation. The reported incidence and prevalence in Northern European countries range from approximately 0.5 to 1.3 cases per 100,000 person-years and 3.85 to 16.2 cases per 100,000 person-years, respectively (Tabibian et al., 2018). Given the progressive nature of PSC and its

associated morbidity and mortality, there is a large unmet need for disease-specific, reliable, and accurate biomarkers for the assessment and monitoring of liver fibrosis and therapy response. According to current guidelines of the American Association for the Study of Liver Diseases and the European Association for the Study of the Liver, imaging is essential for confirming the diagnosis of PSC and identification of possible complications (Khoshpouri et al., 2019; Chapman et al., 2010). Using mapping techniques as a part of MRI examination for the assessment of liver fibrosis severity can be advantageous due to its ability to encompass the liver entirely. This is particularly important in patients with PSC, who present with heterogeneous diffuse parenchymal changes (Khoshpouri et al., 2019). In our study, using MRE-derived liver stiffness as a reference standard, we found strong correlations between hepatic ECV and liver stiffness with a correlation coefficient (r) of 0.69 ($P < 0.001$). Hepatic ECV showed a high diagnostic performance to diagnose significant fibrosis ($F \geq 2$) with an AUC of 0.858. These results are concordant and contribute to the previous data, demonstrating the ability of T1 and ECV mapping to detect and stage liver fibrosis (Luetkens et al., 2018; Müller et al., 2017; Hoy et al., 2018). Similar to patients with AIH the diagnostic performance of ECV was higher than that of all non-invasive laboratory tests under investigation.

There are however some issues limiting the interpretation of quantitative mapping parameters for liver fibrosis assessment. In particular, it is known that T1 relaxation times can be affected not only by fibrosis but other important confounders such as edema due to the accompanying active inflammation, fat, and iron deposition (Welle et al., 2022; Ahn et al., 2021). This poses a challenge as compared to the myocardium, hepatic tissue exhibits a more complex structure and architecture. The influence of the aforementioned factors on mapping parameters should be taken into account when assessing the fibrosis stage, especially in CLD patients in an active stage, where inflammation may dominate and potentially lead to false positive interpretations. This, however, was taken into account in both above-mentioned studies. On the other hand, the advantage of parametric mapping is that it is a part of comprehensive liver tissue assessment alongside with other quantitative techniques (e.g., for the assessment of iron deposition, fat fraction, and edema). Therefore, the results of our studies support the clinical application of MRI quantitative mapping in the assessment of liver fibrosis in patients with AIH and PSC.

Despite underlying etiology, the progression of CLD over time leads to its terminal stage – liver cirrhosis. Up until recently, the scarring process of cirrhosis was thought to be irreversible.

Recent studies have suggested the effectiveness of anti-fibrogenic therapies and their ability not only to prevent severe scarring but also to reverse it (Kisseleva und Brenner, 2011; Nakano et al., 2020). Stem cells and/or liver cell transplantation represent other promising approaches, which are currently under active investigation (Esrefoglu, 2013; Yu et al., 2012; Hu et al., 2023). Nevertheless, liver cirrhosis remains the leading cause of death among nonmalignant diseases worldwide (2020). Development of liver cirrhosis includes an asymptomatic (so-called compensated) stage, followed by a progressive stage (so-called decompensated) characterized by portal hypertension and liver dysfunction to failure, ascites, spontaneous bacterial peritonitis, variceal hemorrhage, hepatorenal syndrome, encephalopathy. Regardless of etiology of CLD, the assessment of liver cirrhosis severity and stage is crucial for prognosis estimation and procedural planning. For these purposes, different clinical scores were developed and implemented with Child-Pugh score as the most established and used one. According to the studies, the 1-year median survival for Class A is nearly 100%, Class B is 80%, and Class C is 45%; 5-year median survival for Class A is ~64%, Class B is 60-75%, Class C is 34-50% (Peng et al., 2016). However, one of the main disadvantages of clinical scores is that they include laboratory and clinical parameters, which can be influenced by factors outside the liver. However, in our studies, we did not intend to advocate the use of clinical scores but to consider probably more specific, and accurate imaging-based biomarkers, which would add a piece of valuable information and, therefore, improve patients' management.

In this regard, various MRI techniques have been tried out to assess the functional aspect of liver disease or cirrhosis severity, e.g., using DWI extended to intravoxel incoherent motion (Ye et al., 2020), contrast-enhanced T1 techniques using different techniques and contrast media (e.g., hepatocyte-specific vs. extracellular (Lee et al., 2016)), and even T1 rho mapping (Chen et al., 2018). However, these techniques suffer from a lack of standardization (e.g., DWI and contrast-enhanced MRI) and availability across institutions (e.g., T1 rho mapping). Quantitative MRI mapping using T1 mapping techniques with a calculation of ECV may potentially overcome these limitations and allow for the assessment of liver disease severity (Kupczyk et al., 2021). A representative hepatic T1 map can be acquired during a single breath-hold and T1 values can be fast and directly obtained from the parametric map (Mesropyan et al., 2022). Therefore, this technique can be cost-effectively integrated into the clinical routine.

Therefore, in our next study, we explored the diagnostic utility of MRI-derived hepatic ECV for the assessment of liver cirrhosis severity in a broad range of patients with CLDs of different etiologies. We demonstrated that both hepatic native T1 and MRI-derived ECV showed significant correlations with the Child–Pugh score (r = 0,45 and 0.64, P < 0.001 in each case, respectively) and, MRI-derived hepatic ECV allowed differentiation between Child–Pugh classes A and B, and B and C with an AUC of 0.785 and 0.944 (P < 0.001, respectively). To our best knowledge, this was the first study focusing on the ability of ECV to assess liver cirrhosis severity and to discriminate between different classes of liver cirrhosis severity. Therefore, the results of our study contribute to the existing data, expanding the clinical application of quantitative mapping, also in specific patient cohorts, which have been insufficiently described in the previous literature.

Another crucial therapeutic target in patients with liver cirrhosis is portal hypertension. Portal hypertension is defined as an increase in pressure in the portal venous system with portal venous pressure of more than 10 mmHg (La Mura et al., 2015). In advanced liver disease, portal hypertension develops because of increased intrahepatic resistance to the passage of blood flow through the liver as a consequence of hepatic fibrosis. A precise diagnosis of portal hypertension is crucial in clinical management and early interventions for the prevention of severe complications. Currently, the hepatic venous pressure gradient (HVPG) is considered the reference standard for the assessment of portal hypertension (La Mura et al., 2015). However, this is an invasive procedure that carries risks of periprocedural complications. Therefore, alternative methods for portal pressure measurements and monitoring are needed.

In our next proof-of-concept study, we investigated whether spleen mapping parameters could be used to predict portal pressure. In our study, splenic ECV demonstrated a perfect diagnostic performance for clinically significant portal hypertension with an AUC of 1.000 (P<0,001). Although not statistically significant, the diagnostic performance of splenic ECV was superior to that of the liver, possibly because liver fibrosis reflects only one aspect of pathophysiological changes in portal hypertension, while splenic ECV directly reflects all consequences of portal hypertension, namely congestion, tissue hyperplasia, and fibrosis. In this regard, splenomegaly in liver disease is likely to be a consequence of portal congestion with blood pooling as well as pulp hyperplasia and fibrosis (Bolognesi et al., 2002). Furthermore, ECV measurements showed a higher diagnostic performance compared to T1

and T2 mapping parameters, likely because ECV is a physiologically normalized measure and more accurately reflects changes in splenic parenchyma. A previous study had mentioned post-contrast T1 as a non-invasive marker for portal hypertension (Hoy et al., 2018; Levick et al., 2019). These results were not confirmed in our study. One of the reasons for this discrepancy might be the differences in patient cohorts, e.g., the mean direct HVPG in our study cohort was 20.71 ± 5.49 mmHg, whereas in the study of Levick et al. only half of the cohort (47%) had significant portal hypertension (Levick et al., 2019). Another reason for these controversial results might be that post-contrast T1 values are known to vary depending on the gadolinium dose, renal clearance rate, scanning time, body composition, and hematocrit levels.

In line with previous data, we contributed to the investigation of the diagnostic value of MRI mapping in the assessment of CLDs, also in specific patient cohorts, and expanded the application of quantitative mapping-derived parameters beyond morphology for the assessment of liver cirrhosis and portal hypertension severity.

The next step for further and broader implementation of mapping techniques into routine clinical practice is to make their acquisition and analysis as simple as possible. For this reason, assuming a known linear relationship between blood hematocrit and longitudinal relaxivity of T1 we hypothesized that ECV could be calculated without hematocrit sampling (Treibel et al., 2016). Therefore, in the final study, we implemented a method to easily obtain synthetic ECV measurement using hematocrit derived from pre-contrast blood T1. The linear relationship between hematocrit and $R1_{blood}$ has been sufficiently investigated, and, therefore, we used R1 for curve fitting (Treibel et al., 2016). We demonstrated a strong correlation between conventional and synthetic ECV in both the validation as well as the whole study cohort with $r = 0.97$ and 0.99, respectively ($P < 0.001$ in each case). As far as the results of this study can be compared with the results of existing cardiac studies, these findings support previous data, demonstrating high correlations between synthetic and conventional ECV (Treibel et al., 2016). It can be explained by the fact that ECV has other dependencies and additional terms, making it a more stable and robust parameter. However, regardless of the excellent linear regression fit and in general strong correlations between blood and synthetic hematocrit as well as conventional and synthetic ECV values, the main disadvantage of synthetic ECV application is that it might lead to considerable errors in individual cases (Raucci et al., 2017). The variability in laboratory hematocrit and calibration of conventional ECV to blood

hematocrit may also lead to miscategorization. Hence, a precise clinical evaluation based on medical history, laboratory examinations as well as MRI in individual patients is needed to minimize potential discrepancies between synthetic and conventional values, and, thereby, its influence on clinical decision-making.

The studies presented in this cumulative habilitation thesis have several limitations. The main limitation of the first two studies was the absence of liver biopsy at the time of the MRI examination. Liver biopsy with its clear drawbacks was performed only once at the time of initial diagnosis. No follow-up liver biopsies were performed to correlate the histopathological findings with mapping parameters in the first two studies. Therefore, we considered MRE-derived and TE-derived liver stiffness measurements as the reference standards for the assessment of liver fibrosis severity. Another limitation to all studies was the relatively small sample size. One of the reasons for this was the rarity of patients with autoimmune CLD. On the other hand, it was due to the explorative nature of the studies presented. Further prospective studies on a larger population, also in correlation with histopathological findings are needed to establish the results of studies and further investigate the diagnostic utility of MRI-derived mapping parameters. Next limitation to all studies was that none of T1 measurements were corrected for hepatic steatosis or hepatic/splenic iron overload, which are known to have an influence on T1 relaxation times. Despite the fact, that the exclusion criterion for all studies was iron overload and steatosis hepatitis, further development and optimization of T1 mapping techniques with a correction to iron and fat overload are needed.

5 Summary

Despite the global burden and clinical importance of CLDs, non-invasive, reliable, accurate, and reproducible imaging-based biomarkers for comprehensive assessment and monitoring of liver disease severity, periprocedural planning, and prognosis estimation are still insufficient. Therefore, active research in this field continues.

In this cumulative habilitation thesis, we presented and discussed studies investigating the diagnostic utility of MRI-derived quantitative mapping parameters for the assessment of liver fibrosis and liver cirrhosis severity. Moreover, we proposed a simple to obtain and reliable method for ECV calculation without the need for hematocrit sampling.

The high diagnostic utility of T1 mapping with the calculation of ECV was demonstrated for the assessment and differentiation between different fibrosis stages in patients with AIH and PSC. The results of these studies support the clinical application of quantitative mapping parameters in these specific patient cohorts for the non-invasive assessment and monitoring of liver fibrosis. Furthermore, we expanded the clinical application of quantitative mapping techniques in patients with CLDs demonstrating their value and high diagnostic performance for the assessment of liver cirrhosis severity as defined by the Child-Pugh score. In particular, hepatic ECV revealed high diagnostic performance in discrimination between different Child-Pugh classes of liver cirrhosis. Hepatic ECV also outperformed other mapping parameters and clinical markers/scores in differentiation between different Child-Pugh classes of liver cirrhosis. Additionally, not only hepatic mapping parameters were shown to be useful for the assessment of liver cirrhosis severity, but splenic parameters were as well. In particular, we demonstrated and discussed significant correlations between splenic ECV and invasive portal pressure measurements.

Interestingly, among all quantitative mapping parameters being under investigation in the presented studies, hepatic and splenic ECV have proven to be more accurate and reliable biomarkers. They outperformed native T1, post-contrast T1, and T2 in both staging liver fibrosis and assessing liver cirrhosis severity. Further, the results of our studies suggest that mapping parameters may overcome the limitation of conventional morphological imaging and provide valuable information beyond morphology in a single imaging setting. Further prospective studies are needed to establish the results of these studies and to ensure further

development, validation and implementation of non-invasive imaging-based parameters into routine clinical practice.

Last but not least, the proposed method of synthetic ECV calculation without hematocrit sampling was shown to be reliable, accurate, and reproducible. The use of synthetic ECV may overcome a limitation related to hematocrit sampling and allow for broader ECV implementation into routine clinical practice for hepatic applications.

In summary, this cumulative work broadens our understanding and knowledge of clinical applications of quantitative MRI biomarkers for the assessment of liver disease severity in patients with CLD, including autoimmune liver diseases, and highlights the importance of novel imaging-based biomarkers in the detection and characterization of liver fibrosis and liver cirrhosis severity. Therefore, based on the finding of our studies the clinical application of quantitative mapping techniques for hepatic applications should be expanded.

6 Overlap

Darstellung der Überlappung durch geteilte Autorenschaft

Die vorliegende Habilitationsschrift hat fünf publizierte Originalarbeiten zur Grundlage. Vier der Arbeiten habe ich als Erstautor (Mesropyan et al., Abdom Radiol (NY) 2021; Mesropyan et al., BMC Med Imaging 2021; Mesropyan et al Abdom Radiol (NY) 2021; Mesropyan et al., Eur Radiol 2021) und eine der Arbeiten als geteilte Erstautor veröffentlicht (Mesropyan, Kupczyk et al., Sci Rep 2022).

Die letztgenannte Arbeit habe ich in enger Kooperation mit meinem geschätzten Kollegen Herrn Dr. Kupczyk aus der Klinik für Diagnostische und Interventionelle Radiologie Bonn erstellt und die Erstautorenschaft geteilt. Dabei erfolgte die Datenrecherche, Akquisition und Berechnung des extrazellulären Volumens und der klinischen Scores, statistische Auswertung, Erstellung von Grafiken und Zusammenstellung des ersten Manuskripts durch mich (auch teilweise parallel zu Herrn Kupczyk). Die Konzeption, Planung, Patientenakquise und parallele Berechnung der extrazellulären Volumenfraktionen erfolgte durch Herrn Kupczyk. Die endgültige Verschriftlichung mit kritischer Diskussion der Ergebnisse erfolgte gemeinsam, sodass die Teilung der Erstautorenschaft gerechtfertigt ist.

Eine inhaltliche Überlappung der Publikation mit der kumulativen Habilitationsschrift von Herrn Dr. Kupczyk ist zwar gegeben, jedoch werden mit dem gemeinsamen Werk jeweils nur Teilaspekte beider Schriften behandelt. Da meine Habilitationsschrift einen Fokus auf den Stellenwert der quantitativen Mapping-Sequenzen inkl. extrazellulären Volumens als bildgebend-basierte nicht-invasive Biomarker für Leberfibrose und Schwergrad der chronischen Lebererkrankung und Zirrhose legen wird, keine größeren Schnittmengen zwischen beiden Habilitationsschriften zu erwarten sind.

7 Bibliography

Ahn J-H, Yu J-S, Park K-S, Kang SH, Huh JH, Chang JS, Lee J-H, Kim MY, Nickel MD, Kannengiesser S, Kim J-Y, Koh S-B. Effect of hepatic steatosis on native T1 mapping of 3T magnetic resonance imaging in the assessment of T1 values for patients with non-alcoholic fatty liver disease. Magnetic resonance imaging 2021; 80: 1–8

Aleknavičiūtė-Valienė G, Banys V. Clinical importance of laboratory biomarkers in liver fibrosis. Biochemia medica 2022; 32: 30501

Baranova A, Lal P, Birerdinc A, Younossi ZM. Non-invasive markers for hepatic fibrosis. BMC gastroenterology 2011; 11: 91

Bissell DM. Assessing fibrosis without a liver biopsy: are we there yet? Gastroenterology 2004; 127: 1847–1849

Bolognesi M, Merkel C, Sacerdoti D, Nava V, Gatta A. Role of spleen enlargement in cirrhosis with portal hypertension. Digestive and liver disease : official journal of the Italian Society of Gastroenterology and the Italian Association for the Study of the Liver 2002; 34: 144–150

Bonekamp S, Torbenson MS, Kamel IR. Diffusion-weighted magnetic resonance imaging for the staging of liver fibrosis. Journal of clinical gastroenterology 2011; 45: 885–892

Cassinotto C, Feldis M, Vergniol J, Mouries A, Cochet H, Lapuyade B, Hocquelet A, Juanola E, Foucher J, Laurent F, Ledinghen V de. MR relaxometry in chronic liver diseases: Comparison of T1 mapping, T2 mapping, and diffusion-weighted imaging for assessing cirrhosis diagnosis and severity. European journal of radiology 2015; 84: 1459–1465

Chapman R, Fevery J, Kalloo A, Nagorney DM, Boberg KM, Shneider B, Gores GJ. Diagnosis and management of primary sclerosing cholangitis. Hepatology (Baltimore, Md.) 2010; 51: 660–678

Cheemerla S, Balakrishnan M. Global Epidemiology of Chronic Liver Disease. Clinical liver disease 2021; 17: 365–370

Chen W, Chen X, Yang L, Wang G, Li J, Wang S, Chan Q, Xu D. Quantitative assessment of liver function with whole-liver T1rho mapping at 3.0T. Magnetic resonance imaging 2018; 46: 75–80

Choi KJ, Jang JK, Lee SS, Sung YS, Shim WH, Kim HS, Yun J, Choi J-Y, Lee Y, Kang B-K, Kim JH, Kim SY, Yu ES. Development and Validation of a Deep Learning System for Staging Liver Fibrosis by Using Contrast Agent-enhanced CT Images in the Liver. Radiology 2018; 289: 688–697

Choi YR, Lee JM, Yoon JH, Han JK, Choi BI. Comparison of magnetic resonance elastography and gadoxetate disodium-enhanced magnetic resonance imaging for the evaluation of hepatic fibrosis. Investigative radiology 2013; 48: 607–613

Chon YE, Choi EH, Song KJ, Park JY, Kim DY, Han K-H, Chon CY, Ahn SH, Kim SU. Performance of transient elastography for the staging of liver fibrosis in patients with chronic hepatitis B: a meta-analysis. PloS one 2012; 7: e44930

Chowdhury AB, Mehta KJ. Liver biopsy for assessment of chronic liver diseases: a synopsis. Clinical and experimental medicine 2023; 23: 273–285

Diao K-Y, Yang Z-G, Xu H-Y, Liu X, Zhang Q, Shi K, Jiang L, Xie L-J, Wen L-Y, Guo Y-K. Histologic validation of myocardial fibrosis measured by T1 mapping: a systematic review and meta-analysis. Journal of cardiovascular magnetic resonance : official journal of the Society for Cardiovascular Magnetic Resonance 2016; 18: 92

Esrefoglu M. Role of stem cells in repair of liver injury: experimental and clinical benefit of transferred stem cells on liver failure. World journal of gastroenterology 2013; 19: 6757–6773

Goodman ZD. Grading and staging systems for inflammation and fibrosis in chronic liver diseases. Journal of hepatology 2007; 47: 598–607

Goshima S, Kanematsu M, Watanabe H, Kondo H, Kawada H, Moriyama N, Bae KT. Gd-EOB-DTPA-enhanced MR imaging: prediction of hepatic fibrosis stages using liver contrast enhancement index and liver-to-spleen volumetric ratio. Journal of magnetic resonance imaging : JMRI 2012; 36: 1148–1153

Guimaraes AR, Siqueira L, Uppal R, Alford J, Fuchs BC, Yamada S, Tanabe K, Chung RT, Lauwers G, Chew ML, Boland GW, Sahani DV, Vangel M, Hahn PF, Caravan P. T2 relaxation time is related to liver fibrosis severity. Quantitative imaging in medicine and surgery 2016; 6: 103–114

Guo SL, Su LN, Zhai YN, Chirume WM, Lei JQ, Zhang H, Yang L, Shen XP, Wen XX, Guo YM. The clinical value of hepatic extracellular volume fraction using routine multiphasic contrast-enhanced liver CT for staging liver fibrosis. Clinical radiology 2017; 72: 242–246

Heneghan MA, Shumbayawonda E, Dennis A, Ahmed RZ, Rahim MN, Ney M, Smith L, Kelly M, Banerjee R, Culver EL. Quantitative magnetic resonance imaging to aid clinical decision making in autoimmune hepatitis. EClinicalMedicine 2022; 46: 101325

Heye T, Yang S-R, Bock M, Brost S, Weigand K, Longerich T, Kauczor H-U, Hosch W. MR relaxometry of the liver: significant elevation of T1 relaxation time in patients with liver cirrhosis. European radiology 2012; 22: 1224–1232

Hoad CL, Palaniyappan N, Kaye P, Chernova Y, James MW, Costigan C, Austin A, Marciani L, Gowland PA, Guha IN, Francis ST, Aithal GP. A study of T_1 relaxation time as a measure of liver fibrosis and the influence of confounding histological factors. NMR in biomedicine 2015; 28: 706–714

Hoffman DH, Ayoola A, Nickel D, Han F, Chandarana H, Shanbhogue KP. T1 mapping, T2 mapping and MR elastography of the liver for detection and staging of liver fibrosis. Abdominal radiology (New York) 2020; 45: 692–700

Hoodeshenas S, Yin M, Venkatesh SK. Magnetic Resonance Elastography of Liver: Current Update. Topics in magnetic resonance imaging : TMRI 2018; 27: 319–333

Hoy AM, McDonald N, Lennen RJ, Milanesi M, Herlihy AH, Kendall TJ, Mungall W, Gyngell M, Banerjee R, Janiczek RL, Murphy PS, Jansen MA, Fallowfield JA. Non-invasive assessment of liver disease in rats using multiparametric magnetic resonance imaging: a feasibility study. Biology open 2018; 7

Hu X-H, Chen L, Wu H, Tang Y-B, Zheng Q-M, Wei X-Y, Wei Q, Huang Q, Chen J, Xu X. Cell therapy in end-stage liver disease: replace and remodel. Stem cell research & therapy 2023; 14: 141

Khoshpouri P, Habibabadi RR, Hazhirkarzar B, Ameli S, Ghadimi M, Ghasabeh MA, Menias CO, Kim A, Li Z, Kamel IR. Imaging Features of Primary Sclerosing Cholangitis: From Diagnosis to Liver Transplant Follow-up. Radiographics : a review publication of the Radiological Society of North America, Inc 2019; 39: 1938–1964
Kisseleva T, Brenner DA. Anti-fibrogenic strategies and the regression of fibrosis. Best practice & research. Clinical gastroenterology 2011; 25: 305–317
Kong P, Yuan T, He Y, Wang S, Zhou X, Cao J. The correlation between magnetic resonance diffusion parameters and Ki-67 and PCNA in hepatic fibrosis and cirrhosis rats. Annals of palliative medicine 2021; 10: 8112–8122
Kupczyk PA, Mesropyan N, Isaak A, Endler C, Faron A, Kuetting D, Sprinkart AM, Mädler B, Thomas D, Attenberger UI, Luetkens JA. Quantitative MRI of the liver: Evaluation of extracellular volume fraction and other quantitative parameters in comparison to MR elastography for the assessment of hepatopathy. Magnetic resonance imaging 2021; 77: 7–13
La Mura V, Nicolini A, Tosetti G, Primignani M. Cirrhosis and portal hypertension: The importance of risk stratification, the role of hepatic venous pressure gradient measurement. World journal of hepatology 2015; 7: 688–695
Le Bihan D, Breton E, Lallemand D, Aubin ML, Vignaud J, Laval-Jeantet M. Separation of diffusion and perfusion in intravoxel incoherent motion MR imaging. Radiology 1988; 168: 497–505
Lee S, Choi D, Jeong WK. Hepatic enhancement of Gd-EOB-DTPA-enhanced 3 Tesla MR imaging: Assessing severity of liver cirrhosis. Journal of magnetic resonance imaging : JMRI 2016; 44: 1339–1345
Levick C, Phillips-Hughes J, Collier J, Banerjee R, Cobbold JF, Wang LM, Piechnik SK, Robson MD, Neubauer S, Barnes E, Pavlides M. Non-invasive assessment of portal hypertension by multi-parametric magnetic resonance imaging of the spleen: A proof of concept study. PloS one 2019; 14: e0221066
Li J, Liu H, Zhang C, Yang S, Wang Y, Chen W, Li X, Wang D. Native T1 mapping compared to ultrasound elastography for staging and monitoring liver fibrosis: an animal study of repeatability, reproducibility, and accuracy. European radiology 2020; 30: 337–345
Li Y, Huang Y-S, Wang Z-Z, Yang Z-R, Sun F, Zhan S-Y, Liu X-E, Zhuang H. Systematic review with meta-analysis: the diagnostic accuracy of transient elastography for the staging of liver fibrosis in patients with chronic hepatitis B. Alimentary pharmacology & therapeutics 2016a; 43: 458–469
Li Z, Sun J, Hu X, Huang N, Han G, Chen L, Zhou Y, Bai W, Yang X. Assessment of liver fibrosis by variable flip angle T1 mapping at 3.0T. Journal of magnetic resonance imaging : JMRI 2016b; 43: 698–703
Low G, Kruse SA, Lomas DJ. General review of magnetic resonance elastography. World journal of radiology 2016; 8: 59–72
Lu Y, Wang Q, Zhang T, Li J, Liu H, Yao D, Hou L, Tu B, Wang D. Staging Liver Fibrosis: Comparison of Native T1 Mapping, T2 Mapping, and T1ρ: An Experimental Study in Rats With Bile Duct Ligation and Carbon Tetrachloride at 11.7 T MRI. Journal of magnetic resonance imaging : JMRI 2022; 55: 507–517

Lubner MG, Pickhardt PJ. Multidetector computed tomography for assessment of hepatic fibrosis. Clinical liver disease 2018; 11: 156–161
Luetkens JA, Klein S, Träber F, Schmeel FC, Sprinkart AM, Kuetting DLR, Block W, Uschner FE, Schierwagen R, Hittatiya K, Kristiansen G, Gieseke J, Schild HH, Trebicka J, Kukuk GM. Quantification of Liver Fibrosis at T1 and T2 Mapping with Extracellular Volume Fraction MRI: Preclinical Results. Radiology 2018; 288: 748–754
Magnetic resonance imaging of parenchymal liver disease: a comparison with ultrasound, radionuclide scintigraphy and X-ray computed tomography. The Clinical NMR Group. Clinical radiology 1987; 38: 495–502
Mesropyan N, Kupczyk PA, Dold L, Praktiknjo M, Chang J, Isaak A, Endler C, Kravchenko D, Bischoff LM, Sprinkart AM, Pieper CC, Kuetting D, Jansen C, Attenberger UI, Luetkens JA. Assessment of liver cirrhosis severity with extracellular volume fraction MRI. Scientific reports 2022; 12: 9422
Messroghli DR, Moon JC, Ferreira VM, Grosse-Wortmann L, He T, Kellman P, Mascherbauer J, Nezafat R, Salerno M, Schelbert EB, Taylor AJ, Thompson R, Ugander M, van Heeswijk RB, Friedrich MG. Clinical recommendations for cardiovascular magnetic resonance mapping of T1, T2, T2* and extracellular volume: A consensus statement by the Society for Cardiovascular Magnetic Resonance (SCMR) endorsed by the European Association for Cardiovascular Imaging (EACVI). Journal of cardiovascular magnetic resonance : official journal of the Society for Cardiovascular Magnetic Resonance 2017; 19: 75
Mewton N, Liu CY, Croisille P, Bluemke D, Lima JAC. Assessment of myocardial fibrosis with cardiovascular magnetic resonance. Journal of the American College of Cardiology 2011; 57: 891–903
Motosugi U, Ichikawa T, Oguri M, Sano K, Sou H, Muhi A, Matsuda M, Fujii H, Enomoto N, Araki T. Staging liver fibrosis by using liver-enhancement ratio of gadoxetic acid-enhanced MR imaging: comparison with aspartate aminotransferase-to-platelet ratio index. Magnetic resonance imaging 2011; 29: 1047–1052
Müller A, Hochrath K, Stroeder J, Hittatiya K, Schneider G, Lammert F, Buecker A, Fries P. Effects of Liver Fibrosis Progression on Tissue Relaxation Times in Different Mouse Models Assessed by Ultrahigh Field Magnetic Resonance Imaging. BioMed research international 2017; 2017: 8720367
Nacif MS, Turkbey EB, Gai N, Nazarian S, van der Geest RJ, Noureldin RA, Sibley CT, Ugander M, Liu S, Arai AE, Lima JAC, Bluemke DA. Myocardial T1 mapping with MRI: comparison of look-locker and MOLLI sequences. Journal of magnetic resonance imaging : JMRI 2011; 34: 1367–1373
Nakano Y, Kamiya A, Sumiyoshi H, Tsuruya K, Kagawa T, Inagaki Y. A Deactivation Factor of Fibrogenic Hepatic Stellate Cells Induces Regression of Liver Fibrosis in Mice. Hepatology (Baltimore, Md.) 2020; 71: 1437–1452
Obmann VC, Berzigotti A, Catucci D, Ebner L, Gräni C, Heverhagen JT, Christe A, Huber AT. T1 mapping of the liver and the spleen in patients with liver fibrosis-does normalization to the blood pool increase the predictive value? European radiology 2021; 31: 4308–4318

O'Brien AT, Gil KE, Varghese J, Simonetti OP, Zareba KM. T2 mapping in myocardial disease: a comprehensive review. Journal of cardiovascular magnetic resonance : official journal of the Society for Cardiovascular Magnetic Resonance 2022; 24: 33
Ou H-Y, Bonekamp S, Bonekamp D, Corona-Villalobos CP, Torbenson MS, Geiger B, Kamel IR. MRI arterial enhancement fraction in hepatic fibrosis and cirrhosis. AJR. American journal of roentgenology 2013; 201: W596-602
Papastergiou V, Tsochatzis E, Burroughs AK. Non-invasive assessment of liver fibrosis. Annals of Gastroenterology 2012; 25: 218–231
Pape S, Schramm C, Gevers TJ. Clinical management of autoimmune hepatitis. United European gastroenterology journal 2019; 7: 1156–1163
Patel K, Sebastiani G. Limitations of non-invasive tests for assessment of liver fibrosis. JHEP reports : innovation in hepatology 2020; 2: 100067
Peng Y, Qi X, Guo X. Child-Pugh Versus MELD Score for the Assessment of Prognosis in Liver Cirrhosis: A Systematic Review and Meta-Analysis of Observational Studies. Medicine 2016; 95: e2877
Perea RJ, Ortiz-Perez JT, Sole M, Cibeira MT, Caralt TM de, Prat-Gonzalez S, Bosch X, Berruezo A, Sanchez M, Blade J. T1 mapping: characterisation of myocardial interstitial space. Insights into imaging 2015; 6: 189–202
Petitclerc L, Gilbert G, Nguyen BN, an Tang. Liver Fibrosis Quantification by Magnetic Resonance Imaging. Topics in magnetic resonance imaging : TMRI 2017; 26: 229–241
Piechnik SK, Ferreira VM, Lewandowski AJ, Ntusi NAB, Banerjee R, Holloway C, Hofman MBM, Sado DM, Maestrini V, White SK, Lazdam M, Karamitsos T, Moon JC, Neubauer S, Leeson P, Robson MD. Normal variation of magnetic resonance T1 relaxation times in the human population at 1.5 T using ShMOLLI. Journal of cardiovascular magnetic resonance : official journal of the Society for Cardiovascular Magnetic Resonance 2013; 15: 13
Premkumar M, Anand AC. Overview of Complications in Cirrhosis. Journal of clinical and experimental hepatology 2022; 12: 1150–1174
Puustinen L, Barner-Rasmussen N, Pukkala E, Färkkilä M. Incidence, prevalence, and causes of death of patients with autoimmune hepatitis: A nationwide register-based cohort study in Finland. Digestive and liver disease : official journal of the Italian Society of Gastroenterology and the Italian Association for the Study of the Liver 2019; 51: 1294–1299
Raucci FJ, Parra DA, Christensen JT, Hernandez LE, Markham LW, Xu M, Slaughter JC, Soslow JH. Synthetic hematocrit derived from the longitudinal relaxation of blood can lead to clinically significant errors in measurement of extracellular volume fraction in pediatric and young adult patients. Journal of cardiovascular magnetic resonance : official journal of the Society for Cardiovascular Magnetic Resonance 2017; 19: 58
Ronot M, Leporq B, van Beers BE, Vilgrain V. CT and MR perfusion techniques to assess diffuse liver disease. Abdominal radiology (New York) 2020; 45: 3496–3506
Rossi E, Adams LA, Bulsara M, Jeffrey GP. Assessing Liver Fibrosis with Serum Marker Models. Clinical Biochemist Reviews 2007; 28: 3–10
Schelbert EB, Messroghli DR. State of the Art: Clinical Applications of Cardiac T1 Mapping. Radiology 2016; 278: 658–676

Shin MK, Song JS, Hwang SB, Hwang HP, Kim YJ, Moon WS. Liver Fibrosis Assessment with Diffusion-Weighted Imaging: Value of Liver Apparent Diffusion Coefficient Normalization Using the Spleen as a Reference Organ. Diagnostics (Basel, Switzerland) 2019; 9
Sigrist RMS, Liau J, Kaffas AE, Chammas MC, Willmann JK. Ultrasound Elastography: Review of Techniques and Clinical Applications. Theranostics 2017; 7: 1303–1329
Singh S, Venkatesh SK, Wang Z, Miller FH, Motosugi U, Low RN, Hassanein T, Asbach P, Godfrey EM, Yin M, Chen J, Keaveny AP, Bridges M, Bohte A, Murad MH, Lomas DJ, Talwalkar JA, Ehman RL. Diagnostic performance of magnetic resonance elastography in staging liver fibrosis: a systematic review and meta-analysis of individual participant data. Clinical gastroenterology and hepatology : the official clinical practice journal of the American Gastroenterological Association 2015; 13: 440-451.e6
Smith AD, Branch CR, Zand K, Subramony C, Zhang H, Thaggard K, Hosch R, Bryan J, Vasanji A, Griswold M, Zhang X. Liver Surface Nodularity Quantification from Routine CT Images as a Biomarker for Detection and Evaluation of Cirrhosis. Radiology 2016; 280: 771–781
Spees WM, Yablonskiy DA, Oswood MC, Ackerman JJ. Water proton MR properties of human blood at 1.5 Tesla: magnetic susceptibility, T(1), T(2), T*(2), and non-Lorentzian signal behavior. Magnetic resonance in medicine 2001; 45: 533–542
Tabibian JH, Ali AH, Lindor KD. Primary Sclerosing Cholangitis, Part 1: Epidemiology, Etiopathogenesis, Clinical Features, and Treatment. Gastroenterology & Hepatology 2018; 14: 293–304
The global, regional, and national burden of cirrhosis by cause in 195 countries and territories, 1990-2017: a systematic analysis for the Global Burden of Disease Study 2017. The lancet. Gastroenterology & hepatology 2020; 5: 245–266
Thomsen C, Christoffersen P, Henriksen O, Juhl E. Prolonged T1 in patients with liver cirrhosis: An in vivo MRI study. Magnetic resonance imaging 1990; 8: 599–604
Treibel TA, Fontana M, Maestrini V, Castelletti S, Rosmini S, Simpson J, Nasis A, Bhuva AN, Bulluck H, Abdel-Gadir A, White SK, Manisty C, Spottiswoode BS, Wong TC, Piechnik SK, Kellman P, Robson MD, Schelbert EB, Moon JC. Automatic Measurement of the Myocardial Interstitium: Synthetic Extracellular Volume Quantification Without Hematocrit Sampling. JACC. Cardiovascular imaging 2016; 9: 54–63
Ulmenstein S von, Bogdanovic S, Honcharova-Biletska H, Blümel S, Deibel AR, Segna D, Jüngst C, Weber A, Kuntzen T, Gubler C, Reiner CS. Assessment of hepatic fibrosis and inflammation with look-locker T1 mapping and magnetic resonance elastography with histopathology as reference standard. Abdominal radiology (New York) 2022; 47: 3746–3757
Vento S, Cainelli F. Chronic liver diseases must be reduced worldwide: it is time to act. The Lancet. Global health 2022; 10: e471-e472
Verloh N, Utpatel K, Haimerl M, Zeman F, Fellner C, Fichtner-Feigl S, Teufel A, Stroszczynski C, Evert M, Wiggermann P. Liver fibrosis and Gd-EOB-DTPA-enhanced MRI: A histopathologic correlation. Scientific reports 2015; 5: 15408
Wang H-Q, Jin K-P, Zeng M-S, Chen C-Z, Rao S-X, Ji Y, Fu C-X, Sheng R-F. Assessing liver fibrosis in chronic hepatitis B using MR extracellular volume measurements: Comparison with serum fibrosis indices. Magnetic resonance imaging 2019; 59: 39–45

Wang Q-B, Zhu H, Liu H-L, Zhang B. Performance of magnetic resonance elastography and diffusion-weighted imaging for the staging of hepatic fibrosis: A meta-analysis. Hepatology (Baltimore, Md.) 2012; 56: 239–247
Wang YXJ, Huang H, Zheng C-J, Xiao B-H, Chevallier O, Wang W. Diffusion-weighted MRI of the liver: challenges and some solutions for the quantification of apparent diffusion coefficient and intravoxel incoherent motion. American Journal of Nuclear Medicine and Molecular Imaging 2021; 11: 107–142
Welle CL, Olson MC, Reeder SB, Venkatesh SK. Magnetic Resonance Imaging of Liver Fibrosis, Fat, and Iron. Radiologic clinics of North America 2022; 60: 705–716
Xu X, Su Y, Song R, Sheng Y, Ai W, Wu X, Liu H. Performance of transient elastography assessing fibrosis of single hepatitis B virus infection: a systematic review and meta-analysis of a diagnostic test. Hepatology international 2015; 9: 558–566
Ye Z, Wei Y, Chen J, Yao S, Song B. Value of intravoxel incoherent motion in detecting and staging liver fibrosis: A meta-analysis. World journal of gastroenterology 2020; 26: 3304–3317
Yu Y, Fisher JE, Lillegard JB, Rodysill B, Amiot B, Nyberg SL. Cell therapies for liver diseases. Liver transplantation : official publication of the American Association for the Study of Liver Diseases and the International Liver Transplantation Society 2012; 18: 9–21
Zhu N-Y, Chen K-M, Chai W-M, Li W-X, Du L-J. Feasibility of diagnosing and staging liver fibrosis with diffusion weighted imaging. Chinese medical sciences journal = Chung-kuo i hsueh k'o hsueh tsa chih 2008; 23: 183–186

8 Acknowledgments

Mein erster und besonderer Dank gilt Frau Prof. Dr. Ulrike Attenberger, die mir seit dem ersten Tag Ihrer Amtszeit Vertrauen und Wertschätzung entgegenbrachte. Durch Ihre Unterstützung ermöglicht Sie es mir, mich weiterhin sowohl klinisch als auch wissenschaftlich weiterzuentwickeln.

Ein herzlicher Dank gilt Prof. Dr. Daniel Thomas, der mir die Arbeit in dieser tollen Klinik ermöglicht hat, die mir so viel Freude täglich bringt.

Mein besonderer und tiefster Dank möchte ich meinem Mentor Priv.-Doz. Julian Luetkens aussprechen. Danke für Deine wertvolle Unterstützung und das Mentoring, die inspirierende und fokussierte Arbeit. Ohne Dich wäre das Ganze überhaupt nicht möglich gewesen.

Als nächstes möchte ich mich ganz herzlich bei Priv.-Doz. Darius Dabir bedanken, der mich von dem ersten Tag an so viel unterstützt und mir so viel beigebracht hat. Danke für Deine immer noch wertvolle Ratschläge, deine Herzlichkeit und Unterstützung.

Ein riesiger Dank geht an die besten Kollegen der Radiologischen Klinik, hier insbesondere an Priv.-Doz. Alexander Isaak, Priv.-Doz. Claus C. Pieper, Dr. Patrick Kupczyk, Priv.-Doz. Daniel Kütting, Dr. Christoph Endler, Dr. Carsten Meyer. Ein großer Dank gilt natürlich dem gesamten radiologischen Team für die zahlreichen Hilfsstellungen und beste Stimmung, ganz besonderes dem MRT-Team.

Ich danke meinem Freund Can für seinen Rückhalt, den er mir gibt und dass Du für mich immer da bist.

Zum Schluss möchte ich mich bei meiner gesamten Familie bedanken. Allen voran aber bei meiner Mutter für Ihre bedingungslose Unterstützung, unendliche Liebe und Geduld. Du bist immer für mich da und ohne Dich wäre nichts möglich gewesen.